University of Louisville

ThinkIR: The University of Louisville's Institutional Repository

12-2016

Optimization models and algorithms for demand response in smart grid.

Guangyang Xu
University of Louisville

OPTIMIZATION MODELS AND ALGORITHMS FOR DEMAND
RESPONSE IN SMART GRID

By

Guangyang Xu
M.S., University of Louisville, 2013

A Dissertation
Submitted to the Faculty of the
J.B. Speed School of Engineering of the University of Louisville
in Partial Fulfillment of the Requirements
for the Degree of

Doctor of Philosophy
in Industrial Engineering

Department of Industrial Egnineering
University of Louisville
Louisville, Kentucky

December 2016

OPTIMIZATION MODELS AND ALGORITHMS FOR DEMAND
RESPONSE IN SMART GRID

By

Guangyang Xu
M.S., University of Louisville, 2013

A Dissertation Approved On

November 28th, 2016

by the following Dissertation Committee

Dr. Lihui Bai, Dissertation Director

Dr. Kihwan Bae

Dr. Jason Saleem

Dr. Michael McIntyre

ACKNOWLEDGEMENTS

ABSTRACT

OPTIMIZATION MODELS AND ALGORITHMS FOR DEMAND RESPONSE IN
SMART GRID

Guangyang Xu

November 28th, 2016

For demand response in smart grid, a utility company wants to minimize
total electricity cost and end users want to maximize their own utility. The latter is
considered to consist of two parts in this research: electricity cost and
convenience/comfort. We first develop a system optimal (SO) model and a user
equilibrium (UE) model for the utility company and end users, respectively and
compare the difference of the two. We consider users' possible preference on
convenience over cost-saving under the real-time pricing in smart grid, and each
user is assumed to have a preferred time window for using a particular appliance.
As a result, each user in the proposed energy consumption game wishes to maximize
a payoff or utility consisting of two parts: the negative of electricity cost and the
convenience of using appliances during their preferred time windows. Numerical
results show that users with less flexibility on their preferred usage times have larger
impact on the system performance at equilibrium.

Second, we found that instead of minimizing total cost, if utility company is
regulated to maximize the social welfare, the user equilibrium model can achieve
identical optimal solution as the system optimal model. We then design a demand
response pricing frame work to accomplish this goal under alternative secondary

objectives. We also investigate the non-uniqueness of the user equilibrium solution and prove that there exist alternative user equilibrium solutions. In this case, robust pricing is considered using multi-level optimization for the user equilibrium.

Third, we study empirical data from a demand response pilot program in Kentucky in an attempt to understand consumer behavior under demand response and to characterize the thermo dynamics when set point for heat, ventilation and air conditioning (HVAC) is adjusted for demand response. Although sample size is limited, it helps to reveal the great variability in consumers' response to demand response event. Using the real data collected, we consider to minimize the peak demand for a system consisting of smart thermostats, advanced hot water heaters and battery systems for storage. We propose a mixed integer program model as well as a heuristic algorithm for an optimal consumption schedule so that the system peak during a designated period is minimized. Therefore, we propose a consumption scheduling model to optimally control these loads and storage in maximizing efficiency without impacting thermal comfort. The model allows pre-cooling and pre-heating of homes to be performed for variable loads in low-demand times.

We propose several future works. First, we introduce the concept of elastic demand to our SO model and UE model. The system problem maximizes net benefit to the energy consumers and the user problem is the usual one of finding equilibrium with elastic demand. The Karush-Kuhn-Tucker (KKT) conditions can be applied to solve the elastic demand problems. We also propose to develop algorithms for multi-level pricing models and further collect and analyze more field data in order to better understand energy users' consumption behavior.

TABLE OF CONTENTS

LIST OF TABLES

LIST OF FIGURES

CHAPTER 1

INTRODUCTION

"The grid", refers to the electric power grid, a network system that consists of transmission lines, substations, transformers and more (shown in Figure 1). It delivers electricity from the power plant to residential homes or businesses [1]. The first alternating current power grid was built in 1886 in the small city of Great Barrington, MA [2]. Since then, the power grid has been improved dramatically as technology advanced through each decade. The current US power grid consists of more than 9,200 electric generating units with more than 1 million megawatts of generating capacity, which is connected by more than 300,000 miles of transmission lines [1].

Although the electric grid is considered an engineering marvel, it has to face so many challenges today, such as generation diversification, optimal deployment of expensive assets, demand response, energy conservation, and reduction of the industry's overall carbon footprint, that it is not designed and engineered to handle [1][3][4]. The above listed critical issues cannot be addressed within the confines of the existing electricity power grid [3].

The existing electricity grid is one-way communication in nature. Two-thirds of fuel energy is wasted and cannot be converted into electricity. Almost 8% of its output is lost during the transmission from the generation facility to end users. In addition, 20% of its generation capacity exists to meet peak demand, which occurs only 5% of the time. Furthermore, because of the hierarchical topology of its assets, the current power grid experiences domino-impact failures [3]. To move forward, we require another sort of electric grid, which is developed from the base to handle the
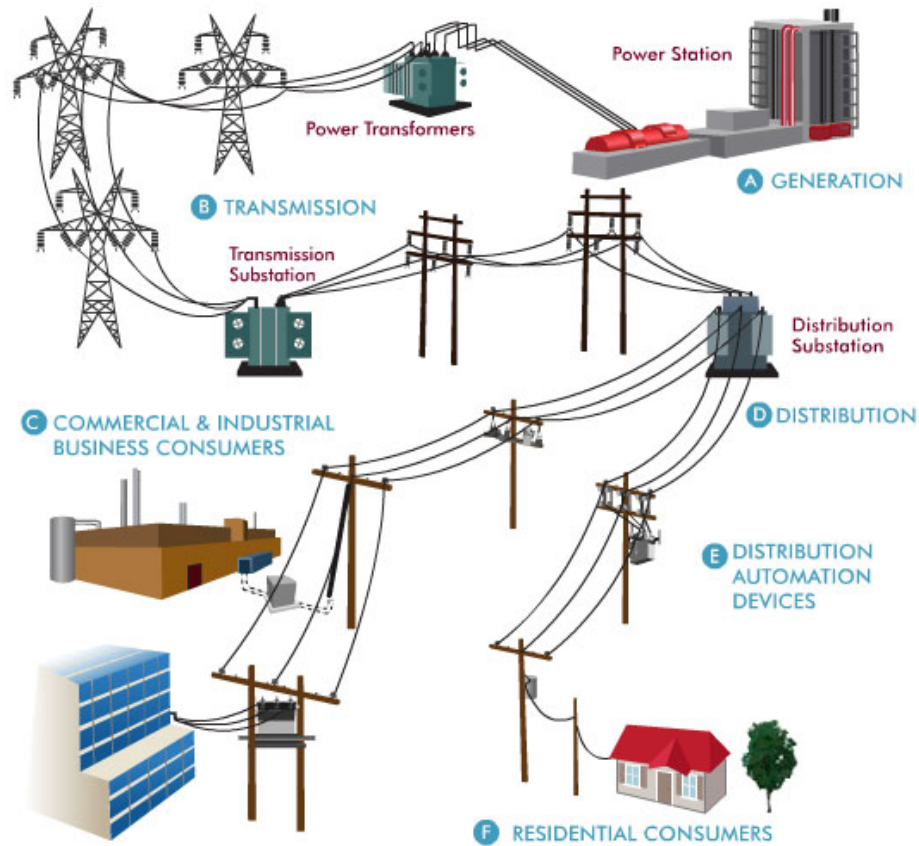
Figure 1. General layout of electricity networks [5]

upsurge of digital and computerized equipment and innovation subject to it – and which can automate and manage the increasing complexity and needs of electricity in the 21st Century. The next-generation electricity grid, which is also called smart grid or intelligent grid, is expected to overcome the major disadvantages of the existing grid.

The smart grid is a modern grid infrastructure to improve efficiency, reliability and security. Using automated control and modern communications technologies, it can smoothly integrate renewable and alternative energy sources [6][7]. Critically, smart grid empowering new network management strategies provide an effective grid integration in Distributed Generation (DG) for demand response (DR) and energy storage for DG load balancing, etc. [8][9]. Under this

circumstance, renewable energy generators is not only a promising technology to reduce fuel consumption and greenhouse gas emissions [10], renewable energy sources (RES) also become part of a reliable grid system. The integration of RES reduces system losses and enhances the reliability, efficiency and security of electricity supply to customers, which are some of the benefits that smart grid system will bring [11]. The existing grid is lack of ability to communicate, while a smart power grid infrastructure is sufficiently strengthened in enhanced sensing and advanced communication and computing abilities (see Figure. 2). Different components of the system are connected together with communication paths and sensors to provide advanced sensing and control, among which are distribution, transmission and other substations, i.e. residential, commercial, and industrial customers [12].
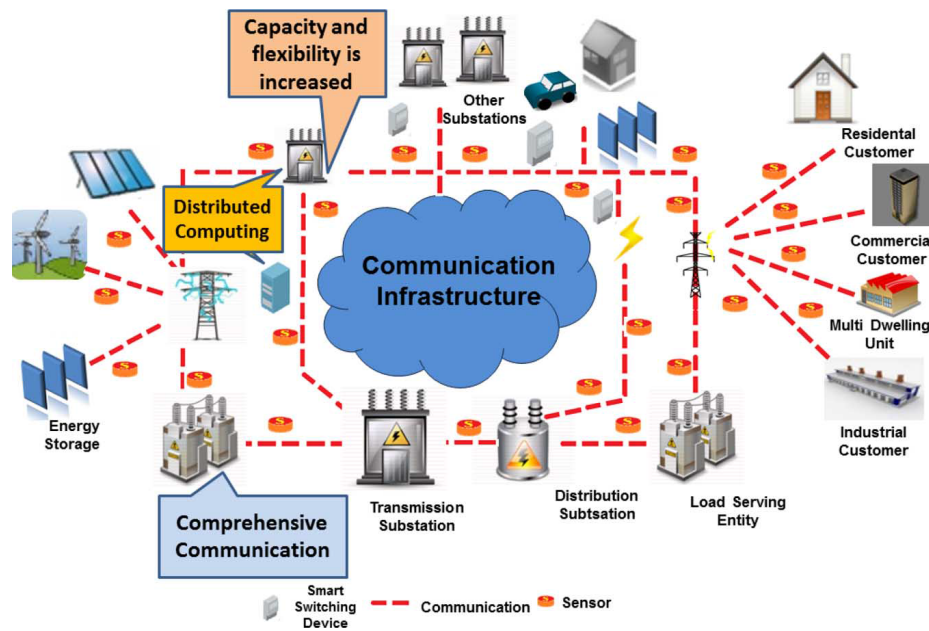
Figure 2. Framework of smart grid [12]

In essence, the smart grid needs to provide the utility companies with full visibility and pervasive control over their assets and services. Advanced metering infrastructure (AMI) for its significant effect in terms of system operation, asset

management, especially in energy saving and emission reduction achieved by DR technology has become the most popular research area throughout the power industry [13]. AMI uses two-way communication network, which can remotely connect and disconnect services, record waveforms, monitor voltage and current, send alarm information back to center within near real-time, and support time-of-use and real-time rate structures [13]-[15].

Additionally, the smart grid is required to be self-healing and resilient to system anomalies. Both simulation models [16][17] and optimization models [18]-[20] have been developed and investigated by many researchers to promote trust in smart grid solutions in safe and cost effective ways. Ghosn et al.[21] design an agent-oriented simulation model which can help understand smart grid issues and identify ways to improve the electrical grid. Their focus is mainly on the self-healing problem on how to activate control solutions in order to either take preventative actions or to handle problems after they occur. Alderson et al. [22] demonstrate a defender-attacker-defender (DAD) sequential game model to plan defenses for an infrastructure system that will enhance that system's resilience against attacks by an intelligent adversary. They also develop a general decomposition algorithm for solving DAD models and it only requires the system-operation model to be continuous and convex.

And last but not least, the smart grid needs to empower its stake holders to define and realize new ways of engaging with each other and performing energy transactions across the system. The integration of RES in smart grid is a challenging task, primarily because of the intermittent and unpredictable nature of the sources, either wind or polar [23]. Significant improvements can be made to the operations of a smart grid by providing information about the likely behavior of renewable energy through both online short-term forecasting and long-term assessments [24]. Another issue concerns the way to support the consumers' participation in the electricity market aiming at minimizing the costs of the system energy consumption [23].

In the advent of smart grid, demand response (DR) presents significant opportunities for load shifting, which helps flatten the demand curves, decrease the peak-to-average ratio, and hence reduce total cost. Managing residential electricity consumption, which accounts for 22% of the US energy consumption in 2008, is an important part to make the system more economical. Particularly, when consumers' use of electricity is mainly driven by convenience, coincident demand occurs, resulting in electric load peaks that greatly increase the generation costs. Early approach of consumer response can date back to the 1980's [25]. More recently, both centralized optimization models and decentralized game-theoretic models have been introduced to study strategies to flatten the load curves in DR and to study consumer behaviors. In centralized models, a central controller is assumed to be able to control and distribute the loads, with the objective of optimizing the total cost and user satisfaction (e.g., Gatsis and Giannakis [26]). With the advancement of communication technologies and smart meters within a smart grid, price signals can reach to the consumers in real time and in some cases the local/central operators can directly control the usage of some appliances. This increased ability for consumers and operators to interact within the power system has sparked interests in more decentralized models for describing individual's energy consumption scheduling and its impact on the power system [27].

Under smart pricing schemes, users are encouraged to individually and voluntarily manage their loads by reducing their energy consumption during peak hours [28]-[30]. In price based programs, time-of-use pricing (TOU), critical-peak pricing (CPP), extreme day CPP (ED-CPP), extreme day pricing (EDP) and real-time pricing (RTP) are among the popular options [31]. For example, in RTP scheme, the price of electricity varies at different hours of the day. The prices are usually higher during the afternoon of hot days in the summer and cold days in the winter [32].

In this dissertation proposal, we first propose a game theoretical approach to

modeling energy consumption scheduling in smart grid with consumer preference. We develop a system optimum model and a user equilibrium model. The objective of the system model is to minimize the total electricity cost of the entire system. In this model, the area central controller determines when and how much each user should use his/her appliances, so that the system can achieve the minimum total electricity cost. But for each user, it may not be the minimum cost for him/her. Also, as the end user, each one has his/her preference on how to use the appliances. They may not want to compromise the convenience to less cost. So in our user equilibrium model, we want to describe users' energy consumption behavior which considers users' possible preference on convenience and cost. This makes the user equilibrium model more realistic. The objective of the user equilibrium model is to maximize each user's payoff or utility, which is the utility function minus the electricity cost. We assume that each user has the knowledge of the usage profile of others. We depict the convenience experienced each user in term of monetary value in the utility function. The user equilibrium solution is always different from the system optimal solution. In terms of the total cost and peak load reduction, it is always worse than the system model.

Second, we develop a pricing model to see if there exists proper pricing scheme that can make the system model and the user equilibrium model share the same users energy consumption profile. The objective of the system model is to maximize the social welfare, which is the convenience-based utility function minus the electricity generation cost function. This is similar to the objective of the user equilibrium model, which is the convenience-based utility function minus the time variant based electricity cost. We show that for a pre-specified system optimal solution, there exists alternative pricing schemes to achieve the desired objective. In this way, the pricing scheme becomes adjustable and the utility company may customize the pricing scheme to achieve proper objectives. We also prove that at the equilibrium, the users' energy consumption pattern of user equilibrium may not

follow the system optimal solution if the user equilibrium has multiple solutions under a given pricing scheme. Then, we propose a robust pricing multi-level optimization problem to maximize the minimum possible social welfare among alternative user equilibrium solutions. The column and constraint generation algorithm or bender's dual cutting plane algorithm might be two of our potential methods to solve the proposed bi-level model.

Third, we study empirical data from a demand response pilot program in Kentucky in an attempt to understand consumer behavior under demand response and to characterize the thermo dynamics when set point for HVAC is adjusted for demand response. Using the real data collected, we consider to minimize the peak demand for a system consisting of smart thermostats, advanced hot water heaters and battery systems for storage. We propose a mixed integer program model as well as a heuristic algorithm for an optimal consumption schedule so that the system peak during a designated period is minimized. Therefore, we propose a consumption scheduling model to optimally control these loads and storage in maximizing efficiency without impacting thermal comfort. The model allows pre-cooling and pre-heating of homes to be performed for variable loads in low-demand times and/or when renewable generation resources are on-line, so as to get maximum utilization from these resources.

The rest of this proposal is organized as follows. Chapter 2 reviews the literature on optimization models and algorithms on DR. Chapter 3 formulates the centralized model and game theoretical model for DR with costumer preference and its numerical results. Chapter 4 presents the pricing model for DR with consumer preference and its computational results. Chapter 5 presents the empirical study of energy consumption in sub-metered homes and the optimal consumption scheduling model. Chapter 6 presents the conclusion and proposed works.

CHAPTER 2

LITERATURE REVIEW

2.1   Direct Load Control

Direct load control (DLC) has been investigated for a long time and there is a large literature of classical DLC on load management. Most optimization methods have been proposed to minimize generation cost [33]-[35]. Particularly, Cohen and Wang [33] develop an effective optimization method for scheduling load management based on an analytic model of the load under control. Their method can be used to minimize different objectives including peak load and production cost. Although it is impossible to determine how close the solutions generated by this method are to the optimal schedules, they have found that the schedules produced are effective in reducing the value of the objective and that they cannot be easily improved upon. Furthermore, the solution method can obtain schedules for difficult problems involving very long periods of peak load and cases where the cycle rate is allowed to vary. Its advantage is to allow any length for the control periods and any cycle rates. While the disadvantage in allowing the cycle rate to vary is that run time will increase almost linearly with the number of allowed cycle rates.

Similarly, Wei and Chen [34] apply multi-pass dynamic programming (MPDP) to determine the required amount of load to be controlled at each time stage in order to reach maximum cost saving and peak load reduction. They test the proposed approach on Taiwan Power Company system to demonstrate its effectiveness. Results show that the peak load reduction and production cost saving are closely related to the energy payback pattern. Furthermore, the MPDP

approach would also yield a load control value for each time stage during the whole study period. They claim that their algorithm is also suitable for the solution of problems with other types of load control operation because of its reasonable results, fast calculation speed and small storage memory requirement.

Another method for DLC dispatch other than dynamic programming is presented by Chen et al. [35]. For a DLC group, their method identifies a set of candidate control patterns in terms of feasibility and cost benefit. Based on the candidate control patterns, they determine the optimal DLC dispatch strategy via a binary flow network model. They also compare their results with a dynamic programming based DLC dispatch method and show their method is very effective.

The second aspect of the DLC's objective is to maximize utility's profit [36]. Ng and Sheble [36] introduce the profit-based load management to examine generic direct load control scheduling. Their aim is to increase the profit of utilities based on the cost/market price function. Their linear programming algorithm controls the number of groups per customer/load type to maximize the profit. They compare their profit-based DLC with the conventional cost-based approach and results show that the former achieves better solution when the rate structure varies each time. Furthermore, the algorithm provides a relatively inexpensive and powerful approach to the scheduling problem.

Minimizing deviation from users' desired consumptions is the third aspect of DLC's objective [37][38]. In order to solve the chronic problem of severe power shortage in the summer for the Taiwan Power Company (TPC), Chu et al. [37] adopt the method of dynamic programming to optimally determine the schedule of the DLC with the objective of minimizing the amount of load reduction to lessen the effects of customers' discomfort and to maintain the TPC's total incomes. They consider the constraints of operation limitations of the compressor and room temperature. They claim that their method is able to dynamically specify the target load level, and should also be helpful for other utilities trying to control the

growth rates of peak loads in their attempt to match their schedules of system planning and thereby to reap the maximal benefit.

Ramanathan and Vittal [38] develop a framework for designing and assessing DLC program with the objective of minimizing end-user discomfort and is formulated as an optimization problem. Two different algorithms for cycling of loads have been presented and Monte Carlo-based dynamic programming approach is applied. The results of the simulations are with regard to the impact of different constraints and parameters on the effectiveness of control. They also claim that their method could be applied in designing and analyzing the effectiveness of other demand-side management programs.

Finally, DLC is sometimes integrated with unit commitment [39]. Hsu and Su [39] integrate the DLC dispatch problem into conventional unit commitment problem. They apply dynamic programming to determine the required amount of load control and generation schedule at each stage in order to maximize fuel cost savings. The total fuel cost can be reduced through peak load reduction and rescheduling of peaking units. It is also observed that the proposed dynamic programming approach would yield a variable amount of load control for each stage over the load control period. Their DLC dispatching strategy will result in more fuel cost savings than the fixed DLC dispatching strategy.

2.2 Distributed and Game Theoretical User Equilibrium Model

Distributed algorithm for coordinated scheduling, is motivated by individualism in decision making in energy consumption and has attracted many researchers in the past decades. Compared to DLC, decentralize/distributed scheduling assumes there is no central controller and all individuals decide or optimize their own energy consumption profiles. As a result, the agent-based approach (e.g., [40]) seems to be a good fit to model individuals' consumption behavior.

For example, Vytelingum et al. [41] implement the agent-based concept in developing a micro-storage management algorithm for the smart grid. In their model, each agent fixes his or her storage profile based on forecasted market price. Vytelingum et al. [41] prove that the average storage profile from their distributed algorithm converges to the Nash Equilibrium. Consequently, average peak demand induced by the optimal storage profile is reduced, thus eliminating the requirements for more costly and carbon-intensive generation plant.

In addition, Vandael et al. [42] propose a multi-agent solution and compared the qualities of this solution with an optimal reference solution obtained by quadratic programming. They use a decentralized model to level the load at each transformer through two coordination strategies: the energy limiter and power limiter. The former only uses predictions about loads, while the latter doesn't use any forecast data. In [42], the multi-agent solution proves to be scalable and adaptable to incomplete and unpredictable information, while still capable of reducing peak demands with an efficiency up to 95% compared to the quadratic scheduler.

In fact, understanding individuals' behavior in energy consumption is considered as one key (among others) to the success of DR, because it will help effectively manage demands via pricing or incentive programs. In the literature, game-theoretic approaches have been the main stream (e.g., Saad et al. [43] and Fadlullah et al. [44]) for modeling the consumer behaviors. Most of these studies assume each consumer optimizes his/her own cost in their energy consumption scheduling.

In [43], Saad et al. provide an overview on the applications of game theory in smart grid networks. In the areas of microgrids, demand-side management, and communications, they have identified the main technical challenges and discussed on how game theory can be applied to address these challenges. Moreover, they propose several future directions for extending these approaches and adopting

11

advanced game theoretic techniques, so as to reduce the gap between theoretical models and practical implementations of future smart grids.

Fadlullah et al. [44] survey a number of game theory-based applications to solve different problems in smart grid. Their survey reveals that game theory can be apparently simple yet become an effective technique to facilitate intelligent decision making in smart grid frameworks. They also notice that many of the game theory applications do not provide the global solution to the considered problem, which might be challenging in applying game theory to solve different optimization problems since the solution may remain stuck to a local minimum. In addition, the time to reach the Nash equilibrium point, in particular the global optimum, should be considered by researchers when applying game theory to solve smart grid communication problems.

More related to our work, Mohsenian-Rad et al. [45] propose a distributed algorithm to study consumers' optimal energy consumption scheduling when they are equipped with communication devices enabling them to talk to each other on energy usage. Their work in [45] assumes that each consumer minimizes his/her "utility payment," while we assume consumers value the convenience of using appliances at preferred times and incorporate this in the model.

In addition, Chen et al. [46] propose a real-time pricing based power scheduling scheme as a demand response mechanism for residential electric power consumption. A Stackelberg game model is formulated to analyze the interaction between a consumer's Energy Management Controller and the service provider. Their scheme can reduce peak load and the mismatch between actual load and planned supply, while avoiding a rebound peak. They allow users to delay the starting time of their usage of the appliances in order to reduce cost. However, users' experience on convenience is not directly modeled in [46] as is in our approach.

Furthermore, Maharjan et al. [47] propose a Stackelberg game between utility companies and end-users to maximize the revenue of each utility company

and the payoff of each user. They assume users will choose different utility companies as the leader in the Stackelberg game and derive analytical results for the Stackelberg equilibrium of the game and prove that a unique solution exists. They also propose a scheme based on the concept of shared reserve power to improve the grid reliability and ensure its dependability.

Finally, Samadi et al. [48] model the users' preferences and their energy consumption patterns in form of selected utility functions based on concepts from microeconomics. They also propose a distributed algorithm which finds the optimal energy consumption levels for each subscriber, so that the aggregate utility of all subscribers in the system is maximized in a fair and efficient way. Samadi et al. [48] show that the energy provider can encourage some desirable consumption patterns among the subscribers by the means of real-time pricing. The simulation results confirm that the proposed distributed algorithm can potentially benefit both subscribers and the energy provider.

2.3 Pricing Schemes

A crucial element in any DR study is the choice of the electricity cost/price, which has been studied rather extensively. Most studies on electricity markets incorporate quadratic functions describing the relationship between cost and electric usage. Furthermore, pricing approaches have been proposed to help shift the electricity load from peak to off-peak hours (e.g., Samadi et al. [48]).

In [49], a piecewise linear approximation is often applied to ease computational burden that would otherwise be experienced by quadratic models. On the other hand, the residential 'time-of-use' (TOU) rate has also been actively studied at various U.S. cities through projects funded by the U.S. Department of Energy over the past decades. The first project to implement the residential TOU rate began in 1975 in Vermont and was documented in [50]. The latter provides a detailed analysis of the TOU experiments in residential areas. Aigner [50] concludes

that effective pricing mechanism to change consumers' behavior is among the most important issues to the success of TOU rates. Other studies focusing on the impacts of TOU rates include [51], [52], [53], and [54].

In order to mitigate peak demand due to the extra load of charging electric vehicles (EVs) , Collins and Mader [51] utilize time-of-day pricing of electricity that causes a driver to shift recharging to periods in the day when electricity price is low. This would increase the utilization of baseload power plants and reduce the average cost of generating electricity.

For the purpose of better understanding the effectiveness of how TOU rates can economically incent off-peak charging in plug-in hybrid electric vehicles (PHEV), Davis and Bradley [52] present a simulation of PHEV total fueling costs and metrics of performance for evaluation of various TOU rate designs. Their results show that TOU rates are not universally effective at incenting off-peak PHEV charging behavior. By analyzing a suite of TOU rate models, the effectiveness and total fueling costs associated with a TOU rate is shown to be a function of the type of vehicle that the consumer is driving, the on:off peak price ratio of the TOU rate, and the length of the off-peak period.

Baladi et al. [53] estimate the response of residential consumers to voluntary TOU electricity pricing, both in terms of their willingness to participate in the rate structure and in their ability to shift usage. They find that the usage patterns of volunteers and non-volunteers were virtually identical under flat rates and on the TOU tariff. The only difference between volunteers and non-volunteers appears to be in their perceived usage patterns and their perceived ability to respond to the rate structure. This raises the issue as to whether education programs might alter these results in the long term, which is not discussed in [53].

Similarly, Hartway et al. [54] describe the results of a TOU rate option experiment which demonstrates that offering a TOU option can be profitable to a utility company. Their finding refutes the common belief that rate options are

necessarily unprofitable to a utility and unwanted by small users.

Other than the TOU rates, real-time pricing (RTP) structure is another intensively investigated pricing scheme by researchers (e.g. [32], [46], [48] and [55]).

Lijesen [32] provides a quantification of the real-time relationship between total peak demand and spot market prices. They find a low value for the real-time price elasticity, which may because not all users observe the spot market price. Their main policy implication is that the real-time elasticity of targeted users should be assessed before expensive demand response measures are taken on a large scale.

Similarly, Mohsenian-Rad and Leon-Garcia [55] point out that the lack of knowledge among users about how to respond to time-varying prices as well as the lack of effective building automation systems are two major barriers for fully utilizing the potential benefits of real-time pricing tariffs. Therefore, they propose an optimal and automatic residential energy consumption scheduling framework to tackle these problems. They attempt to achieve a desired trade-off between minimizing the electricity payment and minimizing the waiting time for the operation of each appliance in household in presence of a real-time pricing tariff combined with inclining block rates. By applying a simple and efficient weighted average price prediction filter to the actual hourly-based prices, Mohsenian-Rad and Leon-Garcia [55] obtain the optimal choices of the coefficients for each day of the week. Simulation results show that the combination of the proposed energy scheduler design and the price predictor leads to significant reduction in users' payments.

In addition to only changing the price, incentive-based demand response approaches are also effective in load shifting (e.g., Zhong et al. [56]). They propose the coupon incentive-based demand response to to induce flexibility in retail customers on a voluntary basis. The main advantages of their scheme are improved social welfare and consumers not exposed to fluctuating wholesale electricity prices. However, there also exists obvious disadvantages, such as increasing the burden of

communications and keeping some potential responsive customers away from the program.

Because all consumers respond to the price signals in adjusting their consumption behaviors, Stackelberg game is used by Meng and Zeng [57] for determining proper incentive. In [57], Meng and Zeng propose a Stackelberg game approach to maximize the profit of the utility company and minimize the payment bills of its customers. They model the interactions between the utility company and its electricity customers as a 1-leader, N-follower Stackelberg game. At the leader's side, they adopt genetic algorithms to maximize its profit while at the followers' side, an analytical solution to the linear programming problem is develop to minimize their bills. Simulation results show that their proposed approach is beneficial for both the customers and the utility company.

Moreover, Fetz and Filippini [58] have studied the economies of vertical integration and economies of scale. Specifically, they use different econometric specifications for panel data, including a random effects and a random-coefficients model, to estimate a quadratic multi-stage cost function for a sample of electricity companies. The empirical results in [58] reflect the presence of considerable economies of vertical integration and economies of scale for most companies considered in the analysis. Moreover, the results suggest a variation in economies of vertical integration across companies due to unobserved heterogeneity.

Finally, concerning the production cost, Martínez-Budría et al. [59] have adapted productivity analysis to the case of a cost model. A normalized quadratic cost function is estimated and discrete data has been used in their research. The main theoretical result in [59] is a productivity index that can be decomposed into modified versions of the contribution of technical change and the effect of the variations in the scale of production. The results also show important productivity gains with both technical change and scale effect playing important roles.

2.4   Customers' Preferences

The dissertation assumes that the consumers take into consideration not only their energy costs but also the convenience of their energy consumption schedule. This is because the fact that people would like to pay more for the convenience to their personal schedule, even if such preference implies a higher system-wide cost. Not much literature we found considers the customers' preferences or convenience.

Sianaki et al. [60] claim that in literature, no approach focuses on the users' point of view at the home level on a continuous basis and in an intelligent way to achieve demand response. They develop an intelligent decision supporting system model at home level for increasing the efficiency of energy consumption in the Smart Grid. They believe that their system will adapt to consumers' preferences and be compatible with demand response in the Smart Grid. The aim of their proposed approach is to urge end users to increase their consumption of renewable sources of energy and decrease the consumption of nonrenewable sources.

Amer et al. [61] propose the algorithm that can manage the household loads according to end user's preset priority and fix the total household power consumption under certain limit. The method in [61] makes the homeowner to automatically perform smart load controls possible. Controls are based on utility programs, customer's preference and load priority . They claim that their work achieves the purpose of reducing electricity expense and clipping the peak-to-average ratio (PAR).

Yoo and Lee [62] present the analysis of the power saving effect and the customer satisfaction level for In-Home Display usage. They analyze the power consumption and consumer preferences through the validation between the experimental group and the control group. From the results obtained from the questionnaire used, they also confirm the customer satisfaction. Yoo and Lee [62] are expected to improve the energy saving effect further, if the service providers supply a variety of devices to the customers to verify their power consumption

information more conveniently in the future.

CHAPTER 3

A GAME THEORETICAL APPROACH FOR DEMAND
RESPONSE WITH CONSUMER PREFERENCE

The department of energy estimates that residential buildings accounted for 37% of the total electricity consumption in 2008, and the percentage will grow much higher upon a broad adoption of electrical vehicles. Thus, energy consumption management in residential buildings becomes a pressing issue for our society to be sustainable. Particularly, when consumers' use of electricity is mainly driven by convenience, coincident demand occurs, resulting in electric load peaks that greatly increase the generation costs. In the advent of smart grid where price and usage data can be exchanged between consumers and utilities, demand side management (DSM) or demand response presents significant opportunities for load shifting and leveling.

Mohsenian-Rad et al. [45] propose a distributed algorithm to study consumers' optimal energy consumption scheduling. Their work assumes that each consumer minimizes his/her utility payment, while we assume consumers value the convenience of using appliances at preferred times and incorporate this in the model. In addition, Chen et al. [46] and Mohsenian-Rad et al. [55] allow users to delay the starting time for using appliances in order to reduce cost. However, users' experience on convenience is not directly modeled in their works as is in our approach. Finally, Maharjan et al. [47] assume users will choose different utility companies through a Stackelberg game. In summary, the current study assumes that consumers take into consideration not only their energy costs but also the convenience of their energy consumption schedule, and the latter is the focus for

subsequent numerical simulations.

In this chapter, we first propose a user (equilibrium) model to describe users' energy consumption behavior that explicitly considers users' possible preference on convenience over cost-saving. In this user equilibrium model, each user maximizes his/her payoff consisting of convenience and cost. To our best knowledge, most DSM literature assumes minimizing cost is the only objective for users, which is unrealistic. Indeed, in a recent smart meter/appliances pilot program by General Electric (GE) and Louisville Gas & Electric Company (LG&E), participants praised the program for it allows them to override the cost-saving based schedule [64]. Second, a centralized system-wide optimization model is developed as a benchmark for the user equilibrium model. The system model is for a central controller to maximize all users' payoffs collectively. Third, extensive sensitivity analysis provides insights on how consumers with various monetary values for convenience and with various flexibility on their energy consumption schedule affect the system equilibrium differently. Numerical experiments further validate both the system and user equilibrium models, and show that system performance is affected by both consumers' preferences and their value for convenience. Users who are less flexible in shifting their consumption schedule have more influence on the equilibrium. Further, consumers who value convenience higher will have a larger impact on the system's total cost.

3.1   Nomenclature

A. Sets and Indices

$\mathcal{A}$ Set of appliances indexed by a

I Set of users indexed by i

i^- Denote all other users in I except user i

20

T Set of time periods indexed by t

$T_{i,a}^0$ The unacceptable time periods for user i to use appliance a

$T_{i,a}^1$ The preferred time periods for user i to use appliance a

B. Parameters

$D_{i,a}$ The daily demand of user i on appliance a

$E_{i,a}$ The maximum electricity that can be consumed by user i on appliance a in one time period

π_i The monetary value of the time-of-use convenience for user i

$c_0,\ c$ Electricity price coefficients in the cost function

C. Variables

$x_{i,a}^t$ Electricity consumption of user i on appliance a at time t

$\mathbf{x_i}$ The electricity usage profile of user i, i.e., a vector of $x_{i,a}^t$ for all appliances and time periods

l_t, l_i^t Total electricity loads/consumptions at time t for all users and user i, respectively

$p_{i,a}$ Electricity consumption of user i on appliance a during preferred times

$\lambda_a^i, \rho_t^i, \gamma_{t,a}^i, \xi_{t,a}^i$ Dual variables for the user model

D. Functions

$f(\cdot)$ Unit electricity cost as of a function of total load

$u_i(\cdot)$ Utility function for user i

3.2 System Optimization Model

Consider a local area power system with n users and a set of appliances $\mathcal{A}$ for each user. Assume each user i has a daily energy demand $D_{i,a}$ for appliance $a \in \mathcal{A}$. We define a 24-hour daily cycle with $t \in T = \{1, 2, \cdots, 24\}$. Further, let $E_{i,a}$ be the maximum amount of energy consumed by user i on appliance a during one unit time. In addition, define a set of unacceptable time intervals $T^0_{i,a} \subset T$ during which user i does not wish to use appliance a, and a set of preferred time intervals $T^1_{i,a} \subset T$ ($T^1_{i,a} \cap T^0_{i,a} = \emptyset$) during which user i prefers to use appliance a. Using this notation and letting decision variable $x^t_{i,a}$ be the amount of energy consumed on appliance a by user i at time t, the system model for the energy controller can be formulated as follows:

$$\text{SO:} \quad \min \quad \sum_{t=1}^{T} f(l_t) \cdot l_t \tag{1}$$

$$\text{s.t.} \quad l_t = \sum_{i=1}^{n} \sum_{a \in A} x^t_{i,a}, \quad \forall t \tag{2}$$

$$\sum_{t=1}^{T} x^t_{i,a} = D_{i,a}, \quad \forall i, a \tag{3}$$

$$x^t_{i,a} \leq E_{i,a}, \quad \forall i, a, t \tag{4}$$

$$x^t_{i,a} = 0, \quad \forall i, a, t \in T^0_{i,a} \tag{5}$$

$$x^t_{i,a} \geq 0, \quad \forall i, a, t \tag{6}$$

where $f(l_t)$ represents the unit electricity (generation) cost at time t, which is a monotone increasing function of the total electricity consumption l_t at time t. In the SO model, the objective in (1) is for the central controller to minimize the total electricity cost required to serve all users. Furthermore, constraints (2) calculate the total energy consumption l_t at time t by all users and constraints (3) ensure that user i's energy demand for appliance a is met. In addition, constraints (4) state that the total energy used by user i's appliance a during each time interval does not exceed $E_{i,a}$, an upper bound due to technical specification. Finally, constraints (5)

22

ensure that user i does not use appliance a at any time interval $t \in T_{i,a}^0$.

Theorem 1. *If $g(z) = f(z)z$ is strictly convex, then the SO model has a unique global solution l^*.*

Proof. Let

$$\mathcal{F} = \{l_t | (2) - (6)\}. \tag{7}$$

Clearly, this feasible region $\mathcal{F}$ is a convex, closed and bounded set. Thus, any local minimum is the global minimum and the uniqueness of the global minimum follows immediately from the strict convexity of the objective function $\sum_{t=1}^{T} g(l_t)$ (see e.g., [65]). ∎

While the above theorem shows the uniqueness of the optimal load vector l_t^* when $g(\cdot)$ is strictly convex, individuals' energy consumption vector $x^{*t}_{i,a}$ may not be unique under the same condition. Below is a counter example.

Consider a system with two users ($n = 2$), two appliances ($|\mathcal{A}| = 2$) and four time intervals ($T = 4$). The demand profiles are: $D_{1,1} = 7, D_{1,2} = 3, D_{2,1} = 6$, and $D_{2,2} = 4$. The Upper bounds are: $E_{1,1} = 3, E_{1,2} = 1, E_{2,1} = 4$, and $E_{2,2} = 3$. The unacceptable usage window $T_{i,a}^0 = \emptyset$ for $i = 1, 2$ and $a = 1, 2$. Suppose $f(l_t) = 10 + 3l_t$, then $g(l_t) = 3l_t^2 + 10l_t$ is strictly convex. The optimal load profile for the SO model is $l_1^* = 6, l_2^* = 6.5, l_3^* = 6.5$, and $l_4^* = 1$. One can easily verify that the following two consumption profiles $\breve{x}_{i,a}^t$ and $\tilde{x}_{i,a}^t$ both yield this optimal load profile.

$$\begin{vmatrix} \breve{x}_{1,1}^1=3, & \breve{x}_{2,2}^1=3, & \tilde{x}_{1,1}^1=3, & \tilde{x}_{2,2}^1=3, \\ \breve{x}_{1,1}^2=1.7875, & \breve{x}_{1,2}^2=1, & \tilde{x}_{1,1}^2=2, & \tilde{x}_{1,2}^2=1, \\ \breve{x}_{2,1}^2=2.7125, & \breve{x}_{2,2}^2=1, & \tilde{x}_{2,1}^2=2.5, & \tilde{x}_{2,2}^2=1, \\ \breve{x}_{1,1}^3=2.2125, & \breve{x}_{1,2}^3=1, & \tilde{x}_{1,1}^3=2, & \tilde{x}_{1,2}^3=1, \\ \breve{x}_{2,1}^3=3.2875, & \breve{x}_{1,2}^4=1, & \tilde{x}_{2,1}^3=3.5, & \tilde{x}_{1,2}^4=1. \end{vmatrix}$$

The SO model assumes a centralized decision system where the central area controller in the power distribution network wishes to coordinate energy consumption for all of its subscribers. Thus, the SO model provides an energy consumption profile with the least electricity cost. On the other hand, in practice

each subscriber may be more interested in their own electricity usage, not so much in others or even the average usage for the entire system. Thus, a user equilibrium model is suitable for describing the individual subscriber's energy consumption behavior.

3.3 User Equilibrium Model

In modeling a user's decision on when and how much to use his/her appliances, we consider not only cost but also the convenience for the user to be able to use an appliance during his/her preferred times. Thus, the user equilibrium model assumes each user i maximizes the following payoff or utility:

$$U_i = -\left[\sum_{t=1}^{T} f(l_t) \cdot l_i^t\right] + u_i(\mathbf{x_i}) \tag{8}$$

where l_i^t is the total electricity consumption by user i at time t, and $\mathbf{x_i}$ is the electricity usage profile of user i, a vector of $x_{i,a}^t$ for all appliances and time periods. In this payoff U_i, the first term represents the total energy cost, thus the disutility, for user i, and the second term defines the convenience experienced by user i, calculated by his/her personal utility function $u_i(\cdot)$ in terms of monetary value. In general, $u_i(\mathbf{x_i})$ can incorporate different monetary values or functions toward different appliances and time periods, e.g., $u_i(\mathbf{x_i}) = \sum_{\mathbf{a}\in\mathcal{A}}\sum_{\mathbf{t}\in\mathbf{T}} \pi_{\mathbf{i,a}}^{\mathbf{t}}\nu_{\mathbf{i,a}}^{\mathbf{t}}(\mathbf{x_{i,a}^t})$, where $\pi_{i,a}^t$ and $\nu_{i,a}^t$ are the monetary value of convenience and the utility function for user i to use appliance a at time t, respectively. Furthermore, the reason, for a user to take into account the unit generation cost to calculate his/her total consumption cost, is the wide use of smart electricity meters which enable the user-to-generator and user-to-user communication in the smart grid. Hence, in a distributed manner, each user solves the following user's problem:

$$\text{UO}_i: \quad \max \quad U_i = -\left[\sum_{t=1}^{T} f(l_i^t + l_{i-}^t) \cdot l_i^t\right] + u_i(\mathbf{x_i}) \tag{9}$$

$$\text{s.t.} \quad l_i^t = \sum_{a \in A} x_{i,a}^t, \quad \forall t \tag{10}$$

$$\sum_{t=1}^{T} x_{i,a}^t = D_{i,a}, \quad \forall a \tag{11}$$

$$x_{i,a}^t \le E_{i,a}, \quad \forall a, t \tag{12}$$

$$x_{i,a}^t = 0, \quad \forall a, t: t \in T_{i,a}^0 \tag{13}$$

$$x_{i,a}^t \ge 0, \quad \forall a, t \tag{14}$$

The UO model is for each user i to maximize his/her payoff assuming the knowledge of others' usage profile $\mathbf{x_{i-}} \triangleq \{\mathbf{x_{j,a}^t}\}_{\mathbf{a,j \neq i}}$, and the decision variables only pertain to user i's energy consumption profile $x_{i,a}^t$ and the resulting load profile l_i^t. Thus, the objective (9) for user i is to minimize the total disutility, i.e., the energy cost less the convenience-based utility. Note that in calculating the energy cost, the generation cost function is rewritten as $f(l_t) = f(l_i^t + l_{i-}^t)$ in order to distinguish user i's decision variable l_i^t from the input parameter l_{i-}^t. Constraints (10)-(14) for the UO model are similar to (2)-(6) in the SO model. Finally, if each user solves his/her own UO_i, then the system of n user problems, i.e., $\{\text{UO}_i\}_{i=1,\cdots,n}$, may reach an equilibrium defined below.

Definition 2. *Let* $X_i = \{\mathbf{x_i}|(\mathbf{10}) - (\mathbf{14})\}$ *be the set of feasible consumption profiles and* $\mathbf{x} \triangleq \{\mathbf{x_i}\}_{\mathbf{i=1,\cdots,n}}$ *be the usage profile for an n-user system. Then,* $\mathbf{x}^*$ *is at user equilibrium if and only if each user i does not have the incentive to unilaterally change his/her optimal consumption profile* $\mathbf{x_i^*}$, *i.e.,*

$$U_i(\mathbf{x_i^*}; \mathbf{x_{i-}^*}) \ge \mathbf{U_i}(\mathbf{x_i}; \mathbf{x_{i-}^*}), \forall \mathbf{x_i} \in \mathbf{X_i}, \ \mathbf{i = 1, \cdots, n}. \tag{15}$$

Theorem 3. *If $g(z) = f(z)z$ is convex and the utility function u_i is concave for all user i, then there exists a user equilibrium consumption profile* $\mathbf{x}^*$ *that satisfies (15).*

25

Proof. Recall that the simultaneous strategy space $\mathcal{F}$ in (7) is a convex, closed and bounded set. Because $g(l_i^t)$ is convex with respect to l_i^t, u_i is concave with respect to $x_{i,a}^t$, and the linear relationship between l_i^t and $x_{i,a}^t$ as defined in (10), the individual's payoff function $U_i = -\sum_t g(l_i^t) + u_i$ is concave with respect to $x_{i,a}^t$. Thus, from Theorem 1 in Rosen [66], a user equilibrium that satisfies (15) exists. ∎

Theorem 4. *If $g(z) = f(z)z$ is strictly convex and the utility function u_i is strictly concave for all user i, then there exists a unique user equilibrium consumption profile $\mathbf{x}^*$ that satisfies (15).*

Proof. Because g is strictly convex with respect to l_i^t, Theorem 2 in Rosen [66] guarantees the uniqueness of the l_i^t part, although not necessarily the $x_{i,a}^t$ part, of the equilibrium solution. On the other hand, the strict convavity of u_i implies the uniqueness of $x_{i,a}^t$ in the equilibrium solution, again due to Theorem 2 in Rose [66]. Therefore, the equilibrium solution $(l_i^t, x_{i,a}^t)$ must be unique. ∎

Theorem 5. *Suppose that $g(z) = f(z)z$ is convex and the utility function u_i is concave for all user i. Further, if the unit cost function f is constant, then the SO model and the UO model with $u_i = 0$ for all i yield the same optimal solution.*

Proof. Let the Karush−Kuhn−Tucker (KKT) conditions (e.g., Bazaraa et al. [65]) for the SO system be KKTSO, and the KKT conditions for UO_i with $u_i = 0$ $(i = 1, \cdots, n)$ be KKTUO(i). Then, it is fairly straightforward that KKTSO and $\{$KKTUO(i)$\}_{i=1,\cdots,n}$ are equivalent when the unit cost function f satisfies $f'(z) = 0$. Thus, if $f = c_0$ is a constant, then the two problems have the optimal solution. ∎

In order to characterize the equilibrium solution $\mathbf{x}^*$, one introduces the Lagrangian multipliers ρ_t^i, λ_a^i, $\gamma_{t,a}^i$, and $\xi_{t,a}^i$ for constraints (10), (11), (12), and (13) in user i's model UO_i, respectively. Consequently, the user equilibrium problem

$\{UO_i\}_{i=1,\cdots,n}$ reduces to the following mixed complementarity problem (MCP),

$$
\begin{aligned}
0 \le x_{i,a}^t \perp \quad & \rho_t^i = u_i'(x_{i,a}^t) + \lambda_a^i + \gamma_{t,a}^i \\
& \quad + \xi_{t,a}^i - \mu_{t,a}^i, && \forall i,a,t : t \in T_{i,a}^0 \\
0 \le x_{i,a}^t \perp \quad & \rho_t^i = u_i'(x_{i,a}^t) + \lambda_a^i + \gamma_{t,a}^i \\
& \quad - \mu_{t,a}^i, && \forall i,a,t : t \in T \setminus T_{i,a}^0 \\
0 \le l_i^t \perp \quad & \rho_t^i = -l_i^t f'(l_i^t + l_{i-}^t) \\
& \quad - f(l_i^t + l_{i-}^t), && \forall i,t \\
0 \le \gamma_{t,a}^i \perp \quad & E_{i,a} - x_{i,a}^t \ge 0, && \forall i,a,t \\
\rho_t^i \perp \quad & l_i^t = \sum_{a \in A} x_{i,a}^t, && \forall i,t \\
\lambda_a^i \perp \quad & \sum_{t=1}^T x_{i,a}^t = D_{i,a}, && \forall i,a \\
\xi_{t,a}^i \perp \quad & x_{i,a}^t = 0, && \forall i,a,t : t \in T_{i,a}^0
\end{aligned}
\tag{16}
$$

where the "$\perp$" sign in $\mathbf{a} \perp \mathbf{b}$ (for $\mathbf{a}, \mathbf{b} \in \mathbf{R^n}$) signifies that componentwise $a_i b_i = 0$ for $i = 1, \cdots, n$. Such a property is referred to as a_i is "complementary" to b_i. In other words, the above MCP defines the KKT optimality conditions for the equilibrium solution $\mathbf{x}^*$ and associated Lagrangian multipliers. Note that formulating the KKT conditions in a MCP form allows for an efficient solution by the PATH solver [67] offered by the nonlinear program software GAMS [68] used in this study.

3.4 Computational Results

In this section, we discuss the results from our numerical simulations for evaluating the proposed system and user equilibrium models. Both SO and UO models were implemented in GAMS [68], a state-of-the-art modeling language for nonlinear programs, where the SO model was solved by the CONOPT solver [69] and the UO model was solved by the PATH solver [67]. All experiments and simulations were run on a 16-core dual Opteron CPU server with 32GB of memory running openSUSE 11 Linux.

Common to all numerical examples and test instances is the way we model

the convenience experienced by users. To do so, we introduce the notion of *preferred usage window*. The "preferred usage window," denoted as $T_{i,a}^1 \subseteq T$, represents a set of time periods when user i prefers to use appliance a. Note that associated with user i and appliance a, there is also a time window $T_{i,a}^0 \subseteq T$ when the user does not wish to use appliance a. Thus, $T_{i,a}^0 \cap T_{i,a}^1 = \emptyset$ holds. Using the "preferred usage window", the (second) convenience term as required in the utility function (8) is defined as

$$u_i(\mathbf{x_i}) = \pi_\mathbf{i} \sum_\mathbf{a} \left(\frac{\mathbf{p_{i,a}}}{\mathbf{D_{i,a}}} \right)^{1/2} \tag{17}$$

where π_i is the utility coefficient representing the monetary value of convenience for user i and $p_{i,a} = \sum_{t \in T_{i,a}^1} x_{i,a}^t$ is the amount of electricity from appliance a used by user i during his/her preferred usage window. Subsequently, u_i is the utility value based on the proportion of total demand for user i that is fulfilled during preferred usage window. We note that this specific form of utility function is widely used in economics and decision analysis for modeling users preference (e.g., Keeney and Raiffa [70] and Clemen [71]).

Without loss of generality, in this section, we simplify the presentation by using $[\alpha, \beta]$ to denote $T \setminus T_{i,a}^0$ and $[\alpha_p, \beta_p]$ to denote $T_{i,a}^1$. Thus, $1 \le \alpha \le \alpha_p \le \beta_p \le \beta \le 24$.

3.4.1 Relationship between UO and SO consumption profiles

To begin the evaluation of the proposed user equilibrium model, we illustrate the difference between the outcomes of the system model and the user equilibrium model in which utilities for all users π_i equal zero. The latter is because we would like to study without introducing the notion of "convenience utility", how the proposed UO model performs against the SO model. In section 3.4.3, we discuss extensively the UO model with non-zero utilities.

Consider two simple numerical examples both with two users, two appliances and four time intervals. The attributes of the two users in these two examples are

summarized in Table 1, where α, β, α_p and β_p are as defined above. One notes that the two examples only differ by the values for β, i.e., $\beta_{\text{ex1}} \neq \beta_{\text{ex2}}$. The purpose of this design will become clear later in this subsection.

TABLE 1
Parameter Values for Examples 1 and 2

user	appliance	$D_{i,a}$	$E_{i,a}$	α	β_{ex1}	β_{ex2}	α_p	β_p
1	1	7	3	1	3	3	1	1
1	2	3	1	2	4	4	4	4
2	1	6	4	2	4	3	3	3
2	2	4	3	1	3	2	2	2

In both examples, for simplicity, we use the unit electricity price $f(l_t) = 10 + 3l_t$. Then, solving the SO and UO models for Example 1 yields the optimal consumption profiles displayed in Table 2, where the SO solution is denoted by $\bar{x}_{i,a}^t$ and the UO solution by $\hat{x}_{i,a}^t$. Note again the UO solution is obtained by setting utilities $\pi_1 = \pi_2 = 0$.

Several observations can be made from Table 2. First, the optimal solutions to the SO and UO models (the latter with zero utilities for both users) are different. This necessitates the study of the user equilibrium model, while using the system model as a benchmark. Second, the total electricity cost for the SO solution is 500.00, less than the that for the UO solution (502.25). This is consistent with the general knowledge that in a non-cooperative game the equilibrium solution does not necessarily yield the maximal system-wide payoff. Third, comparing the costs for user 1 under SO and UO (250 vs. 254.5), he/she is better off in the system solution. However, user 2 is better off in the equilibrium solution (250 vs. 247.75). This suggests that the concern of "making everybody better off" exists for the proposed equilibrium model.

Furthermore, it is interesting to observe the results for Example 2 in Table 3. With slight modifications to the value of β, Example 2 presents a different comparison between the SO and UO solutions. Notably, the two models yields the

TABLE 2

Optimal UO and SO Solutions for Example 1

user	appliance	time	SO-$\bar{x}_{i,a}^t$	UO-$\hat{x}_{i,a}^t$
1	1	1	2.8143	3.0000
1	1	2	2.1761	2.0000
1	1	3	2.0096	2.0000
1	1	4	0.0000	0.0000
1	2	1	0.0000	0.0000
1	2	2	1.0000	1.0000
1	2	3	1.0000	1.0000
1	2	4	1.0000	1.0000
aggregate cost for user 1			250.00	254.50
2	1	1	0.0000	0.0000
2	1	2	0.5004	1.7500
2	1	3	1.4996	1.0000
2	1	4	4.0000	3.2500
2	2	1	2.1857	2.2500
2	2	2	1.3234	0.5000
2	2	3	0.4908	1.2500
2	2	4	0.0000	0.0000
aggregate cost for user 2			250.00	247.75
aggregate cost for the system			500.00	502.25

same total electricity cost 564.50, although from different solutions.

Collectively, Examples 1 and 2 suggest that although in most cases the SO and UO models yield different solutions, it is possible that they lead to the same system-wide optimal cost.

3.4.2 Data generation for extended testing

The data used in extended numerical experiments include two parts. The first part characterizes users profiles, i.e., appliances a, appliances' demand $D_{i,a}$ and maximum amount of energy during a unit time for appliances $E_{i,a}$. In particular, we use dishwasher, plug-in hybrid electric vehicle (PHEV) and air conditioner as prototypical appliances 1, 2 and 3, respectively. The daily demand of each appliance

TABLE 3
Optimal UO and SO Solutions for Example 2

user	appliance	time	SO-$\bar{x}_{i,a}^t$	UO-$\hat{x}_{i,a}^t$
1	1	1	3.0000	3.0000
1	1	2	1.7875	2.0000
1	1	3	2.2125	2.0000
1	1	4	0.0000	0.0000
1	2	1	0.0000	0.0000
1	2	2	1.0000	1.0000
1	2	3	1.0000	1.0000
1	2	4	1.0000	1.0000
aggregate cost for user 1			274.00	274.00
2	1	1	0.0000	0.0000
2	1	2	2.7125	2.5000
2	1	3	3.2875	3.5000
2	1	4	0.0000	0.0000
2	2	1	3.0000	3.0000
2	2	2	1.0000	1.0000
2	2	3	0.0000	0.0000
2	2	4	0.0000	0.0000
aggregate cost for user 2			290.50	290.50
aggregate cost for the system			564.50	564.50

follows a uniform distribution in the range of 0.8 and 1.2 times of the typical daily consumption as reported in [72]. Similarly, the upper bound $E_{i,a}$ is also uniformly distributed between 0.8 and 1.2 times of the typical hourly consumption for each appliance. For example, the typical daily and hourly consumption of a dishwasher is 5.76 kWh and 1.44 kW. Thus, the daily demand for dishwashers $D_{i,a=2}$ is set to follow the uniform distribution between (4.6, 6.9), while the upper bound $E_{i,a}$ follow the uniform distribution between (1.152, 1.728).

The second part of the data involves the unit cost $f(l_t)$, as a function of the load l_t at any time t. We choose to use the linear unit cost function $f(l_t) = c_0 + cl_t$ in our simulation, which leads to a quadratic total cost function $f(l_t)l_t = c_0 l_t + cl_t^2$. The latter is consistent with the commonly used quadratic fuel cost in modeling

power generation. Our choice of c_0 and c is based on the DoE census report on the retail price of electricity for 50 states in the U.S. (see e.g., [73]), with an average of 10 cents per KWh. Given an average gap of approximately 17% between the generation and retail costs among the 50 states, we determine that $c_0 = 7.43$ cents and $c = 1.55$ cents per kWh.

3.4.3 Impacts of various users groups on the equilibrium

This section reports extensive sensitivity analysis for the UO and SO models based on variations to the baseline scenario summarized in Table 4. In words, there are two users, three appliances and 24 time intervals. Setting $[\alpha, \beta] = [1, 24]$ allows both users to be able to use all three appliances any time. Note that both users share the same profile with respect to demand $D_{i,a}$ and upper bound $E_{i,a}$.

TABLE 4
Parameter Values for Baseline Scenario

user	appliance	$D_{i,a}$	$E_{i,a}$	α	β	α_p	β_p
1	1	6.0753	1.1703	1	24	3	10
1	2	13.0305	3.2684	1	24	4	9
1	3	18.5805	2.3439	1	24	5	15
2	1	6.0753	1.1703	1	24	3	13
2	2	13.0305	3.2684	1	24	4	12
2	3	18.5805	2.3439	1	24	5	18
Utilities: $\pi_1 = \pi_2 = 5$							

Given special attention is the design of the "preferred usage window" for users 1 and 2. User 1's preferred usage window for using appliance 1 is [3,10], three hours shorter than that for user 2 ([3,13]). Similar observations can be made for appliances 2 and 3 between user 1 and user 2. Practically, user 1 represent those with less flexibility on their preferred time, while user 2 represents those with more flexibility. One focus of our subsequent sensitivity analysis is how these two groups may affect the equilibrium solution differently.

TABLE 5
Aggregate Measures vs. Utility for User 2

Case	π_1	π_2	SO		UO	
			Cost	Disutility	Cost	Disutility
1	5	5	926.9182	892.1366	927.2219	877.7099
2	5	15	926.9182	871.6919	927.9788	824.936
3	5	25	926.9182	851.2473	929.0919	769.9865
4	5	35	926.9182	830.8027	930.1639	713.6645
5	5	45	926.9182	810.3581	931.4551	656.1449
6	5	55	926.9182	789.9134	932.8704	597.5788
7	5	65	926.9182	769.4688	934.3944	538.0829
8	5	75	926.9182	749.0242	936.0158	477.7459
9	5	85	926.9182	728.5795	937.6911	416.7896
10	5	95	926.9182	708.1349	939.3973	355.3186
11	5	100	926.9182	697.9126	940.2457	324.4142

Table 5 displays the aggregate measures for the SO and UO solutions when varying the utility coefficient for user 2, i.e., π_2. Recall that π_i represents the user i's monetary value for the convenience utility. The aggregate measures include the total electricity cost as well as the total disutility (the total electricity cost minus the total convenience utilities), for both the SO and UO solutions. Note that the SO is independent of utility coefficients, thus the electricity cost for the SO solution is fixed regardless values of π_i. From Table 5, as user 2's monetary value of convenience increases from 5 (the baseline value) to 100, the system-wide electricity cost for the UO solution increases from 927.2219 to 940.2457. On the other hand, the disutility of the UO solution decreases from 877.7099 to 324.4142, which indicates the increase of the electricity cost is dominated by the increase of the convenience. Similarly, the disutility of the SO solution decreases (from 892.1366 to 697.9126) as well when π_2 increases. Finally, for all cases 1 through 11, the disutility of the UO solution is consistently more appealing, i.e., less than that of the SO solution. This validates the user equilibrium model in that the user model provides the best utility for users, whereas the system model provides the best cost for the

central controller.

<div align="center">

TABLE 6
Aggregate Measures vs. Utility for User 1

Case	π_1	π_2	SO		UO	
			Cost	Disutility	Cost	Disutility
1	5	5	926.9182	892.1366	927.2219	877.7099
2	15	5	926.9182	843.0180	928.1562	828.5164
3	25	5	926.9182	793.8994	929.5449	776.5224
4	35	5	926.9182	744.7807	931.2226	722.3303
5	45	5	926.9182	695.6621	933.1827	666.2387
6	55	5	926.9182	646.5435	935.3919	608.4622
7	65	5	926.9182	597.4249	937.8233	549.1673
8	75	5	926.9182	548.3063	939.5396	490.078
9	85	5	926.9182	499.1877	940.0007	432.5708
10	95	5	926.9182	450.0691	941.3545	373.4698
11	100	5	926.9182	425.5098	942.2829	343.3592

</div>

Similarly, Table 6 shows the effect of increasing user 1's utility coefficient. Again, as π_1 increases, the electricity cost for the UO solution increases and the disutility decreases for both the UO and the SO solutions.

More interestingly, when assemble the cost-related results in Tables 5 and 6 together, Figure 3 indicates that user 1 and user 2 have different impact on the system cost at equilibrium. In Figure 3, the "□" series corresponds to the system-wide electricity cost with varying π_1, and the '◇' series with varying π_2. From the figure, the '□' series is consistently above the '◇' series, implying that increasing the utility value for user 1, who has less flexibility on the preferred usage window, has larger effect than increasing that for user 2, who has more flexibility. To illustrate, point A in the '◇' series in Figure 3 represents the case where $\pi_1 = 5$ and $\pi_2 = 55$ and point B in the '□' series represents the case where $\pi_1 = 55$ and $\pi_2 = 5$. Clearly, $\pi_1 = 55$ yields a higher electricity cost (935.3919) than does $\pi_2 = 55$ (932.8704), when compared to the baseline cost for the UO solution (927.2219).

Similarly, Figure 4 depicts different impact of user 1 and user 2 on the
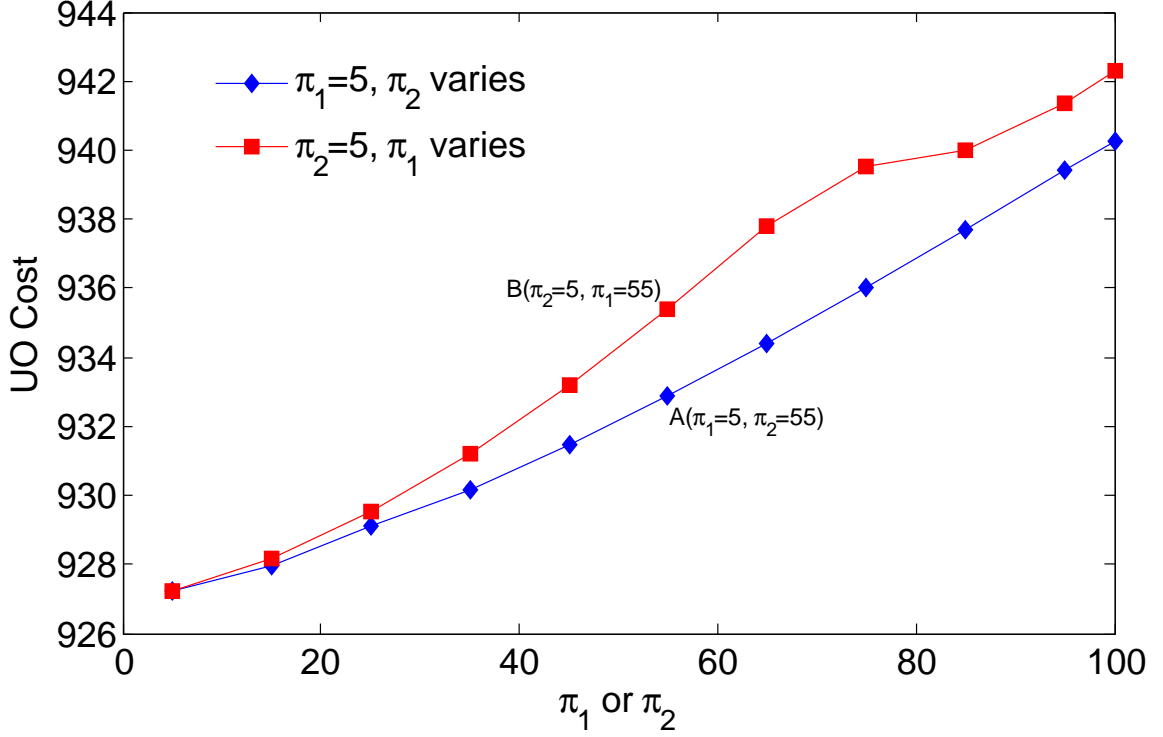
Figure 3. UO Cost vs. Utility

disutility of the equilibrium. Again, the "□" series corresponds to varying π_1 and the '◇' series corresponds to varying π_2. One notes that the UO disutility is consistently higher when varying π_1 than when varying π_2. This is because the increased UO cost (from Figure 3) outweighs the increased convenience.

Finally, we examine the convenience experienced by users for the SO and UO solutions under various scenarios. Recall that the (second) convenience term in the utility function (8) is defined as $u_i(\mathbf{x_i}) = \pi_\mathbf{i} \sum_\mathbf{a} \left(\frac{\mathbf{p_{i,a}}}{\mathbf{D_{i,a}}}\right)^{\mathbf{1/2}}$, where $p_{i,a} = \sum_{t \in T^1_{i,a}} x^t_{i,a}$ is the amount of electricity used from appliance a by user i during the preferred usage window. In subsequent analysis, we define the "average percentage of preferred usage" (APPU) to be $APPU = \frac{\sum_{i=1}^n p_i}{n}$, where $p_i = \frac{\sum_{a \in \mathcal{A}} \frac{p_{i,a}}{D_{i,a}}}{|\mathcal{A}|}$. In other words, p_i is user i's average percentage of preferred usage over all appliances, and APPU is the average of p_i over all users.
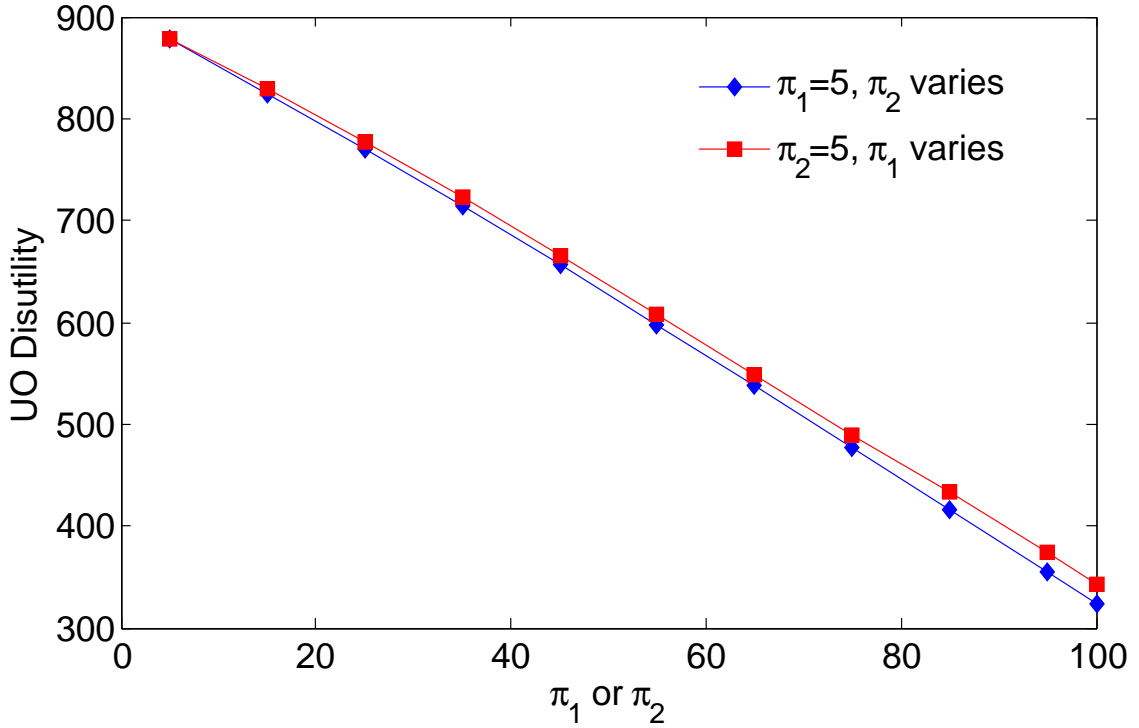
Figure 4. UO Disutility vs. Utility

Figure 5 depicts how p_1 (the "◇" series), p_2 (the "□" series) and APPU (the "△" series) respond to the increase of user 2's utility coefficient π_2. Clearly, when π_2 increases, the average percentage of preferred usage (over three appliances) for user 2 increases, again validating the UO model from the perspective of the convenience utility. On the other hand, the APPU for user 1 decreases as shown in the "◇" series. Finally, looking at the average APPU for two users in the "△" series, it is relatively stable but with a slight increasing trend.

Figure 6 depicts how p_1 (the "×" series), p_2 (the "∗" series) and APPU (the "●" series) respond to the increase of user 1's utility coefficient π_1. In this case, the three series have the same trend as in Figure 5 except that they intercept around $\pi_1 = 25$, where the two users have the same APPU. Finally, Figure 7 compares how the APPU for both users is affected by the change of π_1 and π_2. From this figure,
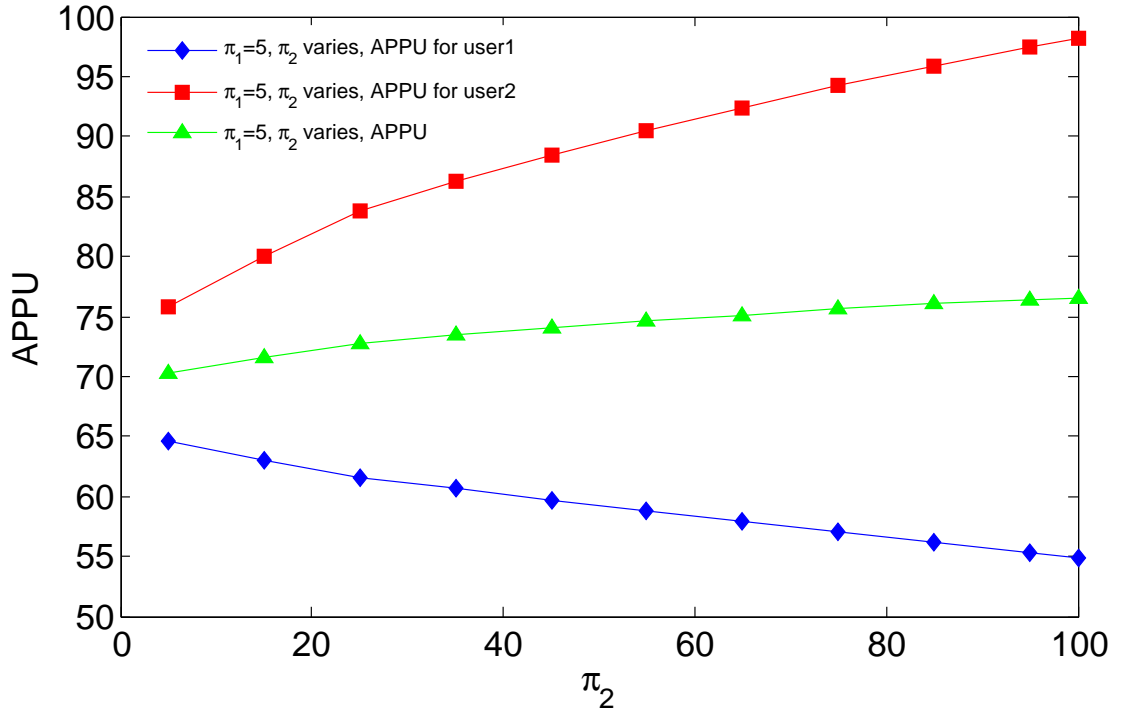
Figure 5. Average Percentage of Preferred Usage vs. Utility 2

the system APPU is higher in the situation where π_2 is fixed and π_1 increases, compared to the situation where π_1 is fixed and π_2 increases. This suggests that user 1 has more influence on the equilibrium in terms of the convenience utility, which is consistent with previous observations in terms of the system costs.

We also study the effect of the changing preferred usage window, i.e., α_p and β_p, on the equilibrium solution. The baseline scenario in this experiment is the same as the baseline in previous sensitivity studies except for $\pi_1 = \pi_2 = 50$. Table 7 displays the SO and UO solutions for four cases. Case 1 corresponds to the baseline. Case 2 is constructed from the baseline by spreading out user 1's preferred windows for the three appliances so that they do not overlap with each other. As a result, the electricity cost and disutiliuty for the UO solution decrease from 949.6517 to 936.6132, and from 412.4361 to 354.4051, respectively. This implies that if a user is
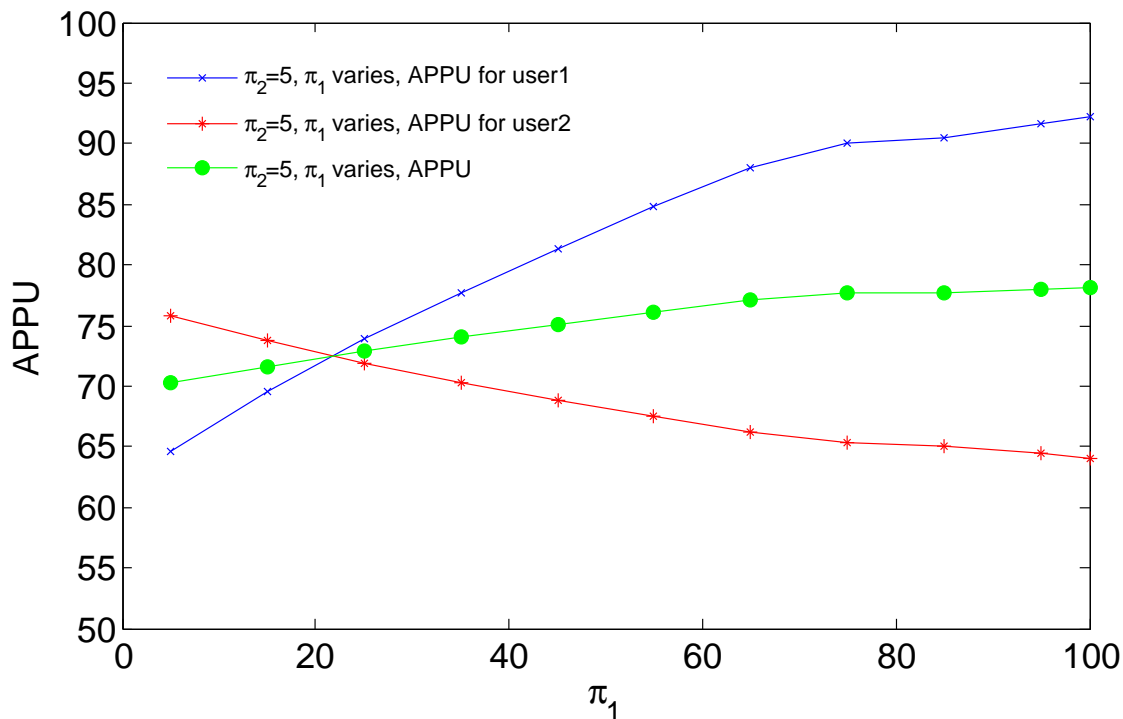
Figure 6. Average Percentage of Preferred Usage vs. Utility 1

willing to spread out his/her preferred usage window between various appliances, the entire system is better off at the equilibrium. Compared to case 1, case 3 spreads out the preferred usage window for user 2, although these intervals still overlap but to lesser degree than in case 1. Similar to case 2, in case 3 the total cost and disutility decreases from 949.6517 to 932.4823, and from 412.4361 to 356.4647, respectively, when compared to the baseline case 1. Finally, case 4 represents a scenario where there is a large overlap amongst all six preferred usage windows for three appliances and two users. Consequently, the system is worse off at equilibrium, experiencing higher cost (952.4703 vs. 949.6517) and disutility (433.5812 vs. 412.4361).
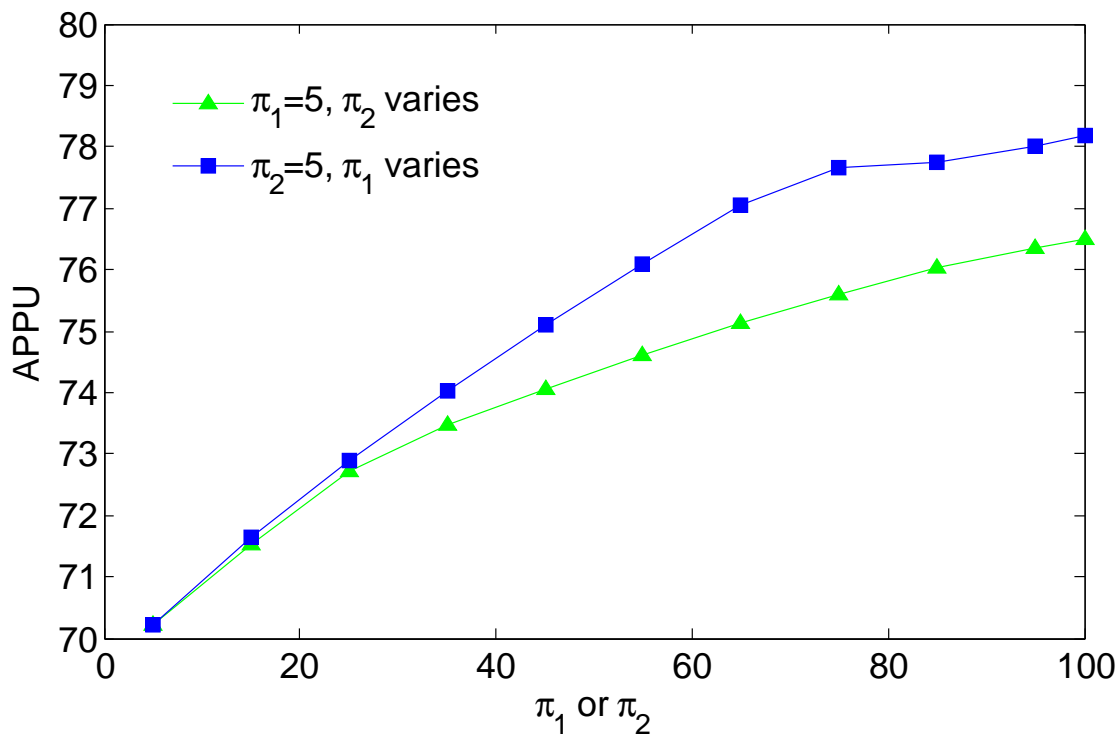
Figure 7. Average Percentage of Preferred Usage vs. Utility

TABLE 7
UO Solutions for Various Preferred Windows

Case	Appliance	User 1 $[\alpha_p, \beta_p]$	User 2 $[\alpha_p, \beta_p]$	UO Cost	UO Disutility
1	1	[3,10]	[3,13]	949.6517	412.4361
	2	[4,9]	[4,12]		
	3	[5,15]	[5,18]		
2	1	[1,8]	[3,13]	936.6132	354.4051
	2	[9,14]	[4,12]		
	3	[14,24]	[5,18]		
3	1	[3,10]	[1,11]	932.4823	356.4647
	2	[4,9]	[16,24]		
	3	[5,15]	[11,24]		
4	1	[3,10]	[3,13]	952.4703	433.5812
	2	[3,8]	[3,11]		
	3	[3,13]	[3,16]		

CHAPTER 4

A PRICING MODEL FOR DEMAND RESPONSE WITH CONSUMER PREFERENCE

In Chapter 3, we consider users possible preference on convenience over cost-saving under the real-time pricing in smart grid. Through numerical analysis, we found that the UE solution is always different from the SO solution. In terms of the total cost and peak load reduction, it is always worse than the SO model. In this chapter, we focus on developing a pricing framework that can make the system model and the user equilibrium model share the same users energy consumption profile. The objective of the system model is different from the one in Chapter 3. The new objective of the system model to maximize the social welfare, which is the convenience-based utility function minus the electricity generation cost function.

Li et al. [63] use dynamic pricing to coordinate the customers' demand responses to the benefit of individual customers and the overall system. Two models are established. In their utility's (system) model, they assume that the utility company is regulated so that instead of maximizing its profit through selling electricity to end users, its objective is to maximize the social welfare. On the other hand, in their customer's or user equilibrium model, each customer aims to maximize his/her own benefit. Both objectives include two parts: a utility function and a cost function. The utility function for the two models are identical while the cost functions are different. Let $x_{i,a}^t$ be the energy consumption by customer i on appliance a at time t, then the total energy drawn by all consumers at time t is $Q = \sum_{i,a} x_{i,a}^t$. the system model assumes the cost function $C(Q,t)$ to be convex and increasing in Q for each t. On the other hand, the user equilibrium model defines

the cost function to be the bill charged to individual user i as $B(Q_i, t) = p(t) \sum_a x^t_{i,a}$, where $p(t)$ is the electricity rate at time t. They show that the pricing scheme defined by $p^*(t) = C'(\sum_i Q^*_i(t)) \geq 0$ for each time t can render the equilibrium solution to be identical to the system solution.

In their paper [63], Li et al. show the existence of a pricing $p^*(t)$ that would reconcile the optimal solutions to the equilibrium and system models. They do not discuss the uniqueness of either the pricing or the equilibrium solution. On the other hand, in the area of traffic networks, congestion toll pricing has been studied for more than a decade [74]. Bergendorff et al. [74] prove that in order to reproduce a fixed choice of system solution, alternative tolls exist. Furthermore, they show that these alternative valid toll vectors can be characterized by a polyhedron, or expressed in a linear system of equalities and inequalities. Thus, in this study we investigate: 1) the nonuniqueness of the demand response pricing under which the user equilibrium solution would reproduce the system optimal solution; 2) the nonuniqueness of the user equilibrium solutions; 3) the development of a framework that optimizes demand response pricing with respect to various objectives, and solution algorithms for the demand response pricing optimization problems.

In this chapter, we first develop a system model for social welfare maximization (SOS) and a game theoretical user equilibrium model for pricing (UEP). We show that the pricing scheme that would induce the equilibrium solution to be identical to the system solution is not unique. With a desired and pre-determined system optimal solution, we show that there exist alternative pricing schemes to achieve the desired objective. In this way, the pricing scheme becomes adjustable and the utility company may customize the pricing scheme to achieve proper objectives, e.g. maximize the profit, minimize the maximum price, etc. Second, we also show that at the equilibrium, the user's solution is not unique. The users' energy consumption pattern is supposed to follow the optimal solution of system model. But when the UEP has multiple solutions under a given pricing

scheme, the design objective will always get worse and the obtained pricing scheme may not be the most desirable. Third, by adopting the risk-averse Second Best Toll Price (SBTP) concept in [75], we propose a bi-level model to solve the problem, which the design objective is worse off when the UEP solution varies under a given pricing scheme. Instead of designing the pricing scheme for the best case scenario, we set the pricing under the worst case scenario. In this case, the design objective will always better off.

The remainder of this chapter is organized as follows. Sections 4.1 and 4.2 present the system optimum and user equilibrium models respectively. Section 4.3 describes a pricing frame work to reproduce the system optimal solution for user equilibrium model. Section 4.4 discusses results from numerical experiments and Section 4.5 demonstrate the non-uniqueness of the valid pricing scheme and that of the UEP solution. Section 4.6 formulates the demand response pricing optimization problem as a bi-level program, especially when the UEP solution is non-unique and a risk-averse pricing model is desired. In addition, discussions are also given on possible decomposition algorithms for the resulting demand response pricing optimization problem.

4.1 System Optimization Model of Maximizing Social Welfare

In our system model, instead of maximizing its profit through selling electricity to end customers, the utility company's objective is to maximize the social welfare. In the way of considering customers' convenience to use an appliance during his/her preferred times, the objective function is the total customers utility minus the utility cost of providing the electricity demanded by all customers. Consider a local area power system with n users and a set of appliances $\mathcal{A}$ for each user. Assume each user i has a daily energy demand $D_{i,a}$ for appliance $a \in \mathcal{A}$. We define a 24-hour daily cycle with $t \in T = \{1, 2, \cdots, 24\}$. Further, let $E_{i,a}$ be the maximum amount of energy consumed by user i on appliance a during one unit

time. In addition, define a set of preferred time intervals $T_{i,a}^1 \subset T$ during which user i prefers to use appliance a. Using this notation and letting decision variable $x_{i,a}^t$ be the amount of energy consumed on appliance a by user i at time t, the system optimal for social welfare maximization (SOS) model to maximizing social welfare for the utility company can be formulated as follows:

Utility's objective (max social welfare):

SOS:

$$\max_{x_{i,a}^t} \sum_i \pi_i \cdot \sum_a 2 \left(\frac{\sum_{t \in T_{i,a}^1} x_{i,a}^t}{D_{i,a}} \right)^{1/2} - \sum_{t=1}^T [(c_0 + c \cdot \sum_{i,a} x_{i,a}^t) \cdot \sum_{i,a} x_{i,a}^t] \quad (18)$$

s.t.

$$\lambda_a^i \cdots \quad \sum_t x_{i,a}^t = D_{i,a}, \quad \forall i, a \quad (19)$$

$$\gamma_{t,a}^i \cdots \quad x_{i,a}^t \le E_{i,a}, \quad \forall i, a, t \quad (20)$$

$$\mu_{t,a}^i \cdots \quad x_{i,a}^t \ge 0, \quad \forall i, a, t \quad (21)$$

In the SOS model, the objective (18) is for the utility company to maximize the total social welfare considering all users' utility. The first term in (18) represents the utility function of all users, in which π_i is the monetary value of the time-of-use convenience for user i. Specifically, the "utility" herein stands for the convenience users have experienced by being able to use their appliances at preferred times. The second term represents the unit electricity (generation) cost. As mentioned previously, at any given time t, this cost function is monotone increasing in the total electricity consumption $\sum_{i,a} x_{i,a}^t$ at time t. c_0 and c are the electricity generation cost coefficients. Furthermore, constraints (19) ensure that user i's energy demand for appliance a is met. Constraints (20) state that the total energy used by user i's appliance a during each time interval does not exceed $E_{i,a}$, an upper bound due to technical specification. Finally, constraints (21) ensure that all $x_{i,a}^t$ are non-negative.

Let $\lambda_{i,a}$, $\gamma_{i,a}^t \geq 0$ and $\mu_{i,a}^t \geq 0$ be the Lagrange multipliers of constraints (19) to (21), respectively. The Lagrange equation and the Karush-Kuhn-Tucker (KKT) system of the SOS model is as follows:

Lagrange Equation:

$$
\begin{aligned}
SL(x_{i,a}^t; \lambda, \mu, \gamma) = {}& \sum_{t=1}^T [(c_0 + c \cdot \sum_{i,a} x_{i,a}^t) \cdot \sum_{i,a} x_{i,a}^t] - \sum_i \pi_i \cdot \sum_a 2 \left(\frac{\sum_{t \in T_{i,a}^1} x_{i,a}^t}{D_{i,a}} \right)^{1/2} \\
& + \sum_{i,a} \lambda_{i,a} \cdot (\sum_{t=1}^T x_{i,a}^t - D_{i,a}) \\
& + \sum_{t,i,a} \gamma_{i,a}^t \cdot (x_{i,a}^t - E_{i,a}) \\
& - \sum_{t,i,a} \mu_{i,a}^t \cdot x_{i,a}^t
\end{aligned}
\tag{22}
$$

The KKT conditions for the system optimal model (KKTSOS):

$$
\sum_t x_{i,a}^t = D_{i,a}, \quad \forall i, a \tag{23}
$$

$$
x_{i,a}^t \leq E_{i,a}, \quad \forall i, a, t \tag{24}
$$

$$
-x_{i,a}^t \leq 0, \quad \forall i, a, t \tag{25}
$$

$\left(\frac{\partial SL}{\partial x_{i,a}^t} \mid_{t \in T_{i,a}^1} = 0 \right)$ $(c_0 + 2c \cdot \sum_{i,a} x_{i,a}^t) - \pi_i \cdot [(\sum_{t \in T_{i,a}^1} x_{i,a}^t) \cdot D_{i,a}]^{-1/2}$

$$
+ \lambda_{i,a} + \gamma_{i,a}^t - \mu_{i,a}^t = 0, \quad \forall i, a, t \tag{26}
$$

$\left(\frac{\partial SL}{\partial x_{i,a}^t} \mid_{t \notin T_{i,a}^1} = 0 \right)$ $(c_0 + 2c \cdot \sum_{i,a} x_{i,a}^t)$

$$
+ \lambda_{i,a} + \gamma_{i,a}^t - \mu_{i,a}^t = 0, \quad \forall i, a, t \tag{27}
$$

$$
(x_{i,a}^t - E_{i,a}) \cdot \gamma_{i,a}^t = 0, \quad \forall i, a, t \tag{28}
$$

$$
x_{i,a}^t \cdot \mu_{i,a}^t = 0, \quad \forall i, a, t \tag{29}
$$

$$
\gamma_{i,a}^t, \mu_{i,a}^t \geq 0, \quad \forall i, a, t \tag{30}
$$

The SOS model assumes a centralized decision system where the central area controller in the power distribution network wishes to coordinate energy consumption for all of its subscribers. Thus, the SOS model provides an energy consumption profile with the maximal social welfare. On the other hand, in practice each subscriber may be more interested in their own electricity usage, not so much in others or even the average usage for the entire system. Thus, a user equilibrium

model is suitable for describing the individual subscriber's energy consumption behavior.

4.2 User Equilibrium Model of Maximizing Own Benefit

Different from the SOS model, a user's decision is on when and how much to use his/her appliances. We consider only the convenience for this user to be able to use an appliance during his/her preferred times. Thus, the user equilibrium model assumes each user i maximizes the his/her own benefit or utility. Hence, in a distributed manner, each user solves the following user's problem:

Customer i's objective (max own benefit):

$$UEP_i: \quad \max_{y_{i,a}^t} \quad \pi_i \cdot \sum_a 2 \left(\frac{\sum_{t \in T_{i,a}^1} y_{i,a}^t}{D_{i,a}} \right)^{1/2} - \sum_{t=1}^T p(t) \cdot \left(\sum_a y_{i,a}^t \right) \tag{31}$$

s.t.

$$\alpha_{i,a} \cdots \quad \sum_t y_{i,a}^t = D_{i,a}, \quad \forall a \tag{32}$$

$$\beta_{i,a}^t \cdots \quad y_{i,a}^t \leq E_{i,a}, \quad \forall a, t \tag{33}$$

$$\rho_{i,a}^t \cdots \quad -y_{i,a}^t \leq 0, \quad \forall a, t \tag{34}$$

The UEP model is for each user i to maximize his/her payoff assuming the knowledge of time-of-use pricing scheme $p(t)$, and the decision variables only pertain to user i's energy consumption profile $y_{i,a}^t$. Thus, the objective (31) for user i is to maximize his/her own benefit, i.e., the electricity cost less the convenience-based utility. Note that in calculating the electricity cost, the pricing scheme $p(t)$ is designed by the utility company and informed to customers in advance. Constraints (32)-(34) for the UEP model are similar to (19)-(21) in the SOS model. Finally, if each user solves his/her own UEP_i, then the system of n user problems, i.e.,

$\{UE_i\}_{i=1,\cdots,n}$, may reach an equilibrium. Let $\alpha_{i,a}$, $\beta_{i,a}^t$ and $\rho_{i,a}^t$ be the Lagrange multipliers of constraints (32) to (34), respectively, the Lagrange equation and the KKT system of the UEP$_i$ model is shown as follows:

Lagrange Equation:

$$
\begin{aligned}
UL(y_{i,a}^t; \alpha, \beta, \rho) = \ & \sum_{t=1}^{T} p(t) \cdot \left(\sum_a y_{i,a}^t\right) - \pi_i \cdot \sum_a 2 \left(\frac{\sum_{t \in T_{i,a}^1} y_{i,a}^t}{D_{i,a}}\right)^{1/2} \\
& + \sum_a \alpha_{i,a} \cdot \left(\sum_t y_{i,a}^t - D_{i,a}\right) \\
& + \sum_{t,a} \beta_{i,a}^t \cdot (y_{i,a}^t - E_{i,a}) \\
& - \sum_{t,a} \rho_{i,a}^t \cdot y_{i,a}^t
\end{aligned}
\tag{35}
$$

The KKT conditions for the user equilibrium KKT(KKTUEP):

$$
\sum_t y_{i,a}^t = D_{i,a}, \quad \forall a \tag{36}
$$

$$
y_{i,a}^t \le E_{i,a}, \quad \forall a, t \tag{37}
$$

$$
-y_{i,a}^t \le 0, \quad \forall a, t \tag{38}
$$

$$
\left(\frac{\partial UL}{\partial y_{i,a}^t} \big|_{t \in T_{i,a}^1} = 0\right) \quad p(t) - \pi_i \cdot [(\textstyle\sum_{t \in T_{i,a}^1} y_{i,a}^t) \cdot D_{i,a}]^{-1/2}
$$
$$
+ \alpha_{i,a} + \beta_{i,a}^t - \rho_{i,a}^t = 0, \quad \forall a, t \tag{39}
$$

$$
\left(\frac{\partial UL}{\partial x_{i,a}^t} \big|_{t \notin T_{i,a}^1} = 0\right) \quad p(t) + \alpha_{i,a} + \beta_{i,a}^t - \rho_{i,a}^t = 0, \quad \forall a, t \tag{40}
$$

$$
(y_{i,a}^t - E_{i,a}) \cdot \beta_{i,a}^t = 0, \quad \forall a, t \tag{41}
$$

$$
y_{i,a}^t \cdot \rho_{i,a}^t = 0, \quad \forall a, t \tag{42}
$$

$$
\beta_{i,a}^t, \rho_{i,a}^t \ge 0, \quad \forall a, t \tag{43}
$$

In Li et al.'s paper [63], they claim that if the utility company set the time-of-use electricity price equal to the first derivative of the electricity generation cost function, the customers' consumption profile $(y_{i,a}^t)$ will be the same as the system optimum model solution $x_{i,a}^t$. This is a direct result comparing KKTSOS and KKTUEP. If three pairs of Lagrange multipliers are equal to each other, i.e. $\lambda_{i,a} = \alpha_{i,a}$, $\gamma_{i,a}^t = \beta_{i,a}^t$ and $\mu_{i,a}^t = \rho_{i,a}^t$, then $p^*(t) = c_0 + 2c \cdot \sum_{i,a} x_{i,a}^t$ will make these two KKT systems [(23)-(30) and (36)-(43)] identical. Thus, user's energy

consumption profile of UEP $(y_{i,a}^t)$ under this pricing scheme $(p^*(t))$ will be the solution of the SOS model.

However, this is only one feasible pricing scheme that renders the UEP solution to reproduce the SOS model. Below we define a set of pricing schemes $\mathcal{P} = \{p(t)|(44) - (48)$ hold for some α, β and $\rho\}$. We show that: 1) set $\mathcal{P}$ is nonempty; 2) for any $p(t) \in \mathcal{P}$, the UEP solution would be identical to the system solution; 3) set $\mathcal{P}$ is convex.

$$p(t) - \pi_i \cdot [(\textstyle\sum_{t \in T_{i,a}^1} x_{i,a}^t) \cdot D_{i,a}]^{-1/2} + \alpha_{i,a} + \beta_{i,a}^t - \rho_{i,a}^t = 0, \quad \forall a, t \qquad (44)$$

$$p(t) + \alpha_{i,a} + \beta_{i,a}^t - \rho_{i,a}^t = 0, \quad \forall a, t \qquad (45)$$

$$(x_{i,a}^t - E_{i,a}) \cdot \beta_{i,a}^t = 0, \quad \forall a, t \qquad (46)$$

$$x_{i,a}^t \cdot \rho_{i,a}^t = 0, \quad \forall a, t \qquad (47)$$

$$\beta_{i,a}^t, \rho_{i,a}^t \geq 0, \quad \forall a, t \qquad (48)$$

where $x_{i,a}^t$ is the solution set of SOS model, computed by equations (18) to (21). By setting different objectives, we may find different solution sets of $S \equiv \{p(t), \alpha_{i,a}, \beta_{i,a}^t, \rho_{i,a}^t\}$ that can solve equations (44) to (48). If we can find such set S and because equations (44) to (48) are the KKT system of the UE, we can prove that the SOS model and the UEP may share the same solution set $x_{i,a}^t = y_{i,a}^t$. We show our computational results for multiple pricing schemes in section 4.4. We also show in section 4.4 that under the given pricing scheme, UEP has multiple solutions and it is always worse than the optimal objective value achieved by the SOS model.

Note that the third assertion above is true only when the SOS model has a unique optimal solution. This requires the cost function of the SOS model to be strictly convex. If the SOS has multiple optimal solutions, then we can find sets of pricing schemes $\mathcal{P}_1, \mathcal{P}_2, ...$ that can make the UEP model render the same solution as the SOS model. Then the union of all sets $\{\mathcal{P}_1 \cup \mathcal{P}_2 \cup ...\}$ may or may not be convex.

1. Solve the SOS model and let X^{S} solves (18)-(21).

2. Identify the set $\mathcal{P}$ of valid pricing schemes for demand response by substituting X^{S} into (44)-(48).

3. Solve the following pricing problem for a desired demand response pricing scheme.

$$\min\{g(p)|p \in \mathcal{P} \text{ from Step 2.}\}$$

4.3   A DR Pricing Framework

We propose a framework of demand response pricing whose goal is that the user equilibrium solution under such pricing will reproduce the system solution. The framework offers alternative pricing schemes depending on various pricing objectives chosen by utility authorities.

4.4   Computational Results

4.4.1   Data generation for extended testing

In this section, we discuss the results from our numerical simulations for evaluating the proposed system and user equilibrium models. Both SOS and UEP models were implemented and solved in GAMS [69], a state-of-the-art modeling language for nonlinear programs. All simulations were run on a 16-core dual Opteron CPU server with 32GB of memory running openSUSE 11 Linux.

The data used in extended numerical experiments include two parts. The first part characterizes users profiles, i.e., appliances a, appliances' demand $D_{i,a}$ and maximum amount of energy during a unit time for appliances $E_{i,a}$. In particular, we use dishwasher, plug-in hybrid electric vehicle (PHEV) and air conditioner as prototypical appliances 1, 2 and 3, respectively. The daily demand of each appliance follows a uniform distribution in the range of 0.8 and 1.2 times of the typical daily

consumption as reported in [72]. Similarly, the upper bound $E_{i,a}$ is also uniformly distributed between 0.8 and 1.2 times of the typical hourly consumption for each appliance. For example, the typical daily and hourly consumption of a dishwasher is 5.76 kWh and 1.44 kW. Thus, the daily demand for dishwashers $D_{i,a=2}$ is set to follow the uniform distribution between (4.6, 6.9), while the upper bound $E_{i,a}$ follow the uniform distribution between (1.152, 1.728).

The second part of the data involves the unit cost $f(\sum_{i,a} x_{i,a}^t)$, as a function of the load $\sum_{i,a} x_{i,a}^t$ at any time t. We choose to use the linear unit cost function $f(\sum_{i,a} x_{i,a}^t) = c_0 + c \sum_{i,a} x_{i,a}^t$ in our simulation, which leads to a quadratic total cost function $f(\sum_{i,a} x_{i,a}^t) l_t = c_0 \sum_{i,a} x_{i,a}^t + c(\sum_{i,a} x_{i,a}^t)^2$. The latter is consistent with the commonly used quadratic fuel cost in modeling power generation. Our choice of c_0 and c is based on the DoE census report on the retail price of electricity for 50 states in the U.S. (see e.g., [73]), with an average of 10 cents per KWh. Given an average gap of approximately 17% between the generation and retail costs among the 50 states, we determine that $c_0 = 7.43$ cents and $c = 1.55$ cents per kWh.

4.4.2 Pricing scheme design and results

This section reports pricing scheme design for various objectives based on scenario summarized in Table 8. In words, there are two users, three appliances and 24 time intervals. Setting $[\alpha, \beta] = [1, 24]$ allows both users to be able to use all three appliances any time. Note that both users share the same profile with respect to demand $D_{i,a}$ and upper bound $E_{i,a}$. The "preferred usage windows" for users 1 and 2 are different. For example, user 1's preferred usage window for using appliance 1 is [3,10] and that for user 2 is [3,13]. Similar observations can be made for appliances 2 and 3 between user 1 and user 2.

In order to obtain different pricing schemes, we design various objective function scenarios and describe them as follows.

Marginal Pricing (MP): Let $p(t)$ be the first derivative of the electricity

TABLE 8

Parameter Values for Baseline Scenario

user	appliance	$D_{i,a}$	$E_{i,a}$	α	β	α_p	β_p
1	1	6.0753	1.1703	1	24	3	10
1	2	13.0305	3.2684	1	24	4	9
1	3	18.5805	2.3439	1	24	5	15
2	1	6.0753	1.1703	1	24	3	13
2	2	13.0305	3.2684	1	24	4	12
2	3	18.5805	2.3439	1	24	5	18

Utilities: $\pi_1=\pi_2=5$

generation cost function, which equals to $c_0 + 2c \cdot \sum_{i,a} x_{i,a}^t$ in our case. This is the pricing scheme claimed by Li et al. in [63].

Minimum Total (MinT): The objective is set to be the minimum of the total revenue for the utility company, or the total financial burden for the consumers.

Minimum of Maximum (MinMax): The objective is to minimize the maximum of all possible $p(t)$.

Netzero Total (Net0): The objective is set to be net zero profit for the utility company. This scheme can have two applications. One awards some kind of credits (i.e., negative cost) to users when they use appliances during designated off-peak hours. The other allows for users to discharge and sell the electricity at a certain rate when they are equipped with battery storage devices.

Maximum Total (MaxT): The objective is set to be the maximum of total profit for the utility company with an upper bound of $p(t) \leq P$. P is the constant and can be properly chosen by the utility company. In our case, we randomly choose $P = 1, 9, 10$ or 15 .

Table 9 displays various pricing schemes for different objectives shown in Scenarios 1 to 5. In the second column, we list the solution profile for SOS model. The $p(t)$ of scenario 1 to 4 are listed in column 3 to 6 in Table 9. For scenario 5, the $p(t)$ with upper bound of 1, 9, 10 or 15 are listed in column 7 to 10, respectively.

The bottom row of Table 9 displays total profit in each scenario. It proves that various pricing schemes exist, under which the UEP may have the same users' energy consumption profile as the optimal solution of SOS model. Given this solution profile $x_{i,a}^t$, we solve equations (44) to (48) with various designed objective functions to get $S \equiv \{p(t), \alpha_{i,a}, \beta_{i,a}^t, \rho_{i,a}^t\}$. Adopting this method, the utility company can properly design their electricity pricing scheme to achieve their desired objective. For example, if the utility company is willing to maximize their profit and there is a regulation limiting the highest electricity price to less than or equal to an exact price, i.e. 10, the utility company can set its pricing scheme following column 9 and the maximum profit is 737.29.

TABLE 9
Various pricing schemes

Time	$\sum_{i,a} x_{i,a}^t$	MP	MinT	MinMax	Net0	MaxT			
						$P=1$	$P=9$	$P=10$	$P=15$
1	3.0711	16.9504	0	0	-0.22	0.5619	8.5619	9.5619	14.5619
2	3.0711	16.9504	0	0	-0.22	0.5619	8.5619	9.5619	14.5619
3	3.0711	16.9504	0	0	-0.22	0.5619	8.5619	9.5619	14.5619
4	3.2124	17.3885	0.4381	0.4381	0.2181	1	9	10	15
5	3.2124	17.3885	0.4381	0.4381	0.2181	1	9	10	15
6	3.2124	17.3885	0.4381	0.4381	0.2181	1	9	10	15
7	3.2124	17.3885	0.4381	0.4381	0.2181	1	9	10	15
8	3.2124	17.3885	0.4381	0.4381	0.2181	1	9	10	15
9	3.2124	17.3885	0.4381	0.4381	0.2181	1	9	10	15
10	3.2124	17.3885	0.4381	0.4381	0.2181	1	9	10	15
11	3.2124	17.3885	0.4381	0.4381	0.2181	1	9	10	15
12	3.2124	17.3885	0.4381	0.4381	0.2181	1	9	10	15
13	3.2124	17.3885	0.4381	0.4381	0.2181	1	9	10	15
14	3.1977	17.3428	0.3924	0.3924	0.1724	0.9543	8.9543	9.9543	14.9543
15	3.1977	17.3428	0.3924	0.3924	0.1724	0.9543	8.9543	9.9543	14.9543
16	3.0711	16.9504	0	0	-0.22	0.5619	8.5619	9.5619	14.5619
17	3.0711	16.9504	0	0	-0.22	0.5619	8.5619	9.5619	14.5619
18	3.0711	16.9504	0	0	-0.22	0.5619	8.5619	9.5619	14.5619
19	3.0711	16.9504	0	0	-0.22	0.5619	8.5619	9.5619	14.5619
20	3.0711	16.9504	0	0	-0.22	0.5619	8.5619	9.5619	14.5619
21	3.0711	16.9504	0	0	-0.22	0.5619	8.5619	9.5619	14.5619
22	3.0711	16.9504	0	0	-0.22	0.5619	8.5619	9.5619	14.5619
23	3.0711	16.9504	0	0	-0.22	0.5619	8.5619	9.5619	14.5619
24	3.0711	16.9504	0	0	-0.22	0.5619	8.5619	9.5619	14.5619
Total reveneu		1294.18	16.58	16.58	0.00	58.93	661.92	737.29	1114.15

4.5   Non-uniqueness of UEP_i Model

Observations on Non-Uniqueness of UEP Solutions: Our preliminary experiments show that the UEP may have multiple solutions under a given pricing scheme, i.e., the users' energy consumption pattern may not follow the optimal solution of system model. For example, when substituting the marginal pricing (MP) in Table 9 into UEP_i model, the corresponding KKTUEP system with (36)-(43) yields an UEP solution (the last column in Table 10) with a total welfare of -1086.6029. This is less desirable than that of the SOS solution (-876.5805). Thus considerations ought to be given to the non-uniqueness of the UEP solution when designing a pricing scheme. This motivates the robust pricing in Section 4.6.

4.6 A Robust Pricing Model

As noted previously, for a given pricing scheme p the UEP solution may not be unique. Thus, we propose the following robust pricing multi-level optimization problem to maximize the minimum possible social welfare among alternative UEP solutions.

$$\text{(RPDR)} \quad \max_p \quad \min_{y \in S_y(p)} SW(y) \tag{49}$$

$$\text{s.t.} \quad L \leq p_t \leq U, \ \forall t \tag{50}$$

where $S_y(p) = \{y \in \text{KKTUEP}:(36) - (43)\}$ is the set of UEP solutions given p, and

$$SW(y) = \sum_i \pi_i \cdot \sum_a 2 \left(\frac{\sum_{t \in T_{i,a}^1} y_{i,a}^t}{D_{i,a}} \right)^{1/2} - \sum_{t=1}^T [(c_0 + c \cdot \sum_{i,a} y_{i,a}^t) \cdot \sum_{i,a} y_{i,a}^t]$$ is the

social welfare for UEP solution y. L and U are the lower bound and upper bound of p_t, respectively.

TABLE 10

Energy consumption profile of SOS and UEP under the MP scheme

Time	$p(t)$	$\sum_{i,a} x_{i,a}^t$	$\sum_{i,a} y_{i,a}^t$
1	16.9504	3.0711	1.9319
2	16.9504	3.0711	3.7903
3	16.9504	3.0711	7.1828
4	17.3885	3.2124	6.5792
5	17.3885	3.2124	9.6446
6	17.3885	3.2124	5.5697
7	17.3885	3.2124	2.9916
8	17.3885	3.2124	3.0861
9	17.3885	3.2124	7.2570
10	17.3885	3.2124	2.9916
11	17.3885	3.2124	3.2764
12	17.3885	3.2124	1.3033
13	17.3885	3.2124	1.1901
14	17.3428	3.1977	1.1901
15	17.3428	3.1977	1.1901
16	16.9504	3.0711	2.1356
17	16.9504	3.0711	2.1356
18	16.9504	3.0711	3.7131
19	16.9504	3.0711	1.9319
20	16.9504	3.0711	1.9319
21	16.9504	3.0711	1.9319
22	16.9504	3.0711	1.9319
23	16.9504	3.0711	0.4856
24	16.9504	3.0711	0.0000
Social welfare		-876.5805	-1086.6029

CHAPTER 5

AN EMPIRICAL STUDY OF ENERGY CONSUMPTION IN
SUB-METERED HOMES AND AN OPTIMAL CONSUMPTION
SCHEDULING METHOD

This chapter focuses on DLC in smart grid at the micro-level for major
energy-consuming appliances, which account for up to 30% of the residential
electricity consumption [76]. We study empirical data from a DR pilot program in
Kentucky in an attempt to understand consumer behavior under DR event. We
expect that the real data collected can be integrated to models developed in
Chapters 3 and 4.

In the literature, many have studied DLC under the smart grid framework.
For example, in order to solve the chronic problem of severe power shortage in the
summer for the Taiwan Power Company (TPC), Chu et al. [37] adopt the method
of dynamic programming to optimally determine the schedule of the DLC with the
objective of minimizing the amount of load reduction to lessen the effects of
customers' discomfort and to maintain the TPC's total incomes. Ramanathan and
Vittal [38] develop a an optimization problem for designing and assessing DLC
program with the objective of minimizing end-user discomfort. More related to our
work, McIntyre et al. [76] conduct a multi-phase study, in which different DR
strategies are tested and energy consumption is measured during each phase. Their
results show that the use of highly energy efficient appliances can achieve a
significant reduction in energy consumption under real-world conditions. They also
demonstrate the ability of smart appliances to react to remote pricing signals, which

can produce a measurable decrease in energy consumption during high price periods and may help utilities manage their demand peaks.

While the above mentioned research focuses on the DLC methods under various conditions, it is desirable to have a micro-level and/or detailed analysis on real data to reveal how customers may act upon a DR event. One contribution of this chapter is that it is the first study of demand response in smart grid revealing real life sub-metered data. In particular, this chapter consists of three parts. First, detailed home energy consumption profiles obtained from a pilot study by a local utility company are reported and investigated for clustering analysis. A total of 10 local homes equipped with sub-meters enabling measurements at individual appliance level have been studied. They are divided into 6 clusters based on their daily and peak-period energy consumption in the summer, and 2 clusters in the winter. Second, a heuristic scheduling algorithm that coordinates the time and length of the use of smart appliances, i.e. Thermo-Stat (TSTAT), Heat Pump Water Heater (HPWH) and Battery System, is proposed. The goal of this heuristic algorithm is to minimize the peak load during designated period of three hours, which is defined as 2-5pm in the summer and 7-10am in the winter. Finally, consumer survey from the pilot program indicates that many electricity consumers would rely upon central utility to control major appliances such as TSTAT and HPWH, as well as the operation of the battery and inverter units, in order to manage demand during the predicted peak periods. Therefore, a mixed integer programming (MIP) model for energy consumption scheduling is developed to optimally control these loads and storage in minimizing the peak load of the peak window for the entire system.

The rest of this chapter is organized as follows. Section 5.1 presents a detailed home energy consumption profile clustering analysis based on the data from a pilot study by a local utility company. Section 5.2 establishes a heuristic rotation model for the energy consumption scheduling problem. Section 5.3 develops the two

MIP models for the optimal energy consumption scheduling. Section 5.5 reports the numerical results.

5.1 Clustering Analysis for Home Energy Consumption Profiles

In 2012~2013, a major US home appliance manufacturer, a local regulation authority and a local utility company in Kentucky together initiated a pilot study with the end goal of DR through the use of smart appliance infrastructure and load shifting. The group wanted to know if through proper incentives, consumers could use smart appliances along with a central control unit to shift appliance loads. Ultimately, this pilot study will help justify and validate an innovative rate structure, which not only charges for the energy consumed each month, but also charges for a home's peak load during the designated system peak window. The appliance types considered in the pilot study are dishwasher, clothes washer, dryer, HVAC, water heater, refrigerator, and range.

30 local homes are engaged in this study with a test group of 20 homes and a control group of 10 homes. Care is taken to make sure that homes within each group are comparable in terms of appliance types. All 30 homes are equipped with sub-meters enabling measurements at the individual appliance level (e.g., HVAC, water heater). The 20 test homes have undergone appliance upgrade with smart appliances and have undergone demand response events in later phases. The 10 control homes, on the other hand, have received no upgrades. Therefore, the energy consumption data at the appliance level for these 10 sub-metered control homes becomes extremely valuable for the micro-level clustering analysis.

Figure 8 displays an example of the energy consumption of a control home in a typical summer day. In Figure 8, the total load is the sum of the HVAC load, water heater load and the baseline load. The time axis represents the starting point of each time interval. In this case, the entire day is divided into 24 continuous time intervals, which means each time interval equals to 1 hour. Time 14 represents the
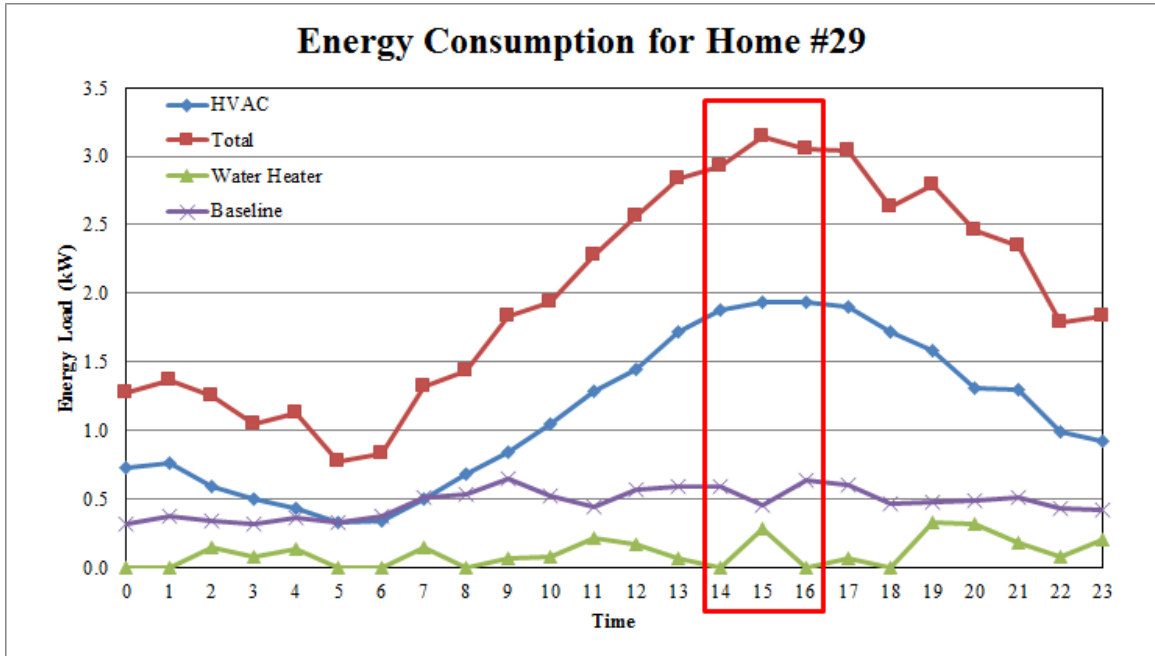
Figure 8. An energy consumption example of a control home in a typical summer day

2-3pm and the time interval between 14 and 16 represents the peak period from 2pm to 5pm. For this particular home #29, its peak load of the day occurs at time 15, which is 3-4pm, with a total load of 3.144 kW.

All 10 control homes are analyzed and grouped using two rules: 1) if the daily peak occurs in the peak period (2-5pm), and 2) the highest kW in the peak period. Based on the above two rules and information in Table 11, all 10 control homes are divided into 6 clusters listed in Table 12. Take home #21 as an example, its daily energy peak load is 4.078 kW, which occurs at 4pm during the system peak period. Three of the other 9 homes also have their daily peak load during the system peak period but with different peak load values. Home #24 has the peak load of over 5 kW at 5pm and home #26 and #29 both have a peak load of around 3.1 kW at 4pm. Therefore, the four homes with peak load inside the system peak period are divided into 3 clusters. For the other 6 homes having their daily peak load outside the system peak period, we distinguish them according to their highest kW between 2pm and 5pm. Home #23 and #30 have highest load in peak period at around 4.5

kW and they are grouped in cluster 4. Similarly, home #22 and home #27's highest
load during peak window are about 3.8 kW, home #25 and home #28 have their
highest load between 2pm and 5pm at about 2.65 kW. Therefore, these four homes
are divided into two clusters, cluster 5 and cluster 6. Hence, all the 10 control homes
are divided into 6 clusters with the frequency of each cluster shown in Table 12.

TABLE 11
10 control homes peak load and timing during a typical summer day

Home#	Peak or Nonpeak between 2-5pm	Highest kW between 2-5pm	Peak time	Peak kW
21	Peak	4.078	4pm	4.078
22	Non-peak	3.775	6pm	4.036
23	Non-peak	4.471	11am	6.122
24	Peak	5.198	5pm	5.198
25	Non-peak	2.649	7pm	4.311
26	Peak	3.148	4pm	3.148
27	Non-peak	3.988	11pm	4.991
28	Non-peak	2.746	9pm	3.209
29	Peak	3.144	4pm	3.144
30	Non-peak	4.626	7pm	5.101

TABLE 12
Clusters of summer homes

Cluster	Representative homes	Frequency
1	#21	0.1
2	#24	0.1
3	#26, #29	0.2
4	#23, #30	0.2
5	#22, #27	0.2
6	#28, #25	0.2

Among the 10 control homes, only home #21 and home #28 are equipped
with electric heater, while the other 8 homes are equipped with gas heater for

winter. Therefore, only home #21 and home #28 are considered in winter home energy consumption profile cluster analysis. The study is based on the similar rules that are used for the summer homes: 1) if the daily peak occurs in the peak period (7-10am), and 2) the highest kW in the peak period. Based on the above two rules and information in Table 13, each of the 2 homes represents its own cluster as listed in Table 14. Take home #21 as an example, its daily energy peak load is 5.134 kW, which occurs at 11pm outside the system peak period. For home #28, its daily peak load is also outside the system peak period at 3.067 kW.

TABLE 13

2 control homes peak load and timing during a typical winter day

Home#	Peak or Nonpeak between 7-10am	Highest kW between 7-10am	Peak time	Peak kW
21	Non-peak	5.134	11pm	5.866
28	Non-peak	3.067	6pm	3.227

TABLE 14

Clusters of winter homes

Cluster	Representative homes	Frequency
1	#21	0.5
2	#28	0.5

We like to note that the relatively small sample size of 10 makes this clustering analysis difficult. The intent here is to propose a method that will be applied to a future work consisting of 330 local homes. We can then divide all the 330 homes into clusters based on the rules described above for both summer and winter. Then either the heuristic algorithm in Section 5.2 or the optimal energy scheduling models in Section 5.3 can be developed based on these clusters.

5.2 A Heuristic Rotation Algorithm for 330 Homes

Consider a local utility company that considers to call for DR event on 330 selected homes. Thus, this and subsequent sections extend the energy consumption sub-metered data from the 10 control homes presented in last section to 330 involved local homes. There are three supporting smart appliances/systems for the demand response system considered in this study. The HPWH allows residents to preheat and elevate ($\sim 165^oF$) the water temperature off peak and control and prevent heating on peak. The programmable TSTAT can be controlled via Wifi to schedule the HVAC temperature set points, thus minimizing peak demand. The battery system stores energy by charging during off-peak periods and discharge during peak periods.

In order to effectively manage demand response supported by these 3 technologies: HPWH, TSTAT and battery system, we develop a heuristic scheduling algorithm that coordinates the time and length of the use of the HPWH, TSTAT and battery system. The goal of this heuristic algorithm is to minimize the peak load during designated system peak period of three hours, which is defined as 2-5pm in the summer and 7-10am in the winter.

The algorithm is described in detail in Table 15, and can be summarized as follows. We consider 3 clusters in this demonstration of the scheduling only. First, the scheduling of the HPWH works as follows. All homes can start at the same time and finish at the same time; no rotation is needed because HPWH is not used during the system peak window. In the Summer, the HPWH starts to work at midnight and lasts for 5 hours to fulfill the daily demand. For the rest of the day, it draws minimal power. Similarly, the HPWH starts to work at 11pm the previous day and lasts for 7 hours in winter days. Second, the operations of TSTAT is designed so as to ensure the maximal thermal comfort level and to minimize the peak load during the peak window. The usage of TSTAT is rotated among three clusters. Each TSTAT incurs a (3,0,3,0,3,3,1.5) consumption pattern for 7 hours,

starting pre-cool at 1pm in summer, and pre-heat at 5am in winter. For example, in summer days, users in cluster 1 can start pre-cool their homes at 1pm. Then users in the following cluster may delay their pre-cool time by τ minutes, and users in cluster n may delay their pre-cool time by $(n-1) * \tau$ minutes. Consequently, all subsequent steps for scheduling TSTAT described in $1b$-$1h$ for cluster n will delay by $(n-1) * \tau$ minutes. Third, the rotation scheduling for TSTAT will not affect the charging of battery system for each user, while the discharging of the battery will be affected. According to the consumption pattern of TSTAT, it requires discharging pattern of (0,0,-3,0,-3,-3,0) from battery. Each Battery gives 3kW for 3 hours, totaling a 9 kWh storage. As we described in step two of battery scheduling, it is discharged to fully or partly mitigate the load of TSTAT during peak window. In this way, the users' thermal comfort level is ensured at a maximal level, and the peak load of the system during peak window is minimized. The scheduling of winter homes is similar to scheduling summer homes as described above.

While the above heuristic rotation algorithm is to minimize the peak load of the system during peak window with the consideration of maximum users' thermal comfort level, it cannot ensure the optimality of the entire system. To achieve the latter, we develop the centralized system peak minimization SPM-1 and SPM-2 models in Section 5.3.

TABLE 15

Outline of heuristic device scheduling algorithm

Devices	Steps for Scheduling
HPWH	1. In the summer, pre-heat starts at midnight and lasts for 5 hours. For the rest of the day, the HPWH draws minimal power. 2. In the winter, pre-heats starts at 11pm the previous day and lasts for 7 hours. For the rest of the day, the HPWH draws minimal power.
TSTAT	1. In the summer when the peak period is 2-5PM, T-stat of first cluster homes works as follows: a. 1 PM. Pre-cool the home at maximal capacity. b. 2 PM. Cool the home at minimum capacity that can avoid room temperature rebound in the near future. c. 3 PM. Cool the home at maximal capacity. d. 4 PM. Cool the home at minimum capacity that can avoid room temperature rebound in the near future. e. 5 PM. Cool the home at maximal capacity. f. 6 PM. Cool the home at maximal capacity. g. 7 PM. Cool the home at medium capacity that can avoid room temperature rebound in the near future. h. All other periods, the T-stat keeps the same consumption pattern as the regular HVAC system. 2. In the winter when the peak period is 7-10AM, T-stat of first cluster homes works as follows: a. 5AM and 6AM. Pre-heat the home at maximal capacity. b. 7AM. Heat the home at minimum capacity that can avoid room temperature rebound in the near future. c. 8AM. Heat the home at maximal capacity. d. 9AM. Heat the home at minimum capacity that can avoid room temperature rebound in the near future. e. 10AM. Heat the home at maximal capacity. f. 11AM. Heat the home at medium capacity that can avoid room temperature rebound in the near future. g. All other periods, the T-stat keeps the same consumption pattern as the regular HVAC system. 3. T-stat of the nth cluster homes start $1a$ or $2a$ late by $(n-1) * \tau$ minutes and complete the process till $1h$ or $2g$.
Battery	1. Battery is charged at midnight per allowed charging rate and hours. 2. Battery is discharged during peak period and, if any, extended periods thereafter, in order to fully or partly mitigate the load required by T-stat and other appliances.

5.3   Development of MIP Models

The goal of the system peak minimization (SPM-1) model is for the utility company to schedule an energy consumption profile for each user so that the user's energy demand is fulfilled while the total peak load for all users collectively is minimized. One objective of the research is to study the effect of newly equipped smart appliance, i.e. HPWH, TSTAT and the battery storage system, on the power grid. Four electricity consumption sources are considered. One is the regular household usage such as heating, lighting, washer and dryer, etc. The other three are the demand of HPWH, TSTAT and battery system. Mathematically, let $t \in \{1, 2, \cdots, T\}$ denote a time interval in a 24-hour cycle. For example, when $T = 24$, each t represents a one-hour interval and when $T = 48$, each t represents a half-hour interval. In addition, T^0 is defined as the low-demand time window and T^1 is defined as the high-demand time window. In our case, if $T = 48$, the high-demand window T^1 of summer days ranges from 27 to 42 for afternoon and evening hours, and the rest is the low-demand window T^0. Inside the high-demand window T^1, the designated system peak window is defined as T^P. T^P ranges from 29 to 34 for summer days. Therefore, $T^P \subset T^1, T^1 \cup T^0 = T, T^1 \cap T^0 = \phi$.

Consider a power distribution network with I users. Let BL_t^i be the regular household baseline demand for user i at time interval t, DH^i, DT^i, DB^i be the daily demand of HPWH, TSTAT and battery for user i, respectively. UH^i, UT^i, UB^i are the power rating for HPWH, TSTAT and battery of user i, respectively. LB^i is the battery discharge rate for user i. Let decision variable x_t^i, y_t^i be the amount of energy consumption of HPWH and TSTAT for user i during time interval t, and u_t^i, v_t^i be the associated binary variables indicating if the HPWH or TSTAT of user i is assigned to use during interval t. In words, $u_t^i = 1$ or $v_t^i = 1$ when HPWH or TSTAT of user i is scheduled to use at time interval t, and $u_t^i = 0$ or $v_t^i = 0$ otherwise. Decision variable z_t^i is the amount of energy charged to or discharged from the battery at time t for user i. r_t^i, s_t^i are the associated binary variables

indicating if the battery of user i is assigned to charge or discharge during interval t. Using the above notation, the SPM-1 model of optimal energy consumption scheduling in sub-metered homes is described below in equations (51)-(67).

$$(\text{SPM-1}) \quad \min \ P \tag{51}$$

$$\text{s.t.} \ \ P \geq M_t, \quad \forall t \in T^P \tag{52}$$

$$M_t = \sum_i (BL_t^i + x_t^i + y_t^i + z_t^i), \quad \forall t \tag{53}$$

$$\sum_t x_t^i = DH^i, \quad \forall i \tag{54}$$

$$x_t^i = UH^i * u_t^i, \quad \forall i, \ t \tag{55}$$

$$\sum_{t \in T^1} x_t^i = 0, \quad \forall i \tag{56}$$

$$\sum_t y_t^i = DT^i, \quad \forall i \tag{57}$$

$$y_t^i = UT^i * v_t^i, \quad \forall i, \ t \tag{58}$$

$$\sum_{t \in T^0} y_t^i = 0, \quad \forall i \tag{59}$$

$$\sum_{t \in T^0} z_t^i = DB^i, \quad \forall i \tag{60}$$

$$\sum_{t \in T^1} z_t^i = -2/3 * DB^i, \quad \forall i \tag{61}$$

$$z_t^i \geq 0, \quad \forall i, \ t \in T^0 \tag{62}$$

$$z_t^i = UB^i * r_t^i, \quad \forall i, \ t \in T^0 \tag{63}$$

$$z_t^i \leq 0, \quad \forall i, \ t \in T^1 \tag{64}$$

$$z_t^i = LB^i * s_t^i, \quad \forall i, \ t \in T^1 \tag{65}$$

$$- z_t^i \leq y_t^i, \quad \forall i, \ t \in T^1 \tag{66}$$

$$u_t^i, \ v_t^i, \ r_t^i, \ s_t^i \in \{0,1\}, \ x_t^i, y_t^i \geq 0, \quad \forall i, \ t \tag{67}$$

In particular, the objective in equation (51) minimizes the peak load during

the peak window for all users in the distribution system. Constraint (52) makes sure that the peak load P is the largest total load M_t of any peak time interval $t \in T^P$. In our case, if $T = 48$, then the peak window T^P ranges from 29 to 34 for afternoon and evening hours (2-5pm). Constraint (53) calculates the total load in each time interval t as the sum of household baseline load, HPWH load, TSTAT load and battery charging or discharging load for all users. Constraints (54) through (56) are constraints for HPWH. Constraint (54) ensures that each user's HPWH daily demand is fulfilled in a 24-hour cycle. Constraint (55) calculates the energy consumption of each user's HPWH at any time interval t. Further, constraint (56) states that no user will use their HPWH during high-demand time window $t \in T^1$. Similarly, constraints (57) through (59) are TSTAT constraints. Constraint (57) ensures that each user's TSTAT daily energy requirement is met. Constraint (58) calculates the energy consumption of each user's TSTAT at any time interval t. Because the energy consumption of TSTAT during low-demand period ($t \in T^0$) remains the same as the HVAC and is included in the household low-demand window $t \in T^0$. In our case, if $T = 48$, then the low-demand window T^0 ranges from 1 to 26 and from 43 to 48. Constraints (60) to (66) pertains to the battery system. Constraint (60) ensures that each user's battery storage is charged to its full capacity during the low-demand period T^0. Constraint (61) states that the battery storage can be discharged 2/3 of its full capacity during the high-demand window T^1 for user i. Constraint (62) states that the battery can only be charged during the low-demand period and constraint (63) calculates the energy consumption of charging battery for each time interval during low-demand times. Similarly, constraint (64) ensures that the battery can only be discharged during the high-demand window and constraint (65) calculates the amount of energy each battery can discharge to the grid at each time interval during high-demand window. Additionally, constraint (66) states that the energy discharged from the battery will not be more than that is consumed by the TSTAT during the high-demand window.

66

Finally, constraint (67) specifies that variables u_t^i, v_t^i, r_t^i and s_t^i are binary indicating if user i will use not use each appliance at time interval t while x_i^t and y_i^t are all non-negative.

The objective of the above SPM-1 model (51)-(67) is to minimize the peak load during the peak window T^P.

Note that one may be interested in minimizing the peak load of the entire day. In this way, we can achieve better performance with the respective to peak-to-average ratio (PAR). Therefore, we can change equation (52) to (68).

$$P \geq M_t, \quad \forall t \tag{68}$$

We may also drop constraint (56), since the goal now is to minimize the peak load of the entire day, the load of HPWH may fill the valley occurs at any time t. Therefore, the following SPM-2 model can be used if the objective is to minimize the system daily peak load.

$$\text{(SPM-2)} \quad \min \left\{ P | (68), (53) - (55), (57) - (67) \right\} \tag{69}$$

5.4   Modification of MIP Models

After the MIP models have been developed, it is important to realize that there are numerous factors which exist in reality and have significant implications on the outcome of the models. These factors include:

1. The preference of consecutive and non-interrupted running of appliances;

2. The different timing of residential and non-residential consumers load on the grid;

3. The unwillingness of certain residential consumers to have their behavior controlled by the centralized decision making system;

4. Thermal comfort needs by consumers.

We will revise the MIP models to reflect each or a combination of the above factors in this section.

We acknowledge that the original model could require frequent run and stop of appliances as determined by the central controller, in reality there is a strong preference that appliances are running on a continuous and uninterrupted basis. This is because starting an appliance to run always consumes extra energy than its normal working load. At the same time, keeping an appliance on and off too frequently can shorten its life span. Therefore one always considers keeping an appliance running for some consecutive time periods once it starts to run.

In the literature, Xu and Bai [77] introduced the fixed setup cost to help reduce the percentage of non-consecutive PHEV charging in a public charging station. Through carefully selected fixed setup cost, the percentage of non-consecutive charging can be reduced by approximately 80%. Unlike public charging during day-time, using an appliance such as HPWH and HVAC at home is difficult to utilize the concept of setup cost.

In this dissertation, we use an alternative approach via the use of binary variables to ensure continuous use of an appliance as in constraints (70) -(72). Assuming once triggered to run, one may consider to keep the HPWH, TSTAT and battery working at least l, m and n time periods, respectively. Note that, for the battery, we only consider to keep it charging for at least n consecutive time periods, but not for the discharging. For the latter, we still use constraint (66) to ensure the energy discharged from the battery will not be more than that is consumed by the TSTAT during the high-demand window.

$$
\begin{aligned}
&u^i_{t+1} - u^i_t + u^i_{t-1} \geq 0, \\
&u^i_{t+2} - u^i_t + u^i_{t-1} \geq 0, \\
&..., \qquad\qquad\qquad\qquad \forall i, \ t \\
&u^i_{t+l-1} - u^i_t + u^i_{t-1} \geq 0,
\end{aligned}
\tag{70}
$$

$$v_{t+1}^i - v_t^i + v_{t-1}^i \geq 0,$$
$$v_{t+2}^i - v_t^i + v_{t-1}^i \geq 0,$$
$$..., \qquad\qquad \forall i, \ t \tag{71}$$
$$v_{t+m-1}^i - v_t^i + v_{t-1}^i \geq 0,$$

$$r_{t+1}^i - r_t^i + r_{t-1}^i \geq 0,$$
$$r_{t+2}^i - r_t^i + r_{t-1}^i \geq 0,$$
$$..., \qquad\qquad \forall i, \ t \in T^0 \tag{72}$$
$$r_{t+n-1}^i - r_t^i + r_{t-1}^i \geq 0,$$

The second factor to consider in revising the model is the difference between residential load and non-residential energy load. From a system point of view, the total system energy load includes not only residential load but also commercial and business load, or non-residential energy load. They affect the system load in different ways and need to be examined separately. While the residential energy consumption is supervised by the central controller as is the purpose of designing the present models, the non-residential consumption is not supervised by the central controller. Therefore, it is critical to include the non-residential energy load when we calculate the hourly total system load. In addition, we want to make sure that we do not create a new peak for the total system by shifting the consumption pattern of the residential users, as for most of the time, especially during day-time when the system peak load is likely to occur, the non-residential load accounts for the majority of the total system load. Here we introduce the pricing mechanism of peak tariff, which is a surcharge that only applies to electricity consumption that incurs within specified time frame. The peak tariff is charged on each user's "coincident load" at the time when system peak load occurs.

Another important factor is that not all homes are willing to give up their appliances' control to the utility company. Some may prefer to take control themselves even though they probably end up paying more on the peak tariff.

Therefore we need to consider these users energy load although it is not controlled by the model.

Let OL_t be the non-participating regular household original total demand at time interval t, NRL_t be the non-residential total energy load at time interval t. Constraint (53) can be rewritten as (73).

$$M_t = \sum_i (BL_t^i + x_t^i + y_t^i + z_t^i) + OL_t + NRL_t, \quad \forall t \tag{73}$$

Together with binary constraint sets (70)-(72) for consecutively using appliances, the following SPM-3 model can be used if

1. only part of the selected residential home owners are willing to participate in the centralized controlled program;

2. non-residential energy load should be considered in the total system load;

3. appliance should be using for at least a consecutive time period once triggered to run.

$$\text{(SPM-3)} \quad \min \{P|(52),(54)-(67),(70)-(73)\} \tag{74}$$

Another critical factor regarding optimal energy consumption scheduling is the users thermal comfort of using the TSTAT. In our previously developed MIP models, this has not been considered as the energy demand has been limited on a per day basis and in a pre-defined time window T^1. In reality the user will base his/her decision to turn on/off the appliances on how they feel, or the ambient temperature. In this case, it is necessary to figure out a way to capture the changing temperature as a result of on/off decisions for the TSTAT.

Similar to the model used by Li et al. ([63]), we use a linear dynamic model to represent an approximate thermal behavior of a house for the purpose of this

dissertation. We denote T_t^i and T_t^O as the temperature at time t inside and outside the house i. As shown in (75) and (76), T_t^i is given by a linear function of house i's previous room temperature T_{t-1}^i, gradient between current outside temperature and previous room temperature $(T_t^O - T_{t-1}^i)$, and energy consumed by HVAC unit at time t for user i, i.e., γy_t^i. Each user may have a particular preferred temperature at which they feel the most comfortable. Although a comfortable temperature is generally believed to be around $70 - 72$ °F, thermal comfort indeed varies by people. Some people may feel most comfortable at 75 °F while others may prefer 65 °F. In our model, we denote $T_{comf,min}^i$ and $T_{comf,max}^i$ as the lower boundary and upper boundary of the comfort temperature window for user i. T^1 denotes the set of time window that the users care about the room temperature.

$$T_t^i = \alpha T_{t-1}^i + \beta(T_t^O - T_{t-1}^i) + \gamma y_t^i, \quad \forall i, \ t \tag{75}$$

$$T_{comf,min}^i \leq T_t^i \leq T_{comf,max}^i, \quad \forall i, \ t \in T^1 \tag{76}$$

By incorporating the thermal comfort constraints, it is unnecessary to keep the TSTAT demand constraint. Also, the HVAC is not always running at its power rating UT^i. LT^i denotes its lower limit of energy consumption once it is on. Thus, we replace the TSTAT demand constraints (57) to (59) with (77).

$$LT^i * v_t^i \leq y_t^i \leq UT^i * v_t^i, \quad \forall i, \ t \tag{77}$$

The modified SPM-4 model shown below can be used by the central controller to optimize the peak load of participating homes with the consideration of non-participating homes load, non-residential energy consumption and user's thermal comfort.

$$(SPM\text{-}4) \quad \min \ \{P|(52), (54) - (56), (60) - (67), (73), (75) - (77)\} \tag{78}$$

5.5 Results and Discussion

5.5.1 Assumptions

When conducting numerical experiments with the proposed rotation scheduling and MIP models, we assume that each home is equipped with the same smart appliances, i.e., HPWH, TSTAT and battery system. We also make the following assumptions according to the information from the smart appliance manufacturer and users' energy consumption profile.

- The daily demand for each HPWH is 2.5 kWh and its power rating is 0.5 kW. Each HPWH needs to run 2.5 hours to fulfill its daily demand.

- The demand for each TSTAT during high-demand hours $(t \in T^1)$ is 13.5 kWh and its power rating is 3 kW. Each TSTAT needs to run 4.5 hours to fulfill this demand. The demand for low-demand hours $(t \in T^0)$ is included in the baseline load (BL).

- The charging demand for each battery system is 13.5 kWh and its power rating is 2.7 kW with an efficiency of 2/3. It can provide 9 kWh energy during high-demand hours $(t \in T^1)$ to the grid to support some of the demand of TSTAT during that time. Each battery needs 5 hours to be fully charged and it can provide power to the TSTAT for 3 hours during $t \in T^1$.

- The new TSTAT can only be scheduled to help users shift their peak load. It still consumes the same amount of energy as the original HVAC. If the original HAVC consumes more than the TSTAT during high-demand hours $(t \in T^1)$, which is 13.5 kWh, then the extra demand is compensated to the time intervals closed to T^1, but cannot surpass its maximum power of 3 kW. This way, the daily demand of TSTAT is kept the same as that of the original HAVC.

Based on the above assumptions, we first get the new energy consumption profile with smart appliance i.e., HPWH, TSTAT and battery system, for home #21. Then we expand this energy consumption profile of home #21 to 330 homes. The 330 homes are with identical energy consumption profile and we evenly divide them into three groups with 110 homes in each group. We only show results of a typical summer day. The winter case should be similar to the summer case, only difference is the peak window for summer is from 2-5pm and for winter, it is 7-10am.

5.5.2   Without Battery System

The battery system can help user mitigate the energy consumption caused by the TSTAT during peak window. However, its high cost and non-necessity nature may prevent users from purchasing it. Therefore, we first study the case that all 330 homes are equipped with only HPWH and TSTAT, but no battery system.

In subsequent analysis, we schedule all 330 homes to use their current appliances simultaneously in the "Original" case (OL) in Figure 9, and all 330 homes to use their smart appliances, i.e., HPWH and TSTAT in the "No Rotation" case and apply the heuristic rotation algorithm for 330 homes all equipped with smart appliances described in Section 5.2 as the "Heuristic" case. Also, as previously stated, we divide the entire day into 48 time intervals and each time interval represents half an hour. We compare the energy consumption of these two scenarios with the original profile and show the results in Figure 9. From Figure 9, we first observe that the peak load during peak window can be reduced from 672.92 kW of the original case to 440.46 kW of the "Heuristic" case due to the effective rotation. Note that under the "No Rotation" case the peak load increases to 689.96 kW, because the maximal power of the new TSTAT is 3 kW, which is higher than that of the original HVAC. Second, the peak load of original case occurs at time interval 31 and 32 and it shifts to time interval 27 and 28 for the "Heuristic" case. Third, the valley load of "No Rotation" case and "Heuristic" case occurs at the

same time intervals as the original load but with a lower energy load. This is due to the more efficient HPWH, which consumes less energy than the original water heater. Overall, for the peak load during peak window, the heuristic rotation algorithm performs significantly better than the other two cases. It can shift the system peak load to non-peak window effectively.
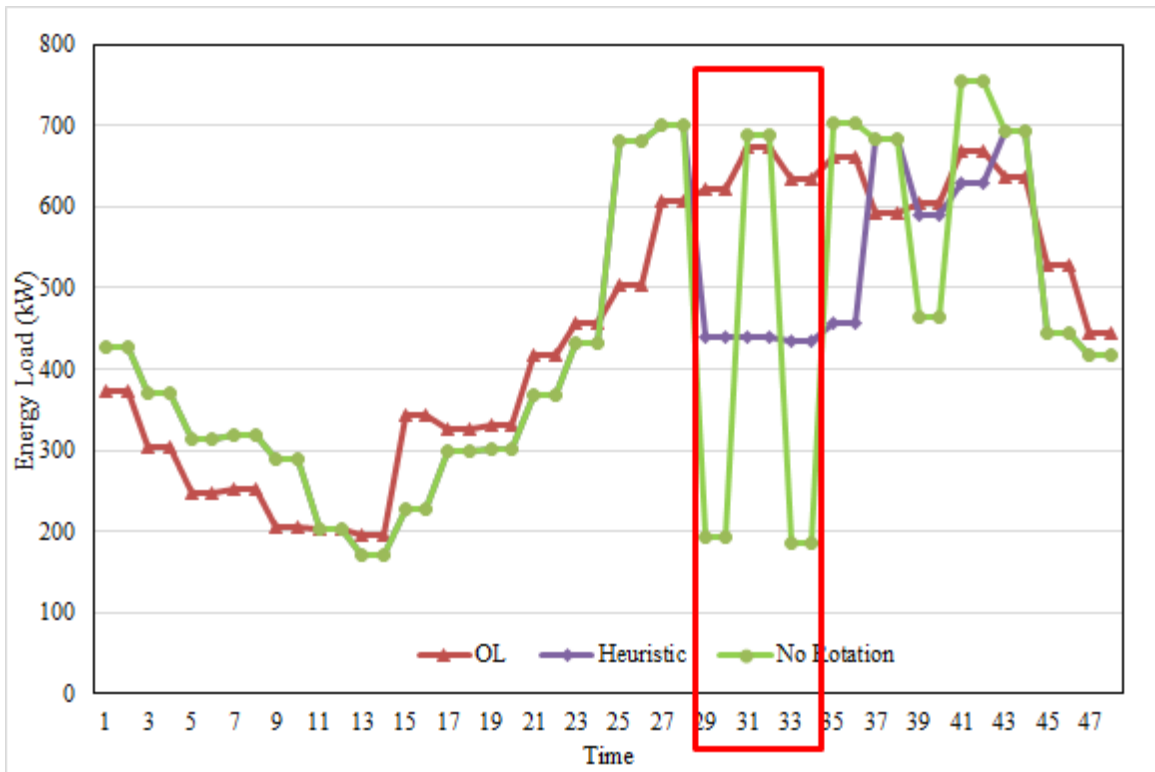

Figure 9. System total energy consumption without battery based on home #21 in a typical summer day

The aggregate results of the above three cases are listed in Table 16. Since the goal of the rotation heuristic is to minimize peak load during peak window, it can be seen the "Heuristic" case can accomplish the goal very well (peak load of 440kW, compared to 672.92kW of "Original" and 687.96kW of "No Rotation"). However, as far as the PAR is concerned, both "No Rotation" case and "Heuristic" case are higher than the original case. This is because the peak load of the former two cases is higher and their valley load is lower than the original case. If we only

compare the "No Rotation" case and the "Heuristic" case, then the "Heuristic" case has a lower PAR. Additionally, the peak load during peak window of "Heuristic" case is much lower than the other two cases. This is consistent with the result we obtain from Figure 9.

TABLE 16
Performance of different scenarios without battery

	Original	No Rotation	Heuristic
PAR	1.49	1.75	1.63
Peak Load in Peak Window (kW)	672.92	687.96	440.46

5.5.3   With Battery System

If all 330 homes are equipped with battery system, then in addition to the three cases discussed in Section 5.5.2, we add two MIP models results to our comparison as shown in Figure 10. The curve of original case is the same as shown in Figure 9. Also, as the battery only works during the high-demand time window (T^1), the parts of curve outside this range for "No Rotation" and "Heuristic" cases are the same as in Figure 9. Because the battery can provide 9 kW of energy totally compensating the TSTAT consumption during this period, both "No Rotation" and "Heuristic" cases have their valley load (192.96 kW), exactly same as the baseline load. For the SPM-1 model, it can achieve the same peak load as the "No Rotation" and "Heuristic" cases, but it does not consider users' comfort level and schedules the TSTAT to work after the midnight and after the high-demand period T^1. There seems no advantage of using the SPM-1 model to minimize the peak load during peak window when the battery system exits. The objective of the SPM-2 model is to minimize the system peak load of the entire day, and the highest load during peak window of SPM-2 model is 412.96 kW, which is higher than "No Rotation",

75

"Heuristic" and SPM-1 cases. However, on the horizon of the entire day , the curve of SPM-2 model is more leveled than all the other cases.
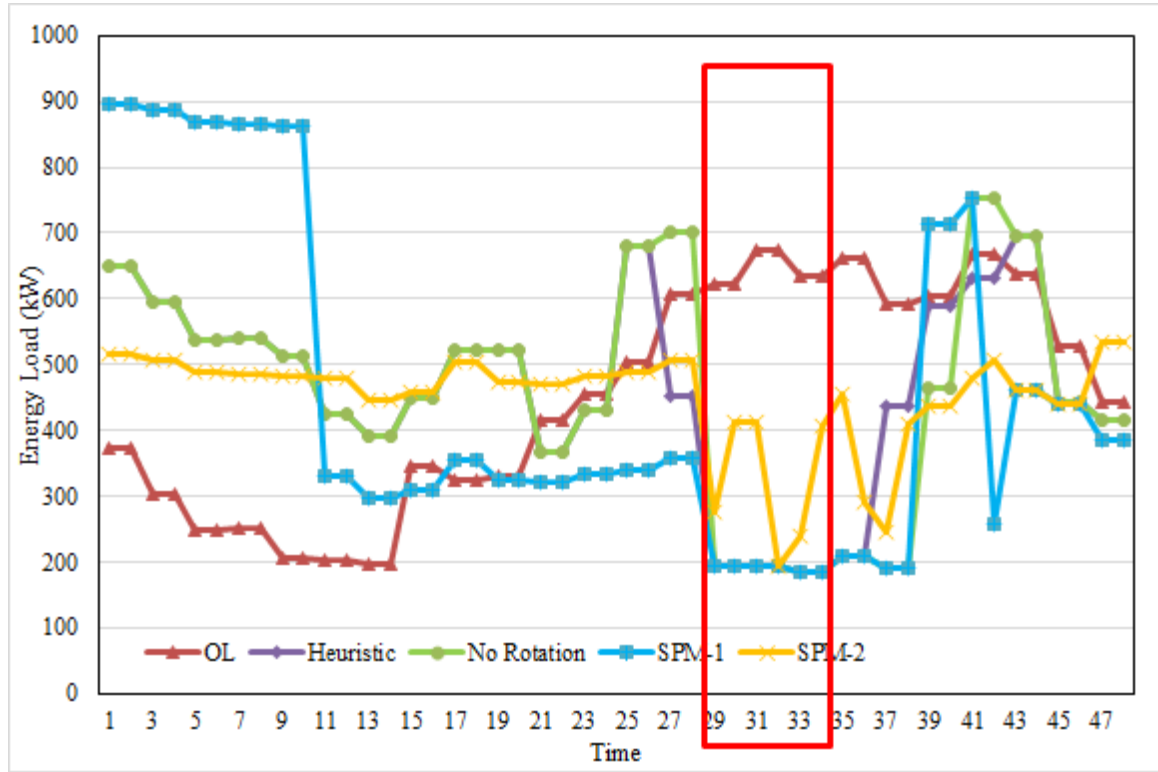

Figure 10. System total energy consumption with battery based on home #21 in a typical summer day

We show the performance results of the above five scenarios in Table 17. Similar to the case without battery system, the "No Rotation", "Heuristic" and SPM-1 models all have higher PAR than the original scenario. However, amongst the three models, the heuristic algorithm can achieve the lowest PAR at 1.5. This is only slightly higher than that of the original scenario. The peak load during peak window under these three scenarios are 192.96 kW, which is much lower than 672.92 kW of the original scenario. Further, we also add the performance result of the SPM-2 model as shown in the last column of Table 17. Although the objective of the SPM-2 model is different from the other three models, we can still compare its performance in terms of the PAR. As expected, the PAR is much lower than those

of "Original", "No Rotation", "Heuristic" and SPM-1 scenarios. It shows that even though the SPM-1 model does not have advantage over the "No Rotation" and "Heuristic" models in minimizing the peak load during the peak window, the SPM-2 model can be applied to level the system load of the entire day and achieve much better performance than all other models.

TABLE 17
Performance of different scenarios with battery

	Original	No Rotation	Heuristic	SPM-1	SPM-2
PAR	1.49	1.63	1.50	1.98	1.19
Peak Load in Peak Window (kW)	672.92	192.96	192.96	192.96	412.96

5.5.4 Results of SPM-3 Model (With Non-Residential Load and Consecutive Usage Constraints)

In this section, we consider the non-residential load when we calculate the system total load. We also assume that only one third of 330 residential homes participate in the program that would allow the central controller to determine when and how much they can use their appliance in order to avoid high cost due to the peak tariff. The rest 220 homes would prefer to take control themselves rather than giving the right of decision to the central controller, even though they may end up paying more during the peak window. In order to show the role of battery system in this optimization problem, we assume that only half of the 110 participating homes are equipped with battery system. The other 55 participating homes and 220 non-participating homes do not have any energy storage system. In addition, we will add the consecutive using constraints and understand how that would change the outcome.

We plot the results of SPM-3 model in Figure 11. There are two levels of

77

comparisons. Both solid lines represent the system load with orange series representing the load without optimization (marked as "OL") and gray representing the load with optimization (marked as "ML"). On the other hand, both dashed lines represent residential load with (gray) and without (orange) optimization. First, we observe that with the consideration of the non-residential load, which contributes more than two thirds of the system total energy consumption, the system peak load is almost certain to occur during the day time when the non-residential load reaches its peak. Second, the peak load of original case occurs at time interval 31 and 32 and it shifts to time interval 27 and 28 for the "ML" case (i.e., with optimization). Third, the residential load of "ML" case during the peak window reduce significantly from the "OL" case. Overall, for the peak load during peak window, the SPM-3 model performs significantly better than the original case. It can reduce the system peak load during peak window effectively.
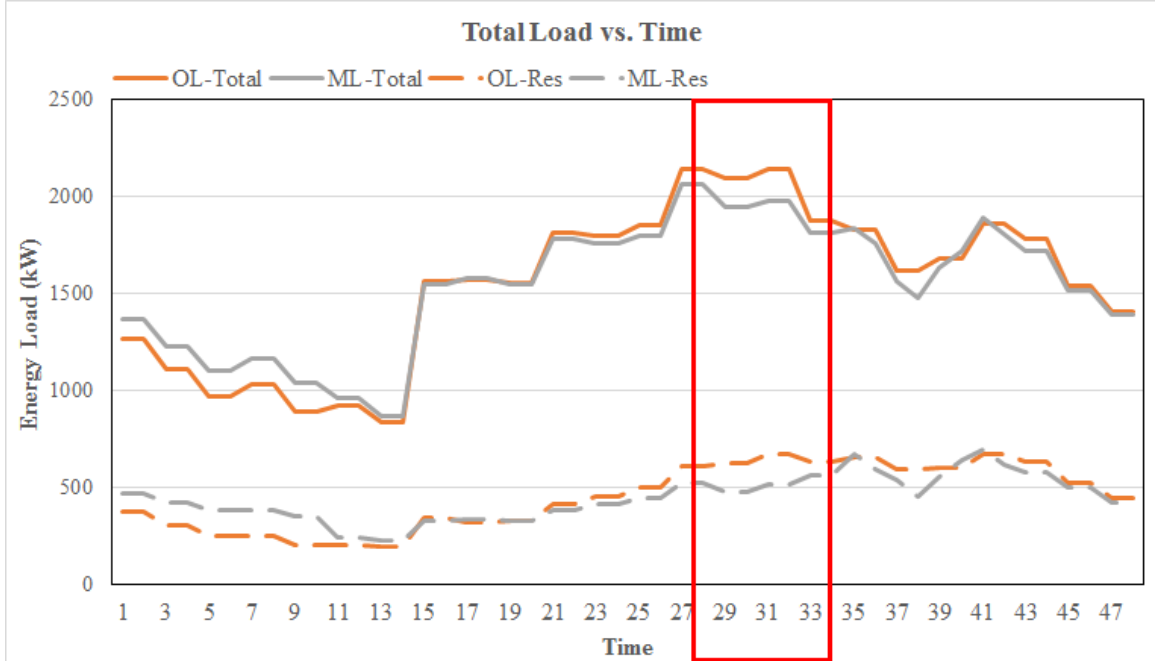
Figure 11. System total energy consumption with non-residential load in a typical summer day

The results of the above two cases are listed in Table 18 and Table 19. Since

the goal of the SPM-3 model is to minimize peak load during peak window, it can be seen from Table 18 that the total system peak load during peak window can be reduced from 2143.46 kW for the original case to 2060.51 kW for the "ML" case. The PAR declines from 1.39 to 1.34. Note that the load of non-residential and non-participating residence has not been optimized by the model, the effect of peak reduction is not as significant as we have seen in Section 5.5.2 and 5.5.3. When focusing just on the residential load, Table 19 shows that the total residential peak load during peak window is reduced from 672.92 kW to 566.81 kW and the PAR declines from 1.49 to 1.27.

TABLE 18
Performance of SPM-3 Model - Total Load

	Original	Modified
PAR	1.39	1.34
Peak Load in Peak Window (kW)	2143.46	2060.51

TABLE 19
Performance of SPM-3 Model - Residential Load

	Original	Modified
PAR	1.49	1.27
Peak Load in Peak Window (kW)	672.92	566.81

The load profile of 110 participating residential homes are shown in Figure 12. It can be observed that all energy consumption due to HPWH and battery charging happens outside the preferred window T^1. More specifically, HPWH and battery only consume energy from time period 1 to 10, when the system load is at its valley. On the other hand, TSTAT only works during the preferred time window T^1, which is from time period 28 to 42. Interestingly, the hourly total energy

79

consumption drawn from the grid in T^1 is less than or equal to the hourly TSTAT load, thanks to the battery energy storage system. It is necessary to look into detailed load profiles of users with and without battery in order to understand the difference of the two groups.
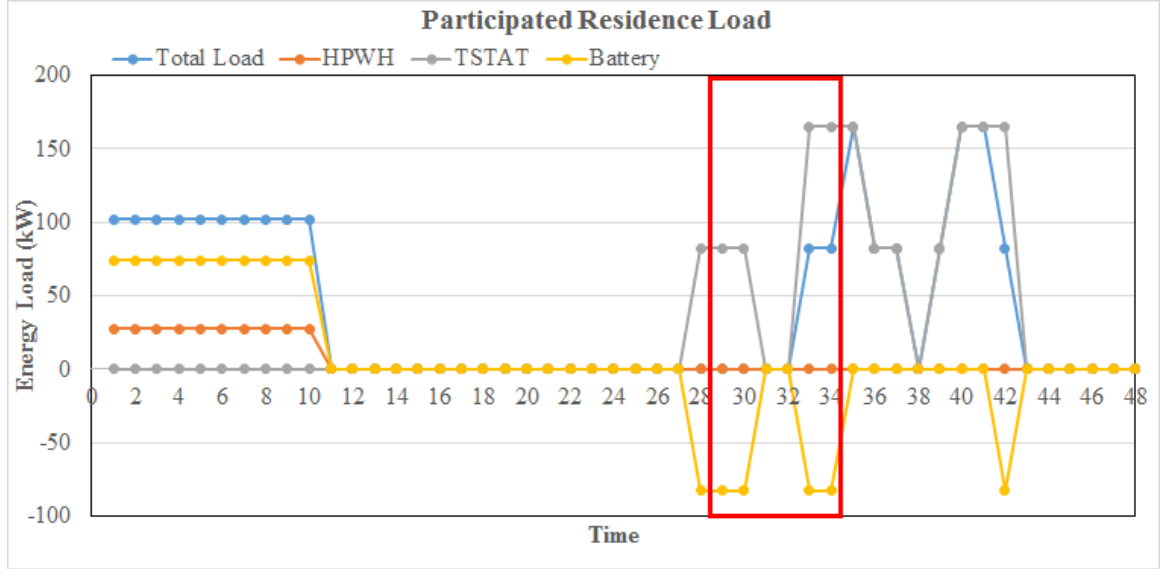

Figure 12. Participating residential energy consumption in a typical summer day

In order to differentiate the users with and without battery system, we label users equipped with battery as Group 1 and the other half without battery as Group 2. Also, we set the consecutive using parameters l, m and n in constraints (70) to (72) at 2, 3 and 3, respectively. In this way, the HPWH works at least two time periods once it starts to run. TSTAT works at least three time periods and battery charges at least three time periods once they start to run. We do not constrain the discharge of the battery and leave it to work with the TSTAT energy consumption.

Figure 13 shows the total load profile of the two groups. Group 1 consumes much more energy during time period 1 to 10, due to charging of the battery system. In returns, Group 1 users consume no energy from the grid during the peak window T^P. Their battery systems provide all loads that are needed by the TSTAT in T^P. This can help them avoid paying any peak tariff. Without the battery,

Group 2 users have to draw energy from the grid from time period 33 to 34 and they have to pay the resulting peak tariff.
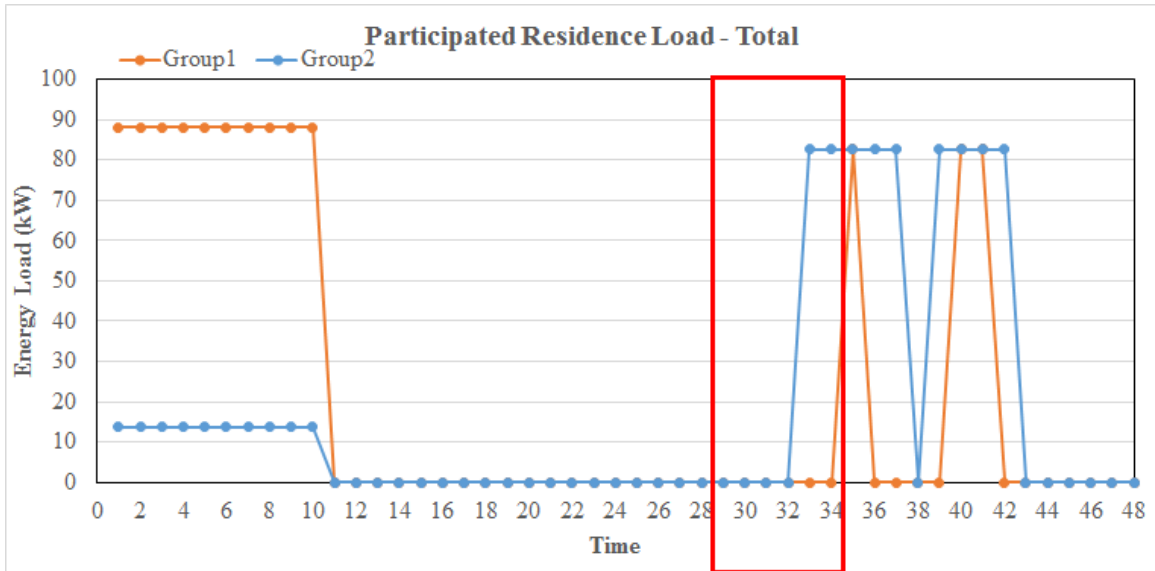
Figure 13. Participating residential total energy consumption in a typical summer day

As shown in Figure 14, the two groups have the same load profile on the HPWH. The HPWH starts to work at time period 1 and continues to run till time 10 to fulfill its daily demand.
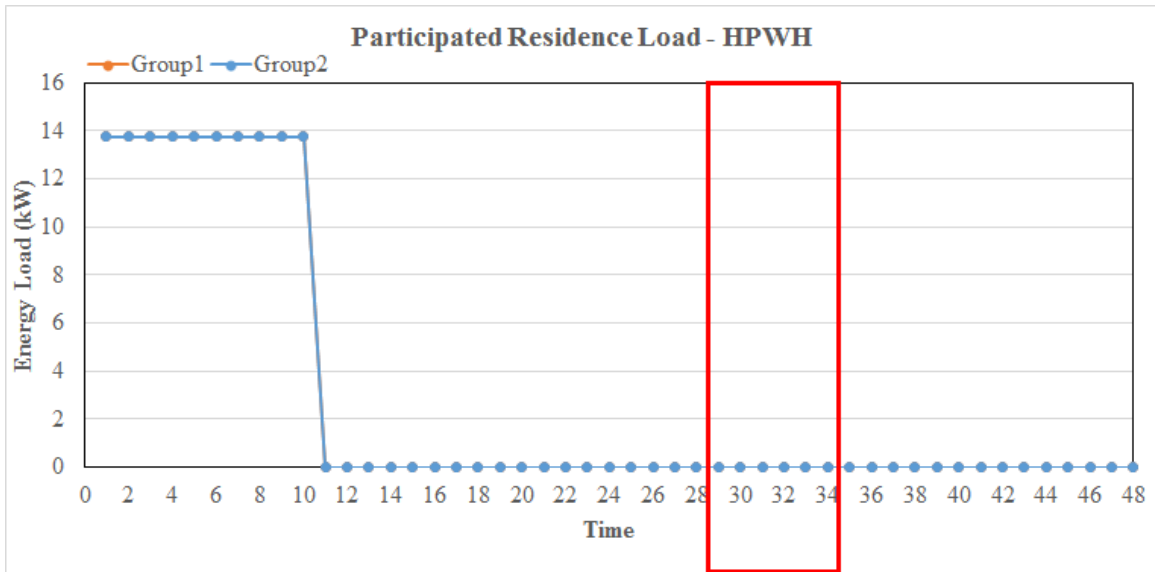
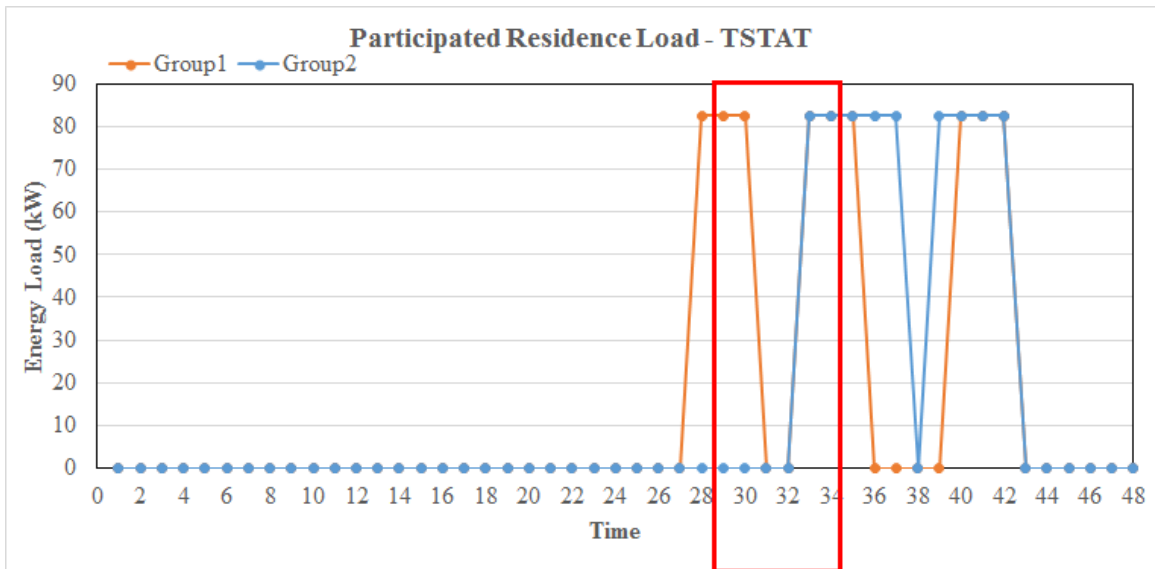Figure 14. Participating residential HPWH energy consumption in a typical summer day

Figure 15. Participating residential TSTAT energy consumption in a typical summer day
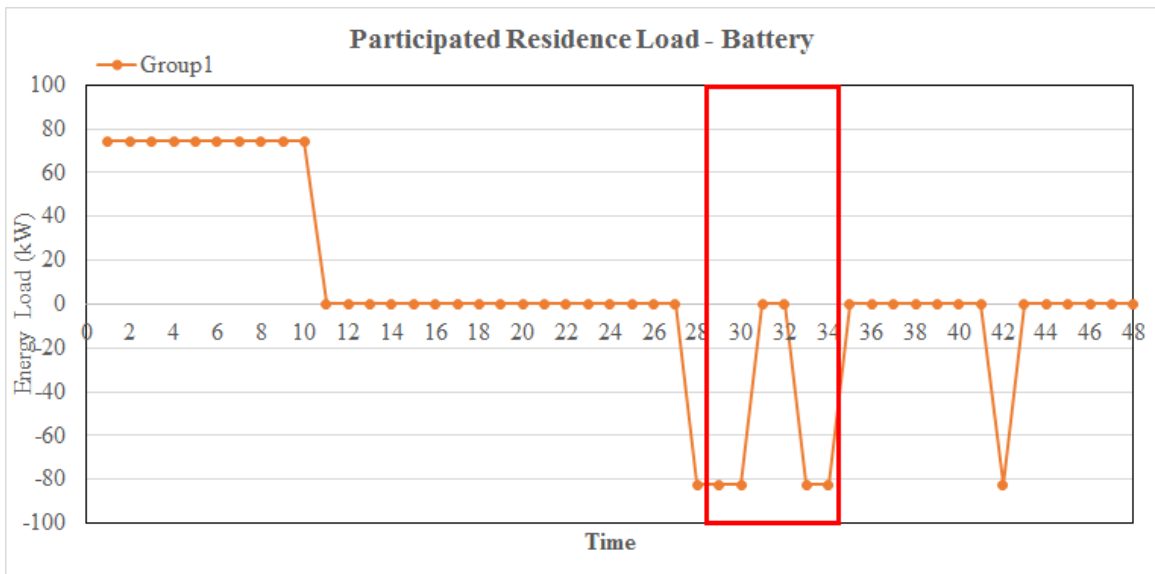
Figure 16. Participating residential battery energy consumption in a typical summer day

Figure 15 describes the detailed TSTAT load profile of two groups. Group 1 homes first use the TSTAT at time 28, right before the peak window T^P, and continue to run it for three time periods. Then at time 33 and 40, they use the TSTAT twice, each for three consecutive time periods. Group 2 users start to use the TSTAT at time 33 for five consecutive time periods. At time 39, they use the TSTAT again for another four time periods.

Figure 16 shows Group 1's battery load profile. As we can see, the user charges his or her battery at time 1 for ten consecutive periods to fulfill the daily battery demand. Then the battery discharges from time 28 to 30, 33 to 34 and 42 to provide energy to the TSTAT. This ensures Group 1's energy consumption during peak window all coming from the battery.
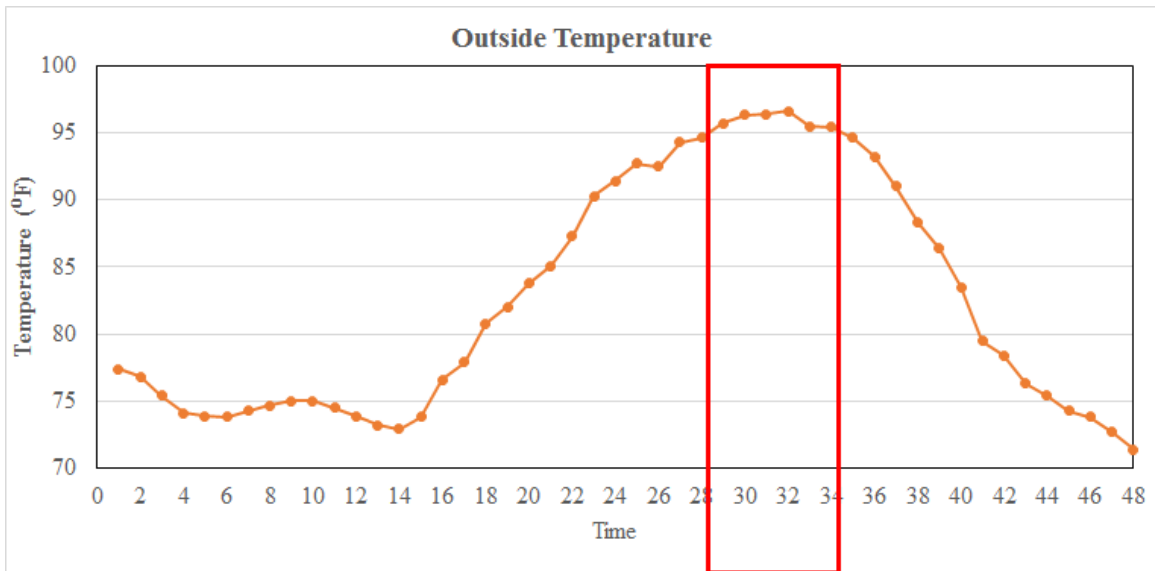
Figure 17. Outside temperature of the study area in a typical summer day

5.5.5 Incorporating Thermal Comfort in MIP models

To incorporate thermal comfort in the MIP model, we first get the 24-hour temperature of the study area for a typical summer day. The temperature change is plotted in Figure 17. As we can see, in a typical summer day, the outside

84

temperature of the study area varies from below 73 °F to over 96 °F.

Khadgi [79] performs a study on how to identify the proper value of parameters in the thermal behavior function. We calibrate his results with the insulation condition and TSTAT power rating of the participating homes. In equation (75), we set the coefficient of previous room temperature $\alpha = 1.00015$, the gradient between previous room temperature and current outside temperature $\beta = 0.010649$ and the coefficient of the TSTAT power rating $\gamma = -0.3821$. The large range of the temperature change makes the parameters selected in constraint (75) persuasive and fit for any summer day in the study area.
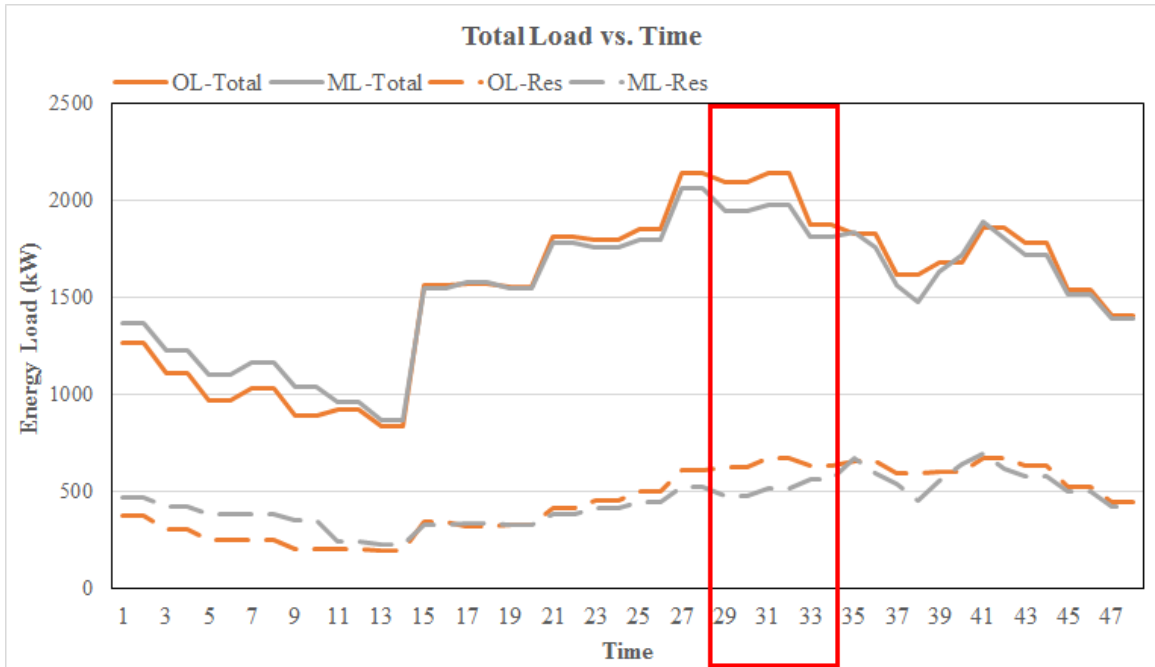
Figure 18. System total energy consumption with thermal comfort in a typical summer day

For the SPM-4 model, we first include the TSTAT demand constraint and the results are shown in Figures 18 to 24. First, when compared to the original case, the average load and peak load are both lower. The PAR decreases from 1.39 to 1.34. Second, users with battery (Group 1) use the HVAC before and during the peak window and the load is provided by the battery. Users without the battery

(Group 2) use the HVAC 2.5 hours after the peak window when the room temperature gets close to the upper limit of the comfort zone. Finally, because the battery can provide energy load for Group 1, the room temperature fluctuates in a relatively smaller range. While the other group without the battery cannot use the HVAC until the temperature hits the upper comfort limit as they want to avoid paying the peak tariff.
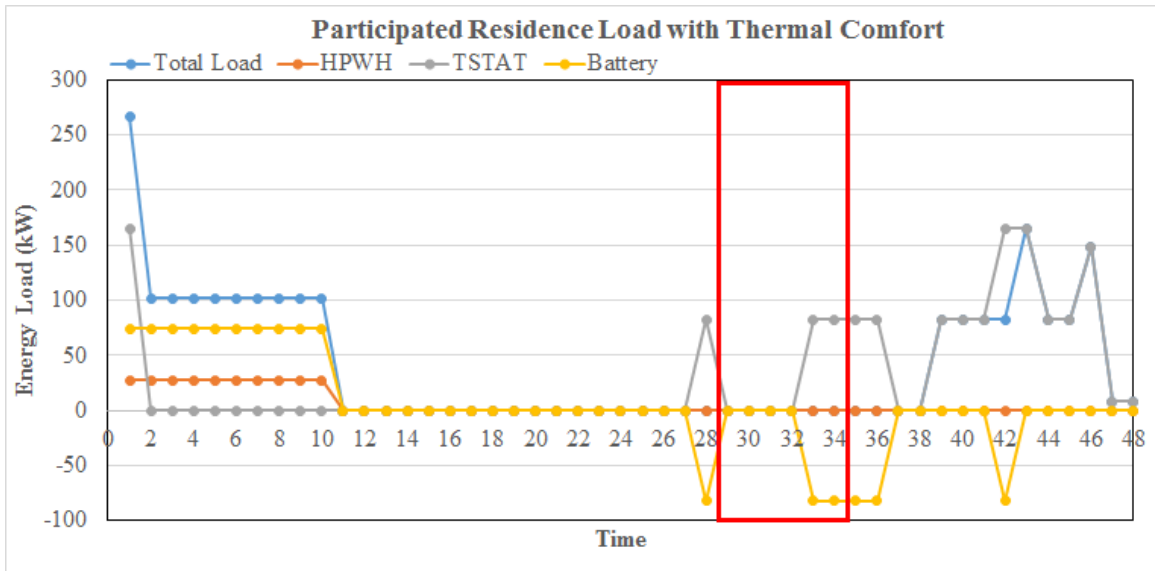

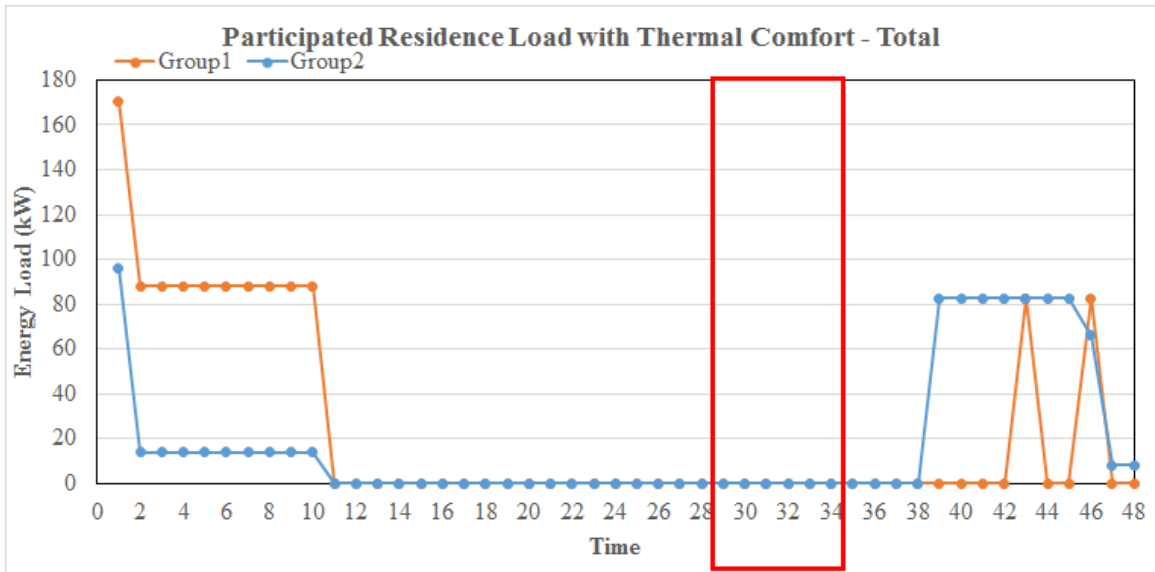Figure 19. Participating residential energy consumption with thermal comfort in a typical summer day

Figure 20. Participating residential total energy consumption with thermal comfort in a typical summer day
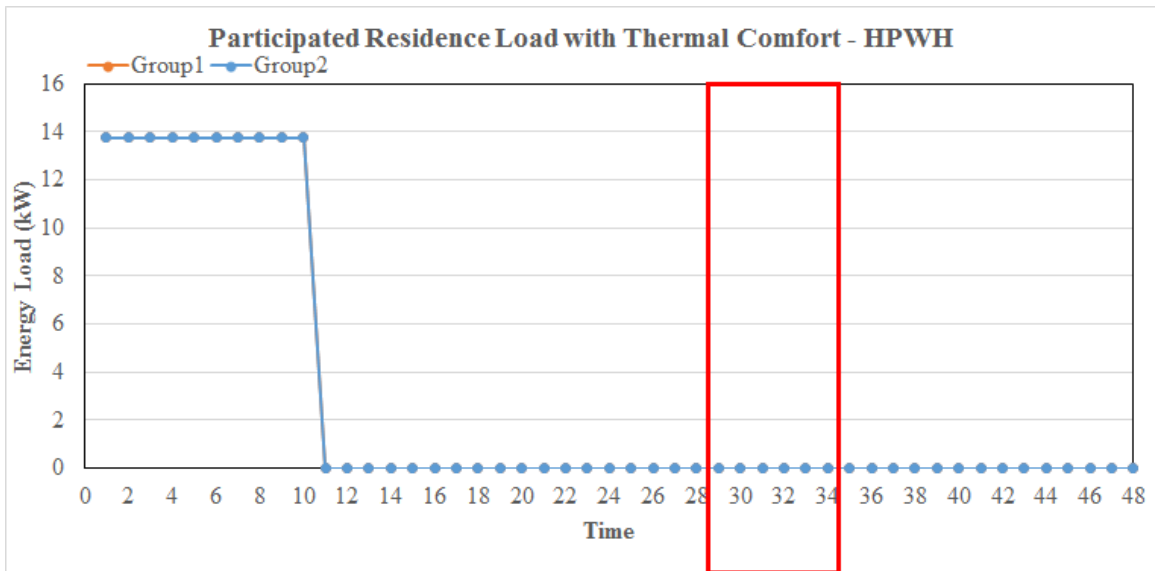

Figure 21. Participating residential HPWH energy consumption with thermal comfort in a typical summer day
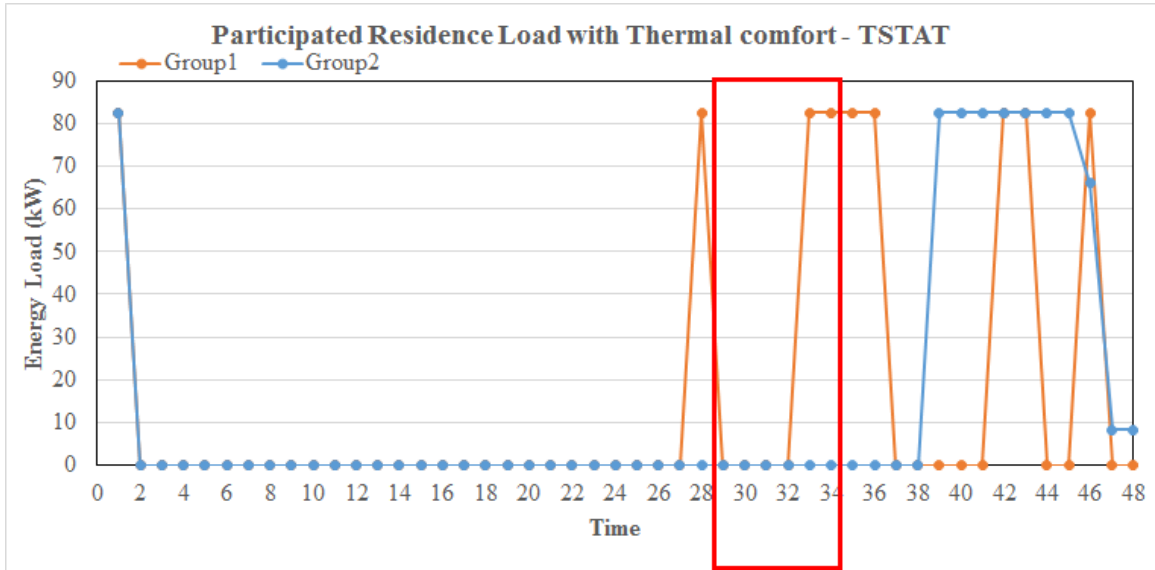
Figure 22. Participating residential TSTAT energy consumption with thermal comfort in a typical summer day
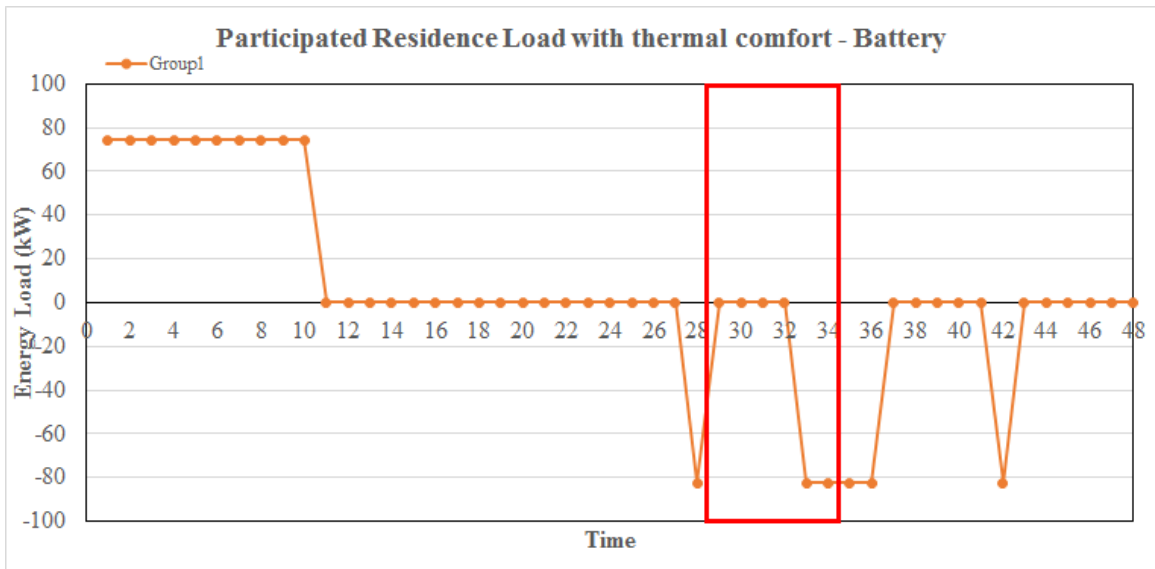

Figure 23. Participating residential battery energy consumption with thermal comfort in a typical summer day
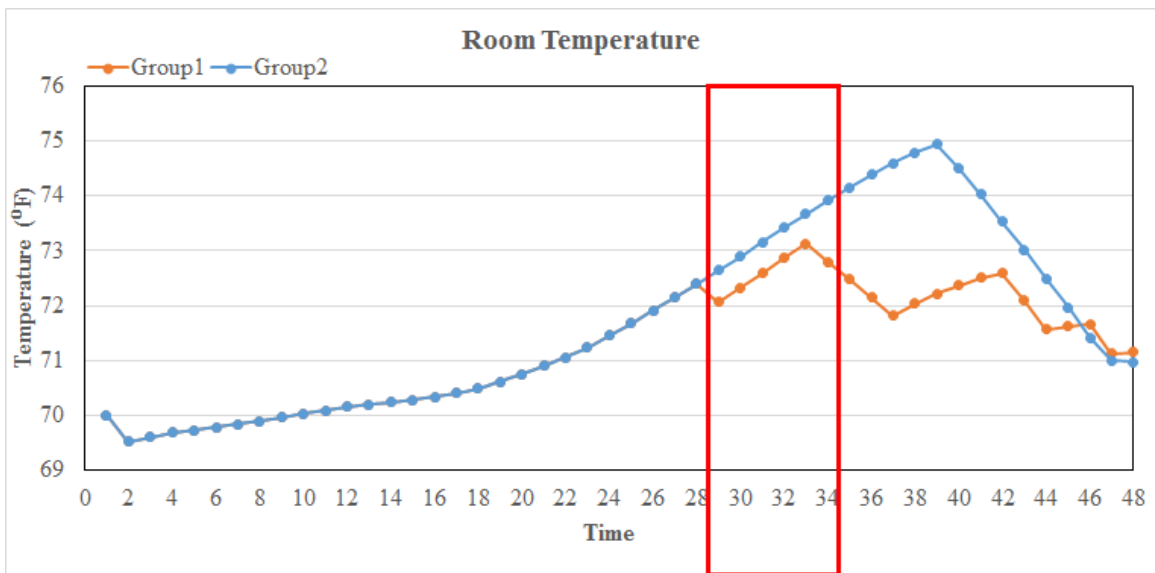
Figure 24. Room temperature of participating home in a typical summer day

We then drop the TSTAT demand and incorporate constraint (77) to allow the TSTAT working based on the thermal comfort. The results are shown in Figures 25 to 30. Because we do not have the TSTAT demand constraint, we cannot compare the total load of the two scenarios. Without the battery, Group 2 can only use the HVAC after the peak window to keep the room temperature below the upper comfort limit. With the battery as the secondary power source, Group 1 can use the HVAC before, during and after the peak window to keep the room temperature in a much more comfortable range.
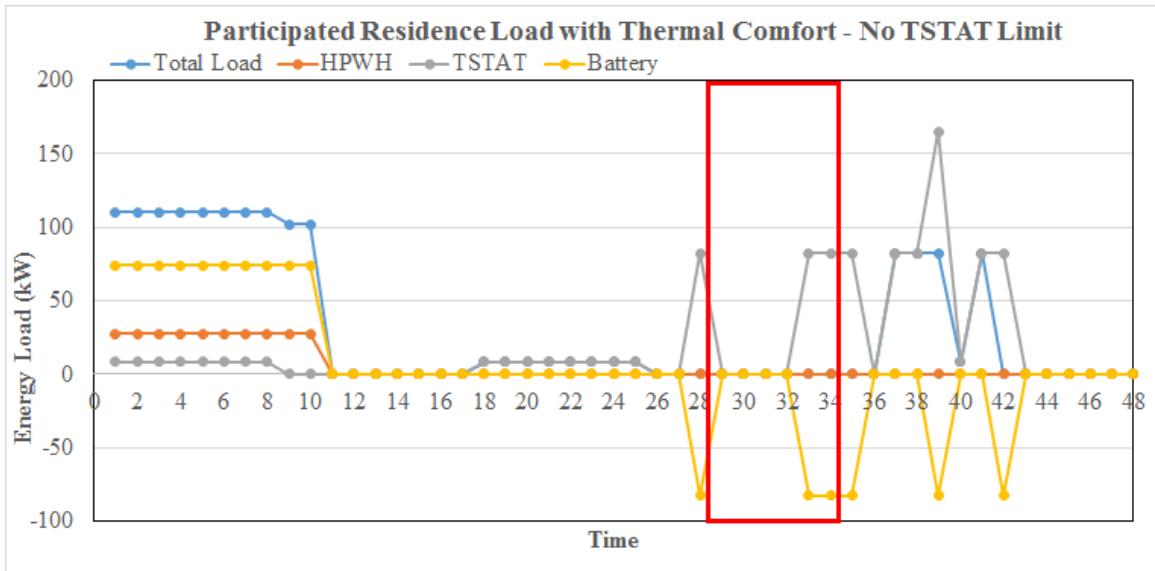

Figure 25. Participating residential energy consumption with thermal comfort and no TSTAT limit in a typical summer day

Figure 26. Participating residential total energy consumption with thermal comfort and no TSTAT limit in a typical summer day

Figure 27. Participating residential HPWH energy consumption with thermal comfort and no TSTAT limit in a typical summer day
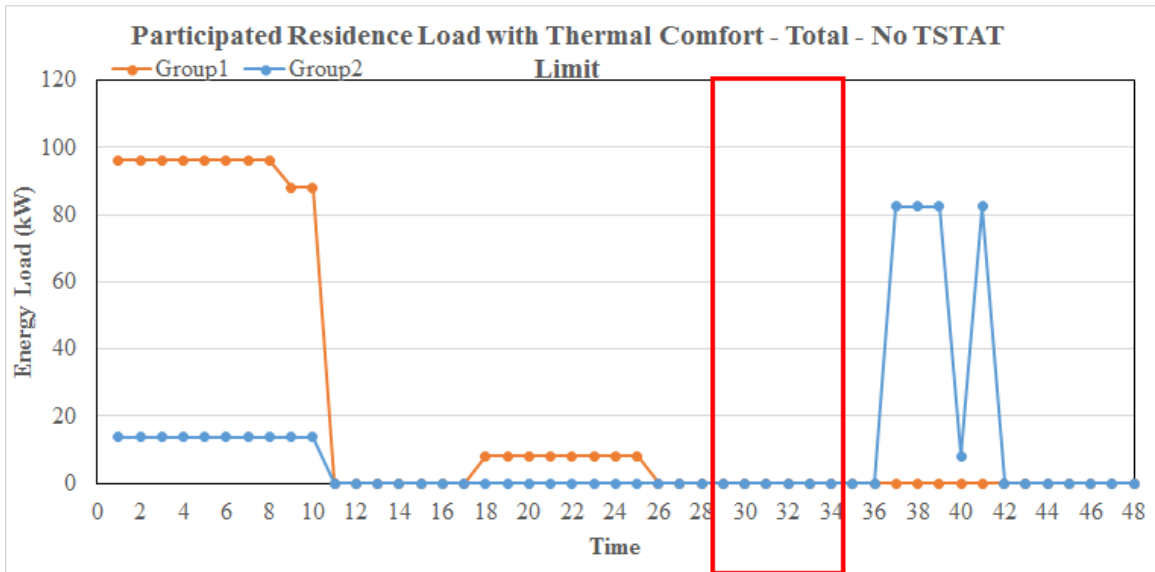
Figure 28. Participating residential TSTAT energy consumption with thermal comfort and no TSTAT limit in a typical summer day
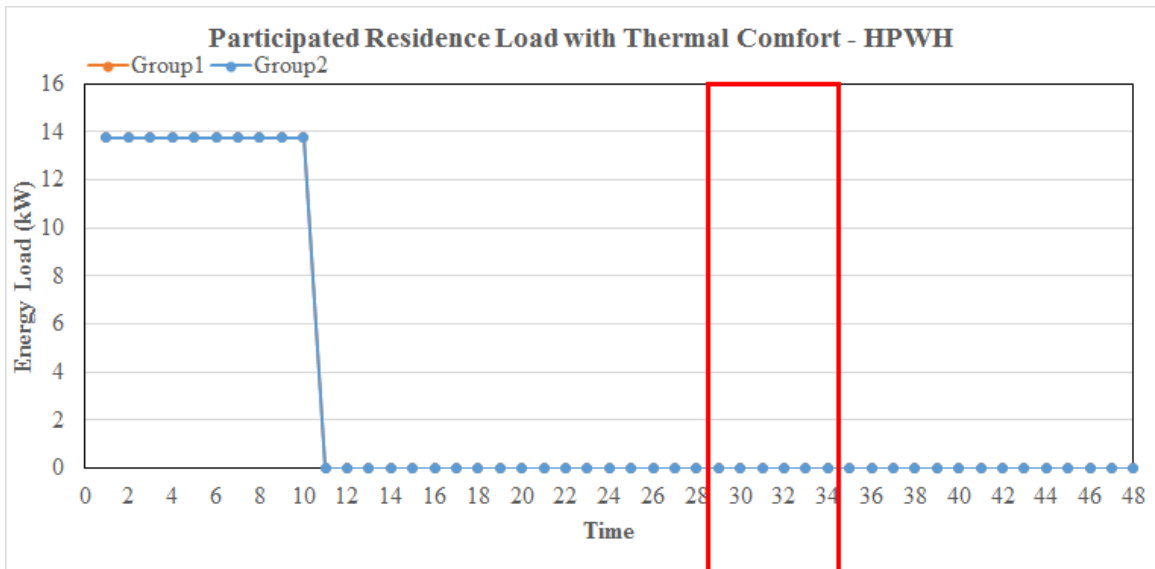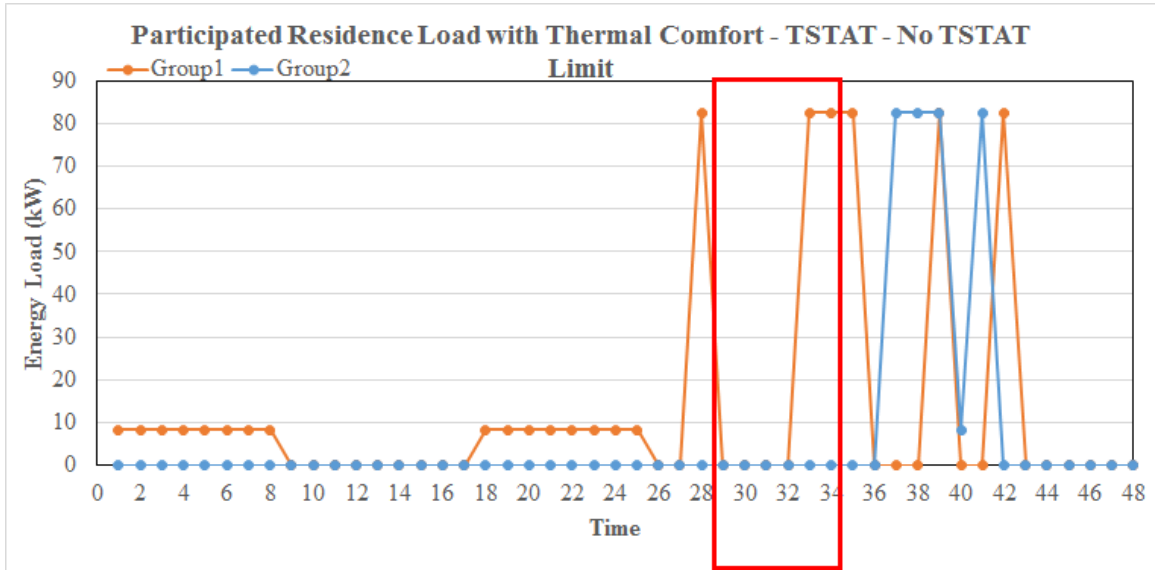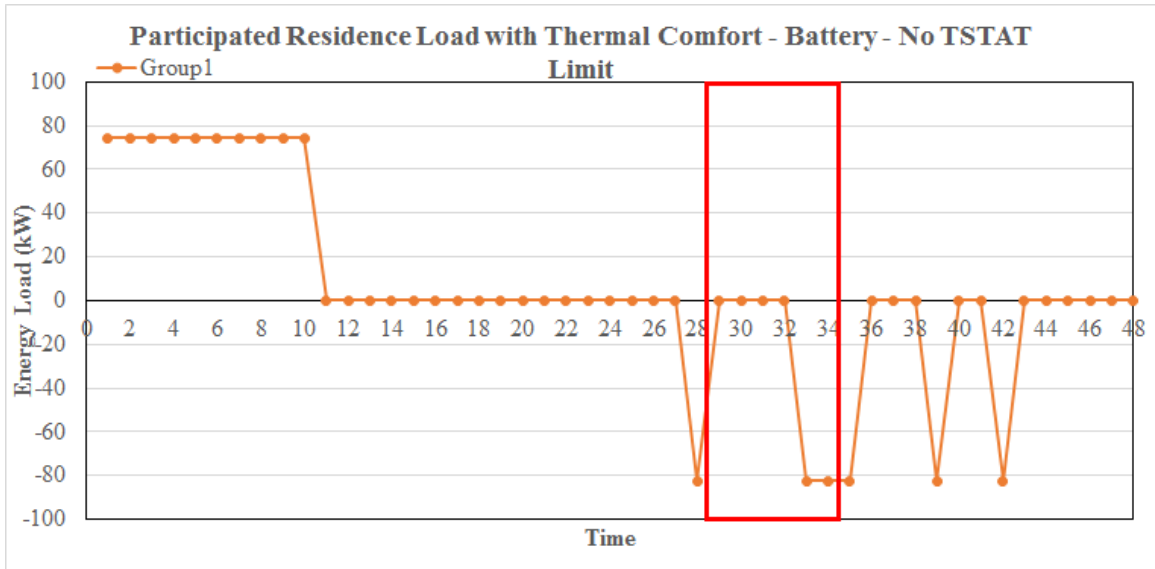

Figure 29. Participating residential battery energy consumption with thermal comfort and no TSTAT limit in a typical summer day
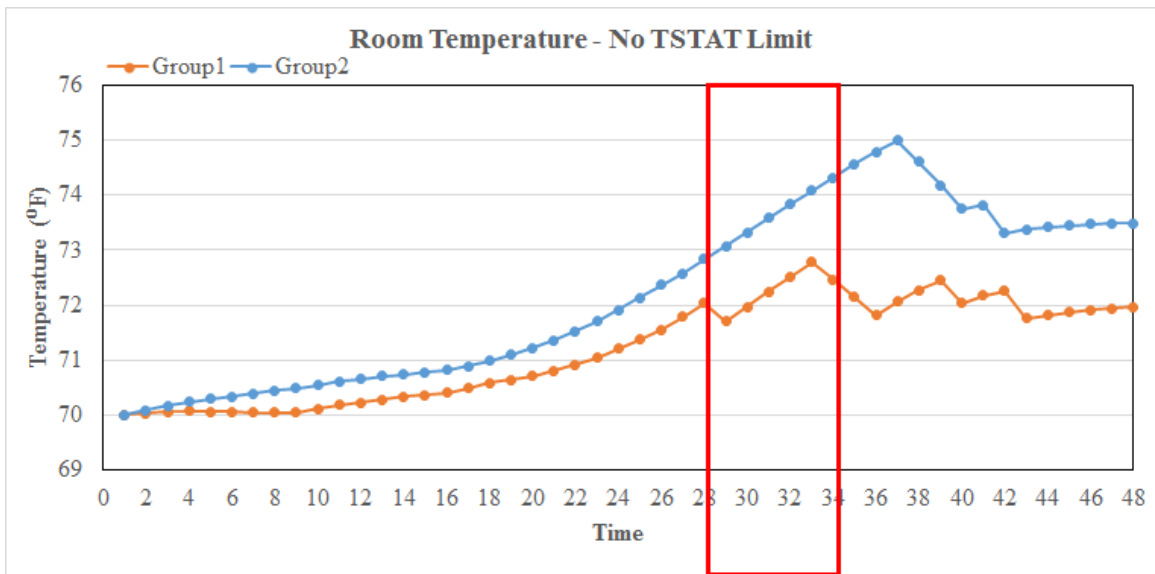
Figure 30. Room temperature of participating homes without TSTAT limit in a typical summer day

CHAPTER 6

CONCLUSIONS AND FUTURE RESEARCH

6.1   Conclusions

Smart grid promises an efficient, reliable and economical power system via advanced models and technologies. Demand side management has gained renewed interests recently in the advent of smart grid, with the focus on increasing energy efficiency from end users. In this study, we consider residential end users who wish not only to minimize their electricity cost but to maximize the utility (e.g., the convenience of using appliances during their preferred times). A user equilibrium model is developed for each user to maximize his/her utility consisting of convenience as well as cost. As a benchmark, a centralized system model is also developed for central controllers to minimize the total system-wide electricity cost. Under mild conditions, we show that the user equilibrium exists and is unique. In addition, we develop the sufficient conditions under which the system and equilibrium models yield the same solution.

Numerically, we demonstrate in general the solutions to the two models are different, even when the convenience utility is not considered. In terms of the total electricity cost of all users, the system model yields lower costs than does the equilibrium model. Our sensitivity analysis suggest that: 1) as users increase their values for convenience, the system's total electricity cost increase at the equilibrium; 2) further, this increase of the electricity cost is dominated by the increase of the users' utility on convenience, thus an increase of the total system-wide utility; 3) users with less flexibility on their preferred time windows for various appliances have

larger impact on the total system-wide measures (e.g., cost and average percentage of preferred usage) at equilibrium; 4) the lesser degree of overlap amongst all users' preferred usage windows for various appliances yields a better system performance (e.g., reduced total cost) at equilibrium. These conclusions provide unique insights for utilities to properly design their demand response programs.

We develop a system model and a game theoretical user equilibrium model to prove that the pricing scheme, which makes the system model and the user equilibrium model share the same users' energy consumption profile, is not unique. By some numerical examples, we show that with a fixed system optimal solution, other pricing schemes exist to achieve the desired objective. In this way, the pricing scheme becomes adjustable and the utility company may customize the pricing scheme to achieve proper objectives. We also prove that at the equilibrium, the users' energy consumption pattern of UEP may not follow the SOS optimal solution if the UEP has multiple solutions under a given pricing scheme. The design objective will always be worse and the obtained pricing scheme may not be the most desirable. By adopting the risk-averse second best toll pricing concept in traffic network area, we propose a bi-level model to solve the problem, where the design objective is worse off.

Based on a pilot study by a major US home appliance manufacturer, a local regulation authority and a local utility company, we analyze the sub-metered homes energy consumption data for summer and winter and develop models for minimize peak load for the system. First, 10 control homes equipped with sub-meters are studied for clustering analysis based on their energy consumption profile for summer days and winter days. In summer days, the 10 homes are sorted into 6 clusters based on the maximum load during peak window and when the peak load occurs. Similarly, 2 clusters are built for winter days. The clustering analysis of the 10 control homes can be applied to the future work, when the pilot study is expanded to 330 local homes enrolled in this project. Secondly, a heuristic rotation algorithm

and four mixed integer programming (MIP) models are developed to minimize the peak load of the entire system. The heuristic algorithm also considers the users' maximum thermal comfort level. Without the expensive battery system, the heuristic rotation algorithm performs better than the "No Rotation" case in two measures of PAR and peak load during peak window. However, with the battery system, the heuristic rotation algorithm and the SPM-1 model does not show advantage over the "No Rotation" case in terms of the peak load during peak window. If the goal is to level the system load of the entire day, the SPM-2 model can reduce the PAR by over 30% compared to the "No Rotation" case.

SPM-3 model is developed to introduce the non-residential consumption into the equation as well as consider the users preference of consecutive using of the appliances. The PAR decreases from 1.39 to 1.34 which appears relatively minor due to the non-residential consumption that is not regulated by the central controller and accounts for over two thirds of total energy consumption.

SPM-4 model further considers the thermal comfort which allows all participating homes to keep the room temperature within their comfortable range and allows the consumers to avoid the peak tariff by using the batteries that provide power supply during peak hours. In addition, this allows the room temperature to fluctuate within a more desired range as compared to the group without the batteries.

Although this dissertation has reached its goals, there were some unavoidable limitations. First, all mathematical models developed in this research were static models. It would be more meaningful and applicable to have dynamic models. Second, some model parameters were based on assumptions for the purpose of theoretical research. If we want to apply the models and results to real world application, the parameters need to go through proper validation processes. Finally, in order for the UE solution to be existence, the cost function needs to be convex and the utility function needs to be concave. In reality, these strict conditions might

not hold.

6.2   Future Research

6.2.1   Energy Consumption Models with Elastic Demand

The price elasticity of demand used in economics assumes a certain relationship between price and quantity demanded in a given time period [80]. It has been widely used in the area of traffic assignment [81] for more than a decade. With the advent of smart grid and demand response, this concept attracts more attention of researchers in electric power system [82][83]. However, they [82][83] only mention the applicability of the elasticity of demand in electricity markets. They do not include the concept in any mathematical models. This section extends the system optimal models and user equilibrium models previously developed for fixed demand energy consumption scheduling to the problem with elastic demand. The system problem maximizes net benefit to the energy consumers and the user problem is the usual one of finding equilibrium with elastic demand.

We first introduce notion and then define the system and user equilibrium models. The system model assumes that the goal of system central controller is to maximize net user benefit, while the equilibrium problem maximizes each user's own benefit.

Employing notation similar to Section 3.1, in addition, let y be the variable of electricity cost.

$$d_{i,a} = v(y) = U_{i,a} - k_{i,a} * y \tag{79}$$

is the the elastic demand function of electricity cost y, where $U_{i,a}$ and $k_{i,a}$ are parameters and $U_{i,a} \geq 0$, $k_{i,a} \geq 0$.

$$w_{i,a}(z) = v^{-1}(z) \tag{80}$$

is the inverse demand function of electricity demand variable z. $w_{i,a}$ is the generalized electricity cost, which is a function of the electricity demand z.

From basic economic principles, the total network wide benefit is

$$\sum_i \sum_a \int_0^{d_{i,a}} w_{i,a}(z)d(z) \tag{81}$$

We can take equations (79) and (80) into equation (81) and get

$$
\begin{aligned}
\int_0^{d_{i,a}} w_{i,a}(z)d(z) \\
&= \tfrac{1}{k_{i,a}}(U_{i,a} - z)dz \\
&= \left(\tfrac{U_{i,a}}{k_{i,a}}z - \tfrac{1}{2k_{i,a}}z^2\right)\Big|_0^{d_{i,a}} \\
&= \tfrac{U_{i,a}}{k_{i,a}}d_{i,a} - \tfrac{1}{2k_{i,a}}d_{i,a}^2
\end{aligned}
$$

Therefore,

$$\int_0^{d_{i,a}} w_{i,a}(z)d(z) = \frac{U_{i,a}}{k_{i,a}}d_{i,a} - \frac{1}{2k_{i,a}}d_{i,a}^2 \tag{82}$$

Note that, z does not really appear in equation (82).

In the system problem, the central controller maximizes net user benefit, the difference between total user benefit and the system cost. and the system cost is defined by $\sum_{t=1}^{T} f(l_t) \cdot l_t$ in the SO model described in Section 3.2. Thus, using minimization in the objective, the elastic demand system problem (SO-ED) is

$$\text{SO-ED:} \quad \min \ \sum_{t=1}^{T} f(\sum_{i,a} x_{i,a}^t) \cdot \sum_{i,a} x_{i,a}^t - \sum_i \sum_a \int_0^{d_{i,a}} w_{i,a}(z)d(z) \tag{83}$$

$$\text{s.t.} \quad \sum_{t=1}^{T} x_{i,a}^t = d_{i,a}, \quad \forall i, a \tag{84}$$

$$x_{i,a}^t \le E_{i,a}, \quad \forall i, a, t \tag{85}$$

$$x_{i,a}^t = 0, \quad \forall i, a, t : \ t \in T_{i,a}^0 \tag{86}$$

$$x_{i,a}^t \ge 0, \quad \forall i, a, t \tag{87}$$

where the objective in (83) is for the central controller to maximize the net user benefit, which is the difference between the total electricity cost required to serve all users and the inverse elastic demand function. Furthermore, constraints (84) - (86)

98

are similar to constraints (3) - (5). The only difference is that in constraint (84), user i's energy demand for appliance a $d_{i,a}$ is no longer fixed. It is the the elastic demand function of electricity cost y and can be written as (79).

Similarly, if we apply the above elastic demand to the SOS model described in Section 4.1, the new SOS-ED model can be characterized as follows:

SOS-ED:

$$\max_{x_{i,a}^t, d_{i,a}} \quad \sum_i \pi_i \cdot \sum_a 2 \left(\frac{\sum\limits_{t \in T_{i,a}^1} x_{i,a}^t}{d_{i,a}} \right)^{1/2} + \sum_i \sum_a \int_0^{d_{i,a}} w_{i,a}(z) d(z)$$

$$- \sum_{t=1}^T [(c_0 + c \cdot \sum_{i,a} x_{i,a}^t) \cdot \sum_{i,a} x_{i,a}^t] \tag{88}$$

s.t.

$$\lambda_a^i \cdots \quad \sum_t x_{i,a}^t = d_{i,a}, \quad \forall i, a \tag{89}$$

$$\gamma_{t,a}^i \cdots \quad x_{i,a}^t \le E_{i,a}, \quad \forall i, a, t \tag{90}$$

$$\mu_{t,a}^i \cdots \quad x_{i,a}^t \ge 0, \quad \forall i, a, t \tag{91}$$

Finally, we apply the elastic demand to the UEP_i model in Section 4.2. We consider the convenience for this user to be able to use an appliance during his/her preferred times and the benefit of the elastic demand. Thus, the user equilibrium model assumes each user i maximizes the his/her own benefit. Hence, in a distributed manner, each user solves the following user's problem under the elastic demand:

UEP_i-ED:

$$\max_{y_{i,a}^t,d_{i,a}} \quad \pi_i \cdot \sum_a 2 \left(\frac{\sum_{t\in T_{i,a}^1} y_{i,a}^t}{d_{i,a}} \right)^{1/2} + \sum_a \int_0^{d_{i,a}} w_{i,a}(z)d(z)$$

$$- \sum_{t=1}^T p(t) \cdot (\sum_a y_{i,a}^t) \tag{92}$$

s.t.

$$\alpha_{i,a} \cdots \quad \sum_t y_{i,a}^t = d_{i,a}, \quad \forall a \tag{93}$$

$$\beta_{i,a}^t \cdots \quad y_{i,a}^t \le E_{i,a}, \quad \forall a,t \tag{94}$$

$$\rho_{i,a}^t \cdots \quad -y_{i,a}^t \le 0, \quad \forall a,t \tag{95}$$

The Lagrange multipliers and KKT conditions method described in Chapter 4 may be applied to solve the above models with elastic demand.

6.2.2   Benders Decomposition Method for Proposed Bi-level Robust Pricing Model

As a follow-up to this dissertation, the Benders Decomposition [84] will be examined as a potential solution method for solving the proposed bi-level model (49)-(50). In Benders decomposition, a subset of variables is solved in the first-stage master problem, and the remaining variables are determined by the second-stage subproblem given the values of the first-stage variables [85]. Benders decomposition is a cutting plane method due to adding a constraint at each iteration. It reduces search region by adding linear constraints while preserving the original feasible region.

In our case, the second-stage subproblem is to minimize the social welfare given a pricing p. The first-stage master problem is to maximize all minimum possible social welfare among alternative pricing with lower and upper boundary

conditions. In this manner, we can get the robust pricing scheme, which can ensure the maximum of all minimum possible social welfare.

REFERENCES

[1] Smartgrid.gov. *What is the Smart Grid*. Retrieved November 19, 2014, from https://www.smartgrid.gov/the_smart_grid.

[2] Edison Tech Center. *The History of Electrification: The Birth of our Power Grid*. Retrieved November 19, 2014, from http://edisontechcenter.org/HistElectPowTrans.html.

[3] Farhangi, H. (2010). The path of the smart grid. *IEEE Power and Energy Magazine*. 8(1), 18-28.

[4] Amin, S. M., and Wollenberg, B. F. (2005). Toward a smart grid: power delivery for the 21st century. *IEEE Power and Energy Magazine*. 3(5), 34-41.

[5] Byrne, C. (2011). *How secure is the smart grid?*. Retrieved December 7, 2014, from http://venturebeat.com/2011/02/01/how-secure-is-the-smart-grid/.

[6] Gungor, V. C., Lu, B., and Hancke, G. P. (2010). Opportunities and challenges of wireless sensor networks in smart grid. *IEEE Transactions on Industrial Electronics*. 57(10), 3557-3564.

[7] Cecati, C., Citro, C., Piccolo, A., and Siano, P. (2011). Smart operation of wind turbines and diesel generators according to economic criteria. *IEEE Transactions on Industrial Electronics*. 58(10), 4514-4525.

[8] Palensky, P., and Dietrich, D. (2011). Demand side management: Demand response, intelligent energy systems, and smart loads. *IEEE Transactions on Industrial Informatics*. 7(3), 381-388.

[9] Calderaro, V., Hadjicostis, C. N., Piccolo, A., and Siano, P. (2011). Failure identification in smart grids based on petri net modeling. *IEEE Transactions on Industrial Electronics.* 58(10), 4613-4623.

[10] Kanchev, H., Lu, D., Colas, F., Lazarov, V., and Francois, B. (2011). Energy management and operational planning of a microgrid with a PV-based active generator for smart grid applications. *IEEE Transactions on Industrial Electronics.* 58(10), 4583-4592.

[11] Vaccaro, A., Velotto, G., and Zobaa, A. F. (2011). A decentralized and cooperative architecture for optimal voltage regulation in smart grids. *IEEE Transactions on Industrial Electronics.* 58(10), 4593-4602.

[12] Gungor, V. C., Sahin, D., Kocak, T., Ergut, S., Buccella, C., Cecati, C., and Hancke, G. P. (2011). Smart grid technologies: communication technologies and standards. *IEEE transactions on Industrial informatics.* 7(4), 529-539.

[13] Luan, Wenpeng. (2009). Advanced metering infrastructure. *Southern Power System Technology.* 3(2), 6-10.

[14] Brown, R. E. (2008). Impact of smart grid on distribution system design. *IEEE in Power and Energy Society General Meeting-Conversion and Delivery of Electrical Energy in the 21st Century.* 1-4. IEEE.

[15] Hart, D. G. (2008). Using AMI to realize the Smart Grid. *IEEE in Power and Energy Society General Meeting-Conversion and Delivery of Electrical Energy in the 21st Century.* 1-2. IEEE.

[16] Pipattanasomporn, M., Feroze, H., and Rahman, S. (2009). Multi-agent systems in a distributed smart grid: Design and implementation. *IEEE/PES Power Systems Conference and Exposition.* 1-8. IEEE.

[17] Karnouskos, S., and De Holanda, T. N. (2009). Simulation of a smart grid city with software agents. *Third UKSim European Symposium in Computer Modeling and Simulation.* 424-429. IEEE.

[18] Cui, S., Han, Z., Kar, S., Kim, T. T., Poor, H. V., and Tajer, A. (2012). Coordinated data-injection attack and detection in the smart grid: A detailed look at enriching detection solutions. *IEEE Signal Processing Magazine.* 29(5), 106-115.

[19] Yuan, Y., Li, Z., and Ren, K. (2011). Modeling load redistribution attacks in power systems. *IEEE Transactions on Smart Grid.* 2(2), 382-390.

[20] Brown, G., Carlyle, W. M., Salmeron, J., and Wood, K. (2004). Analyzing the Vulnerability of Critical Infrastructure to Attack, and Planning Defenses. *IEEE Transactions on Power Systems.* 19(2), 905-912.

[21] Ghosn, S. B., Ranganathan, P., Salem, S., Tang, J., Loegering, D., and Nygard, K. E. (2010). Agent-oriented designs for a self healing smart grid. *2010 First IEEE International Conference in Smart Grid Communications (SmartGridComm).* 461-466. IEEE.

[22] Alderson, D. L., Brown, G. G., Carlyle, W. M., and Wood, R. K. (2011). Solving Defender-Attacker-Defender Models for Infrastructure Defense. *Risk Analysis.* 31, 196-204.

[23] Cecati, C., Citro, C., and Siano, P. (2011). Combined operations of renewable energy systems and responsive demand in a smart grid. *IEEE Transactions on Sustainable Energy.* 2(4), 468-476.

[24] Potter, C. W., Archambault, A., and Westrick, K. (2009). Building a smarter smart grid through better renewable energy information. *IEEE/PES Power Systems Conference and Exposition.* 1-5. IEEE.

[25] Daryanian, B., Bohn, R. E., and Tabors, R. D. (1989). Optimal demand-side response to electricity spot prices for storage-type customers. *IEEE Transactions on Power Systems.* 4(3), 897-903.

[26] Gatsis, N., and Giannakis, G. B. (2012). Residential load control: Distributed scheduling and convergence with lost AMI messages. *IEEE Transactions on Smart Grid).* 3(2), 770-786.

[27] Bai, L., Xu, G., and Zheng, Q. P. (2014). A game theoretical approach to modeling energy consumption with consumer preference. *2014 IEEE/PES General Conference and Exposition.* 1-5. IEEE.

[28] Herter, K. (2007). Residential implementation of critical-peak pricing of electricity. *Energy Policy.* 35(4), 2121-2130.

[29] Triki, C., and Violi, A. (2009). Dynamic pricing of electricity in retail markets. *4OR: A Quarterly Journal of Operations Research.* 7(1), 21-36.

[30] Centolella, P. (2010). The integration of price responsive demand into regional transmission organization (RTO) wholesale power markets and system operations. *Energy.* 35(4), 1568-1574.

[31] Albadi, M. H., and El-Saadany, E. F. (2007). Demand Response in Electricity Markets: An Overview. *In 2007 Power Engineering Society General Meeting.* 1-5. IEEE.

[32] Lijesen, M. G. (2007). The real-time price elasticity of electricity. *Energy economics.* 29(2), 249-258.

[33] Cohen, A. I., and Wang, C. C. (1988). An optimization method for load management scheduling. *IEEE Transactions on Power Systems.* 3(2), 612-618.

[34] Wei, D. C., and Chen, N. (1995). Air conditioner direct load control by multi-pass dynamic programming. *IEEE Transactions on Power Systems.* 10(1), 307-313.

[35] Chen, J., Lee, F. N., Breipohl, A. M., and Adapa, R. (1995). Scheduling direct load control to minimize system operation cost. *IEEE Transactions on Power Systems.* 10(4), 1994-2001.

[36] Ng, K. H., and Sheble, G. B. (1998). Direct load control-A profit-based load management using linear programming. *IEEE Transactions on Power Systems.* 13(2), 688-694.

[37] Chu, W. C., Chen, B. K., and Fu, C. K. (1993). Scheduling of direct load control to minimize load reduction for a utility suffering from generation shortage. *IEEE Transactions on Power Systems.* 8(4), 1525-1530.

[38] Ramanathan, B., and Vittal, V. (2008). A framework for evaluation of advanced direct load control with minimum disruption. *IEEE Transactions on Power Systems.* 23(4), 1681-1688.

[39] Hsu, Y. Y., and Su, C. C. (1991). Dispatch of direct load control using dynamic programming. *IEEE Transactions on Power Systems.* 6(3), 1056-1061.

[40] Bonabeau, E. (2002). Agent-based modeling: Methods and techniques for simulating human systems. *Proceedings of the National Academy of Science.* 99(3), 7280-7287.

[41] Vytelingum, P., Voice, T.D., Ramchurn, S.D., Rogers, A. and Jennings, N.R. (2010, May 10-14). Agent-based micro-storage management for the smart grid. *The Ninth International Conference on Autonomous Agents and Multiagent Systems (AAMAS 2010)*, Toronto, Canada, 39-46.

[42] Vandael, S., Boucke, N., Holvoet, T., and Deconinck, G. (2010, May 10-14). Decentralized demand side management of plug-in hybrid vehicles in a smart grid. *Proceedings of First International Workshop on Agent Technologies for Energy Systems (ATES 2010).* Toronto, Canada, 67-74.

[43] Saad, W., Han, Z., Poor, H. V., and Basar, T. (2012). Game-theoretic methods for the smart grid: An overview of microgrid systems, demand-side management, and smart grid communications. *IEEE Signal Processing Magazine.* 29(5), 86-105.

[44] Fadlullah, Z. M., Nozaki, Y., Takeuchi, A., and Kato, N. (2011). A survey of game theoretic approaches in smart grid. *2011 International Conference on Wireless Communications and Signal Processing (WCSP).* IEEE. 1-4.

[45] Mohsenian-Rad, A. H., Wong, V. W., Jatskevich, J., Schober, R., and Leon-Garcia, A. (2010). Autonomous demand-side management based on game-theoretic energy consumption scheduling for the future smart grid. *IEEE Transactions on Smart Grid.* 1(3), 320-331.

[46] Chen, C., Kishore, S., and Snyder, L. V. (2011). An innovative RTP-based residential power scheduling scheme for smart grids. *2011 IEEE International Conference on Acoustics, Speech and Signal Processing (ICASSP).* IEEE. 5956-5959.

[47] Maharjan, S., Zhu, Q., Zhang, Y., Gjessing, S., and Basar, T. (2013). Dependable demand response management in the smart grid: A stackelberg game approach. *IEEE Transactions on Smart Grid.* 4(1), 120-132.

[48] Samadi, P., Mohsenian-Rad, A.H., Schober, R., Wong, V.W.S. and Jatskevich, J. (2010, October 4-6). Optimal Real-time Pricing Algorithm Based on Utility Maximization for Smart Grid. *2010 First IEEE International Conference on Smart Grid Communication (SmartGridComm).* Gaithersburg, MD, 415-420.

[49] Shahidehpour, M., Yamin, H. and Li, Z. (2002). *Market operations in electric power systems: forecasting, scheduling and risk management.* New York: John Wiley and Sons Inc.

[50] Aigner, D. (1985). The residential electricity time-of-use pricing experiments: what have we learned?. In Hausman, J.A. and Wise, D.A. (Eds.). *Social Experimentation*, Chicago: University of Chicago Press, 11-53.

[51] Collins, M. and Mader, G. (1983). The timing of EV recharging and its effect on utilities. *IEEE Transactions on Vehicular Technology.* 32(1), 90-97.

[52] Davis, M.B. and Bradley, T.H. (2012). The efficacy of electric vehicle time-of-use rates in guiding plug-in hybrid electric vehicle charging behavior. *IEEE Transactions on Smart Grid.* 3(4), 1679-1686.

[53] Baladi, S.M., Herriges, J.A. and Sweeney, J.T. (1998). Residential response to voluntary time-of-use electricity rates. *Resource and Energy Economics.* 20(1998), 225-244.

[54] Hartway, R., Price, S. and Woo, C.K. (1999). Smart meter, customer choice and profitable time-of-use rate option. *Energy.* 24(10), 859-903.

[55] Mohsenian-Rad, A.H. and Leon-Garcia, A. (2010). Optimal residential load control with price prediction in real-time electricity pricing environments. *IEEE Transactions on Smart Grid.* 1(2), 120-133.

[56] Zhong, H., Xie, L., and Xia, Q. (2013). Coupon incentive-based demand response: Theory and case study. *IEEE Transactions on Power Systems.* 28(2), 1266-1276.

[57] Meng, F. L., and Zeng, X. J. (2013). A Stackelberg game-theoretic approach to optimal real-time pricing for the smart grid. *Soft Computing.* 17(12), 2365-2380.

[58] Fetz, A. and Filippini, M. (2010). Economies of vertical integration in the Swiss electricity sector. *Energy Economics.* 32(6), 1325-1330.

[59] Martínez-Budría, E., Jara-Díaz, S. and Ramos-Real, F.J. (2003). Adapting productivity theory to the quadratic cost function: an application to the Spanish electric sector. *Journal of Productivity Analysis.* 20(2), 213-229.

[60] Sianaki, O. A., Hussain, O., Dillon, T., and Tabesh, A. R. (2010). Intelligent Decision Support System for Including Consumers' Preferences in Residential Energy Consumption in Smart Grid. *2010 Second International Conference on Computational Intelligence, Modelling and Simulation (CIMSiM).* 154-159. IEEE.

[61] Amer, M., Naaman, A., M'Sirdi, N. K., and El-Zonkoly, A. M. (2014). A hardware algorithm for PAR reduction in smart home. *International Conference in Applied and Theoretical Electricity (ICATE).* 1-6. IEEE.

[62] Yoo, Y. S., and Lee, I. W. Heuristic Analysis of Energy Information and Preference for Smart Grid Infrastructure. *ICTC2014: The 5th International Conference on ICT Convergence.* 569-571. IEEE.

[63] Li, N., Chen, L., and Low, S. H. (2011). Optimal demand response based on utility maximization in power networks. *2011 IEEE Power and Energy Society General Meeting.* 1-8. IEEE.

[64] LG&E, Louisville Gas & Electric Company. *LG&E Teams with GE To Reshape Energy Usage, Save Consumers Money.* Retrieved July 23, 2013, from http://www.intelligentutility.com/article/08/09/lge-teams-ge-reshape-energy-usage-save-consumers-money?quicktabs_4=1&quicktabs_6=0.

[65] Bazaraa, M. S., Sherali, H. D., and Shetty, C. M. (2013). *Nonlinear programming: theory and algorithms.* John Wiley & Sons.

[66] Rosen, J.B. (1965). Existence and Uniqueness of Equilibrium Points for Concave N-person Games. *Econometrica*. 33(3), 520–534.

[67] Ferris, M. C., and Munson, T. S. (2000). *GAMS/PATH user guide: Version 4.3*. Washington, DC: GAMS Development Corporation.

[68] Brooke, A., Kendrick, D., and Meeraus, A. (1996). *GAMS Release 2.25: A user's guide*. Washington, DC: GAMS Development Corporation.

[69] Drud, A. S. (1994). CONOPT:a large-scale GRG code. *ORSA Journal on Computing*. 6(2), 207-216.

[70] Keeney, R. L., and Raiffa, H. (1993). *Decisions with multiple objectives: preferences and value trade-offs*. Cambridge university press.

[71] Clemen, R. T. (1996). *Making Hard Decisions: An Introduction to Decision Analysis. ed.* Boston: Duxbury Press.

[72] GE Blogs. *Home Appliance Energy Use*. Retrieved July 23, 2013, from http://visualization.geblogs.com/visualization/appliances/.

[73] US Energy Information Administration. *Residential Average Monthly Bill by Census Division, and State*. Retrieved July 23, 2013, from http://www.eia.gov/cneaf/electricity/esr/table5.html.

[74] Bergendorff, P., Hearn, D. W., and Ramana, M. V. (1997). *Congestion toll pricing of traffic networks*. Springer Berlin Heidelberg. Chicago. 51-71.

[75] Ban, X. J., Lu, S., Ferris, M., and Liu, H. X. (2009). Risk averse second best toll pricing. *In Transportation and Traffic Theory 2009: Golden Jubilee.* Springer US. 197-218.

[76] McIntryre, M., Burke, W.J., Latham, J., and Graham, J., (2014). Energy Usage Patterns in Fielded Smart Appliances. *Proc. of the 29th International*

Conference on Computers and Their Applications. March 24-26, Las Vegas, Nevada, 181-188.

[77] Xu, G., and Bai, L. (2013). Heuristic methods for optimal electric vehicle charging scheduling in smart grid. *2013 International Journal of Automation and Logistics.* 1(1), 22-46.

[78] Weather Underground. *Historical temperature of Glasgow, KY.* Retrieved October 23, 2016, from https://www.wunderground.com/history/airport/KGLW/2014/8/1/DailyHistory.html.

[79] Khadgi, P. (2016). Optimizing energy consumption behavior of residential consumers in response to demand side management. *2016 PhD Dissertation.*

[80] Economics Online. *Price elasticity of demand.* Retrieved February 17, 2015, from http://www.economicsonline.co.uk/Competitive_markets/Price_elasticity_of_demand.html.

[81] Hearn, D. W., and Yildirim, M. B. (2002). A toll pricing framework for traffic assignment problems with elastic demand. 135-145. Springer US.

[82] Albadi, M. H., and El-Saadany, E. F. (2008). A summary of demand response in electricity markets. *Electric Power Systems Research.* 78(11), 1989-1996.

[83] Spees, K., and Lave, L. B. (2007). Demand response and electricity market efficiency. *The Electricity Journal.* 20(3), 69-85.

[84] Benders, J. F. (1962). Partitioning procedures for solving mixed-variables programming problems. *Numerische mathematik.* 4(1), 238-252.

[85] Taskin, Z. C. (2010). Benders decomposition. *Wiley Encyclopedia of Operations Research and Management Science.* John Wiley & Sons, Malden (MA).

CURRICULUM VITAE

NAME: Guangyang Xu

ADDRESS: Department of Industrial Engineering

                   University of Louisville

                   Louisville, KY 40292

EDUCATION: B.S. Chemical Engineering

                   China University of Mining and Technology (Beijing)

                   2004

                   M.S. Industrial Engineering

                   University of Louisville

                   2013

PREVIOUS
RESEARCH: Logistics

                   Operations Research

                   Optimization

AWARDS: Leigh Ann Conn Graduate Fellowship - 2012

                   Industrial Engineering Graduate Student Award - 2013

                   Alpha Pi Mu (Industrial Engineering Honor Society)